Microwave Devices and Circuits

Third Edition

SAMUEL Y. LIAO

Professor of Electrical Engineering
California State University, Fresno

PRENTICE HALL, *Englewood Cliffs, New Jersey 07632*

Chapter 9

Microwave Linear-Beam Tubes (O Type)

9-0 INTRODUCTION

We turn now to a quantitative and qualitative analysis of several conventional vacuum tubes and microwave tubes in common use. The conventional vacuum tubes, such as triodes, tetrodes, and pentodes, are still used as signal sources of low output power at low microwave frequencies. The most important microwave tubes at present are the linear-beam tubes (*O* type) tabulated in Table 9-0-1. The paramount *O*-type tube is the two-cavity klystron, and it is followed by the reflex klystron. The helix traveling-wave tube (TWT), the coupled-cavity TWT, the forward-wave amplifier (FWA), and the backward-wave amplifier and oscillator (BWA and BWO) are also *O*-type tubes, but they have nonresonant periodic structures for electron interactions. The Twystron is a hybrid amplifier that uses combinations of klystron and TWT components. The switching tubes such as krytron, thyratron, and planar triode are very useful in laser modulation. Although it is impossible to discuss all such tubes in detail, the common operating principles of many will be described.

The advent of linear-beam tubes began with the Heil oscillators [1] in 1935 and the Varian brothers' klystron amplifier [1] in 1939. The work was advanced by the space-charge-wave propagation theory of Hahn and Ramo [1] in 1939 and continued with the invention of the helix-type traveling-wave tube (TWT) by R. Kompfner in 1944 [2]. From the early 1950s on, the low power output of linear-beam tubes made it possible to achieve high power levels, first rivaling and finally surpassing magnetrons, the early sources of microwave high power. Subsequently, several additional devices were developed, two of which have shown lasting importance. They are the extended interaction klystron [3] and the Twystron hybrid amplifier [4].

TABLE 9-0-1 LINEAR BEAM TUBES (*O* TYPE)

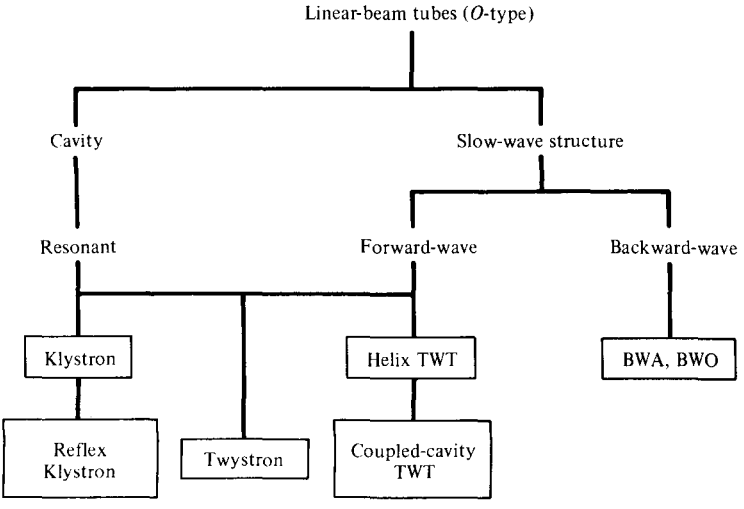

In a linear-beam tube a magnetic field whose axis coincides with that of the electron beam is used to hold the beam together as it travels the length of the tube. *O*-type tubes derive their name from the French *TPO* (*tubes à propagation des ondes*) or from the word *original* (meaning the original type of tube). In these tubes electrons receive potential energy from the dc beam voltage before they arrive in the microwave interaction region, and this energy is converted into their kinetic energy. In the microwave interaction region the electrons are either accelerated or decelerated by the microwave field and then bunched as they drift down the tube. The bunched electrons, in turn, induce current in the output structure. The electrons then give up their kinetic energy to the microwave fields and are collected by the collector.

O-type traveling-wave tubes are suitable for amplification. At present, klystron and TWT amplifiers can deliver a peak power output up to 30 MW (megawatts) with a beam voltage on the order of 100 kV at the frequency of 10 GHz. The average power outputs are up to 700 kW. The gain of these tubes is on the order of 30 to 70 dB, and the efficiency is from 15 to 60%. The bandwidth is from 1 to 8% for klystrons and 10 to 15% for TWTs.

Since the early 1960s, predictions have continued that microwave tubes will be displaced by microwave solid-state devices. This displacement has occurred only at the low-power and receiving circuit level of equipment. Microwave power tubes continue, however, as the only choice for high-power transmitter outputs and are expected to maintain this dominant role throughout the next generation and beyond. Figure 9-0-1 and 9-0-2 show the CW power and peak power state-of-the-art performances for various tube types [5].

The numbers by the data points represent efficiency in percent; the letter in parentheses stands for the developer of the tube. Impressive gain has been made in bandwidth of a single TWT device by Varian. More than 50 dB of gain is available

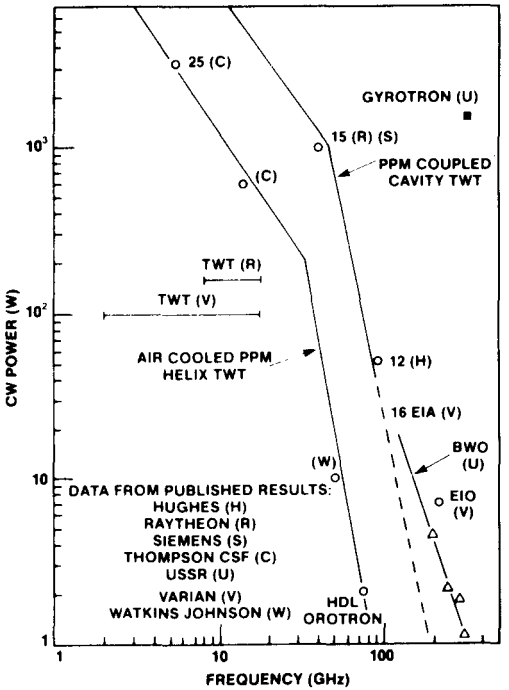

Figure 9-0-1 CW power state-of-the-art performance for various microwave tubes. (*After C. Hieslmair [5], reprinted by permission of* Microwave Journal.)

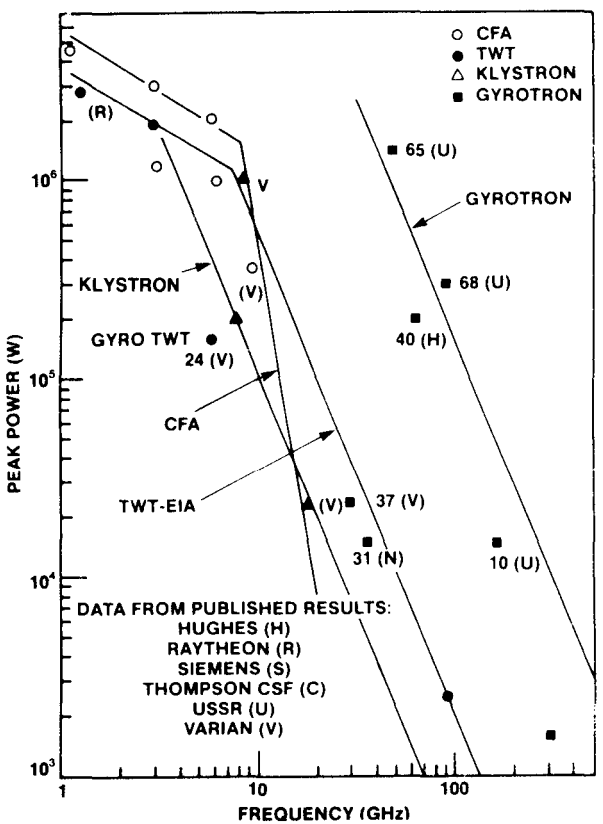

Figure 9-0-2 Peak power state-of-the-art performance for various microwave tubes. (*After C. Hieslmair [5], reprinted by permission of* Microwave Journal.)

in a 93- to 95-GHz TWT at the 50-watt average level by Hughes, and 2-kW peak power at 30-dB gain is provided by Varian. The most impressive power achievements at very good efficiencies continue to occur in the gyrotron area. The Naval Research Laboratory (NRL) reports results of work on a 30% bandwidth gyrotron TWT. Tube reliability continues to improve as a result of low-temperature cathode technology, better materials, and quality control in manufacture.

9-1 CONVENTIONAL VACUUM TRIODES, TETRODES, AND PENTODES

Conventional vacuum triodes, tetrodes, and pentodes are less useful signal sources at frequencies above 1 GHz because of lead-inductance and interelectrode-capacitance effects, transit-angle effects, and gain-bandwidth product limitations. These three effects are analyzed in detail in the following sections.

9-1-1 Lead-Inductance and Interelectrode-Capacitance Effects

At frequencies above 1 GHz conventional vacuum tubes are impaired by parasitic-circuit reactances because the circuit capacitances between tube electrodes and the circuit inductance of the lead wire are too large for a microwave resonant circuit. Furthermore, as the frequency is increased up to the microwave range, the real part of the input admittance may be large enough to cause a serious overload of the input circuit and thereby reduce the operating efficiency of the tube. In order to gain a better understanding of these effects, the triode ciruit shown in Fig. 9-1-1 should be studied carefully.

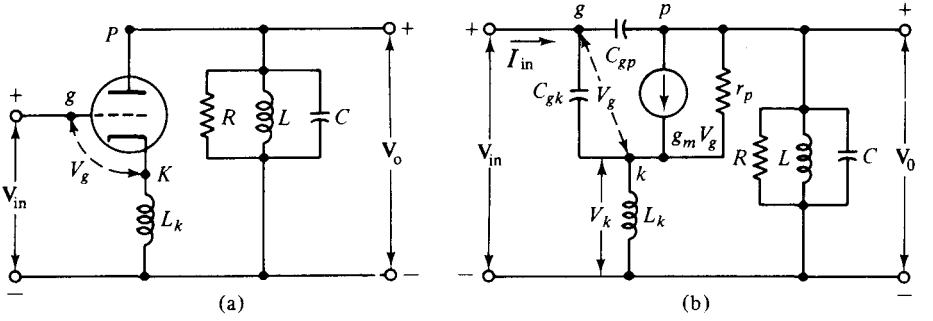

Figure 9-1-1 Triode circuit (a) and its equivalent (b).

Figure 9-1-1(b) shows the equivalent circuit of a triode circuit under the assumption that the interelectrode capacitances and cathode inductance are the only parasitic elements. Since $C_{gp} \ll C_{gk}$ and $\omega L_k \ll 1/(\omega C_{gk})$, the input voltage $\mathbf{V}_{in}$ can be written as

$$\mathbf{V}_{in} = V_g + V_k = V_g + j\omega L_k g_m V_g \tag{9-1-1}$$

and the input current as

$$\mathbf{I}_{in} = j\omega C_{gk} V_g \tag{9-1-2}$$

Substitution of Eq. (9-1-2) in Eq. (9-1-1) yields

$$\mathbf{V}_{in} = \frac{\mathbf{I}_{in}(1 + j\omega L_k g_m)}{j\omega C_{gk}} \tag{9-1-3}$$

The input admittance of the tube is approximately

$$\mathbf{Y}_{in} = \frac{\mathbf{I}_{in}}{\mathbf{V}_{in}} = \frac{j\omega C_{gk}}{1 + j\omega L_k g_m} = \omega^2 L_k C_{gk} g_m + j\omega C_{gk} \tag{9-1-4}$$

in which $\omega L_k g_m \ll 1$ has been replaced. The inequality is almost always true, since the cathode lead is usually short and is quite large in diameter, and the transconductance g_m is generally much less than one millimho.

The input impedance at very high frequencies is given by

$$\mathbf{Z}_{in} = \frac{1}{\omega^2 L_k C_{gk} g_m} - j\frac{1}{\omega^3 L_k^2 C_{gk} g_m^2} \tag{9-1-5}$$

The real part of the impedance is inversely proportional to the square of the frequency, and the imaginary part is inversely proportional to the third order of the frequency. When the frequencies are above 1 GHz, the real part of the impedance becomes small enough to nearly short the signal source. Consequently, the output power is decreased rapidly. Similarly, the input admittance of a pentode circuit is expressed by

$$\mathbf{Y}_{in} = \omega^2 L_k C_{gk} g_m + j\omega (C_{gk} + C_{gs}) \tag{9-1-6}$$

where C_{gs} is the capacitance between the grid and screen, and its input impedance is given by

$$\mathbf{Z}_{in} = \frac{1}{\omega^2 L_k C_{gk} g_m} - j\frac{C_{gk} + C_{gs}}{\omega^3 L_k^2 C_{gk}^2 g_m^2} \tag{9-1-7}$$

There are several ways to minimize the inductance and capacitance effects, such as a reduction in lead length and electrode area. This minimization, however, also limits the power-handling capacity.

9-1-2 Transit-Angle Effects

Another limitation in the application of conventional tubes at microwave frequencies is the electron transit angle between electrodes. The electron transit angle is defined as

$$\theta_g \equiv \omega\tau_g = \frac{\omega d}{v_0} \tag{9-1-8}$$

where $\tau_g = d/v_0$ is the transit time across the gap
d = separation between cathode and grid
$v_0 = 0.593 \times 10^6\sqrt{V_0}$ is the velocity of the electron
V_0 = dc voltage

When frequencies are below microwave range, the transit angle is negligible. At microwave frequencies, however, the transit time (or angle) is large compared to the period of the microwave signal, and the potential between the cathode and the grid may alternate from 10 to 100 times during the electron transit. The grid potential during the negative half cycle thus removes energy that was given to the electron during the positive half cycle. Consequently, the electrons may oscillate back and forth in the cathode-grid space or return to the cathode. The overall result of transit-angle effects is to reduce the operating efficiency of the vacuum tube. The degenerate effect becomes more serious when frequencies are well above 1 GHz. Once electrons pass the grid, they are quickly accelerated to the anode by the high plate voltage.

When the frequency is below 1 GHz, the output delay is negligible in comparison with the phase of the grid voltage. This means that the transadmittance is a large real quantity, which is the usual transconductance g_m. At microwave frequencies the transit angle is not negligible, and the transadmittance becomes a complex number with a relatively small magnitude. This situation indicates that the output is decreased.

From the preceding analysis it is clear that the transit-angle effect can be minimized by first accelerating the electron beam with a very high dc voltage and then velocity-modulating it. This is indeed the principal operation of such microwave tubes as klystrons and magnetrons.

9-1-3 Gain-Bandwidth Product Limitation

In ordinary vacuum tubes the maximum gain is generally achieved by resonating the output circuit as shown in Fig. 9-1-2. In the equivalent circuit (see Fig. 9-1-2) it is assumed that $r_p \gg \omega L_k$. The load voltage is given by

$$\mathbf{V}_\ell = \frac{g_m V_g}{G + j[\omega C - 1/(\omega L)]} \tag{9-1-9}$$

where $G = 1/r_p + 1/R$
r_p = plate resistance
R = load resistance
L, C = tuning elements

The resonant frequency is expressed by

$$f_r = \frac{1}{2\pi\sqrt{LC}} \tag{9-1-10}$$

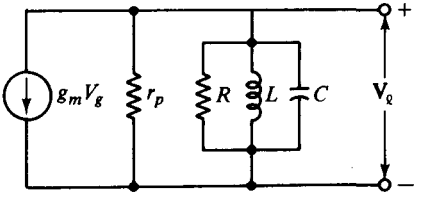

Figure 9-1-2 Output-tuned circuit of a pentode.

and the maximum voltage gain A_{max} at resonance by

$$A_{max} = \frac{g_m}{G} \tag{9-1-11}$$

Since the bandwidth is measured at the half-power point, the denominator of Eq. (9-1-9) must be related by

$$G = \omega C - \frac{1}{\omega L} \tag{9-1-12}$$

The roots of this quadratic equation are given by

$$\omega_1 = \frac{G}{2C} - \sqrt{\left(\frac{G}{2C}\right)^2 + \frac{1}{LC}} \tag{9-1-13}$$

$$\omega_2 = \frac{G}{2C} + \sqrt{\left(\frac{G}{2C}\right)^2 + \frac{1}{LC}} \tag{9-1-14}$$

Then the bandwidth can be expressed by

$$\text{BW} = \omega_2 - \omega_1 = \frac{G}{C} \qquad \text{for } \left(\frac{G}{2C}\right)^2 \gg \frac{1}{LC} \tag{9-1-15}$$

Hence the gain-bandwidth product of the circuit of Fig. 9-1-2 is

$$A_m(\text{BW}) = \frac{g_m}{C} \tag{9-1-16}$$

It is important to note that the gain-bandwidth product is independent of frequency. For a given tube, a higher gain can be achieved only at the expense of a narrower bandwidth. This restriction is applicable to a resonant circuit only. In microwave devices either reentrant cavities or slow-wave structures are used to obtain a possible overall high gain over a broad bandwidth.

9-2 KLYSTRONS

The two-cavity klystron is a widely used microwave amplifier operated by the principles of velocity and current modulation. All electrons injected from the cathode arrive at the first cavity with uniform velocity. Those electrons passing the first cavity gap at zeros of the gap voltage (or signal voltage) pass through with unchanged velocity; those passing through the positive half cycles of the gap voltage undergo an increase in velocity; those passing through the negative swings of the gap voltage undergo a decrease in velocity. As a result of these actions, the electrons gradually bunch together as they travel down the drift space. The variation in electron velocity in the drift space is known as *velocity modulation*. The density of the electrons in the second cavity gap varies cyclically with time. The electron beam contains an ac component and is said to be current-modulated. The maximum bunching should occur approximately midway between the second cavity grids during its retarding

phase; thus the kinetic energy is transferred from the electrons to the field of the second cavity. The electrons then emerge from the second cavity with reduced velocity and finally terminate at the collector. The charateristics of a two-cavity klystron amplifier are as follows:

1. Efficiency: about 40%.
2. Power output: average power (CW power) is up to 500 kW and pulsed power is up to 30 MW at 10 GHz.
3. Power gain: about 30 dB.

Figure 9-2-1 shows the present state of the art for U.S. high-power klystrons. Figure 9-2-2 shows the schematic diagram of a two-cavity klystron amplifier. The cavity close to the cathode is known as the *buncher cavity* or input cavity, which velocity-modulates the electron beam. The other cavity is called the *catcher cavity* or output cavity; it catches energy from the bunched electron beam. The beam then passes through the catcher cavity and is terminated at the collector. The quantitative analysis of a two-cavity klystron can be described in four parts under the following assumptions:

1. The electron beam is assumed to have a uniform density in the cross section of the beam.
2. Space-charge effects are negligible.
3. The magnitude of the microwave signal input is assumed to be much smaller than the dc accelerating voltage.

9-2-1 Reentrant Cavities

At a frequency well below the microwave range, the cavity resonator can be represented by a lumped-constant resonant circuit. When the operating frequency is increased to several tens of megahertz, both the inductance and the capacitance must be reduced to a minimum in order to maintain resonance at the operating frequency. Ultimately the inductance is reduced to a minimum by short wire. Therefore the reentrant cavities are designed for use in klystrons and microwave triodes. A reentrant cavity is one in which the metallic boundaries extend into the interior of the cavity. Several types of reentrant cavities are shown in Fig. 9-2-3. One of the commonly used reentrant cavities is the coaxial cavity shown in Fig. 9-2-4.

It is clear from Fig. 9-2-4 that not only has the inductance been considerably decreased but the resistance losses are markedly reduced as well, and the shelf-shielding enclosure prevents radiation losses. It is difficult to calculate the resonant frequency of the coaxial cavity. An approximation can be made, however, using transmission-line theory. The characteristic impedance of the coaxial line is given by

$$Z_0 = \frac{1}{2\pi}\sqrt{\frac{\mu}{\epsilon}}\,\ell n\frac{b}{a} \quad \text{ohms} \tag{9-2-1}$$

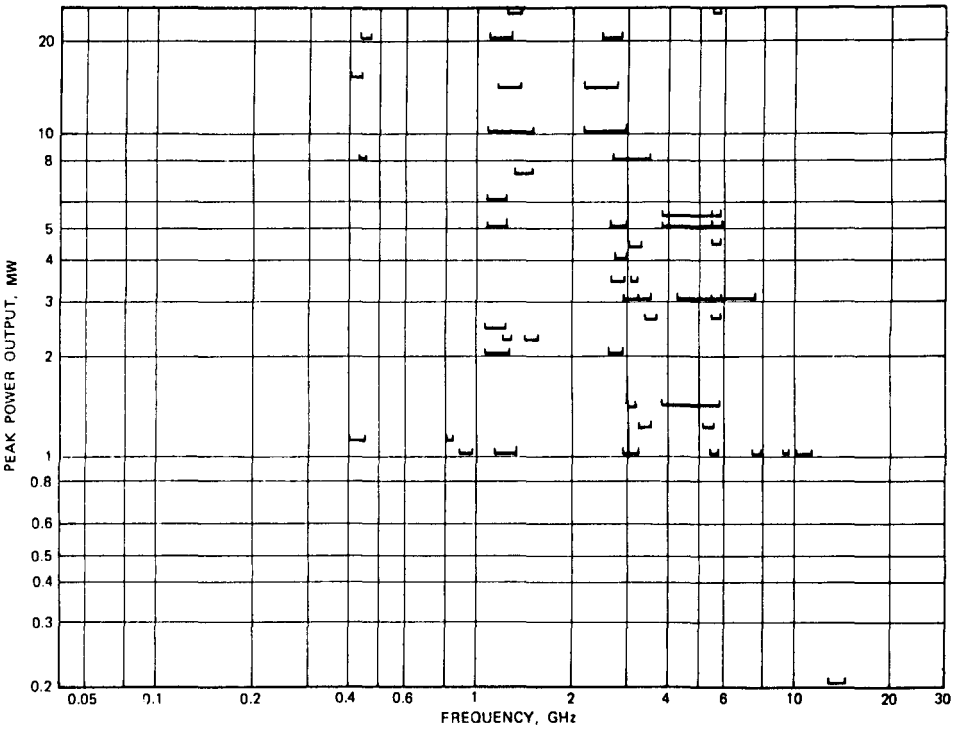

Figure 9-2-1 State of the art for U.S. high-power klystrons.

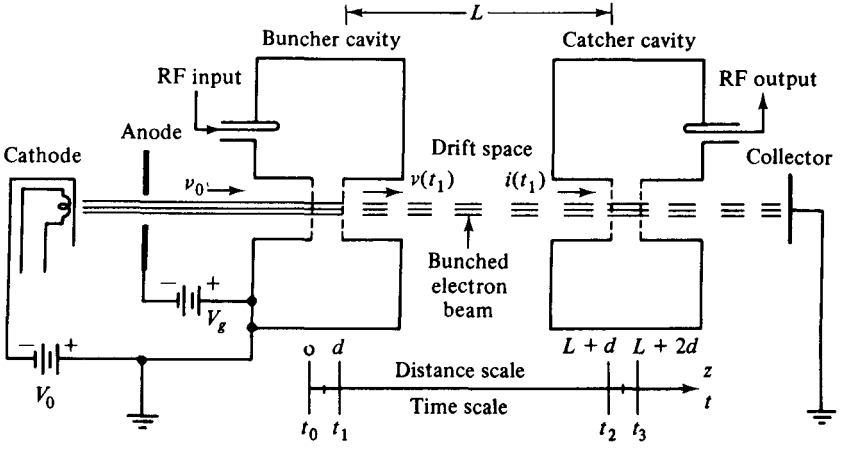

Figure 9-2-2 Two-cavity klystron amplifier.

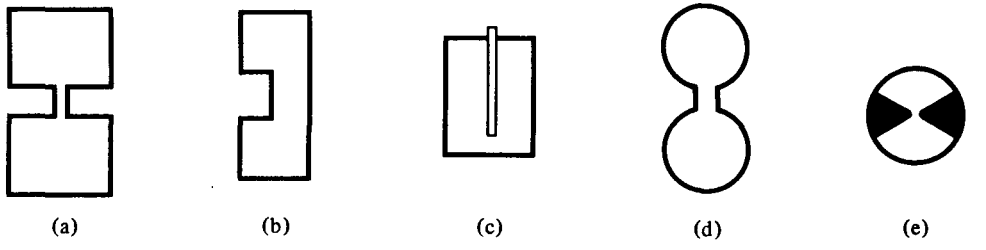

Figure 9-2-3 Reentrant cavities. (a) Coaxial cavity. (b) Radial cavity. (c) Tunable cavity. (d) Toroidal cavity. (e) Butterfly cavity.

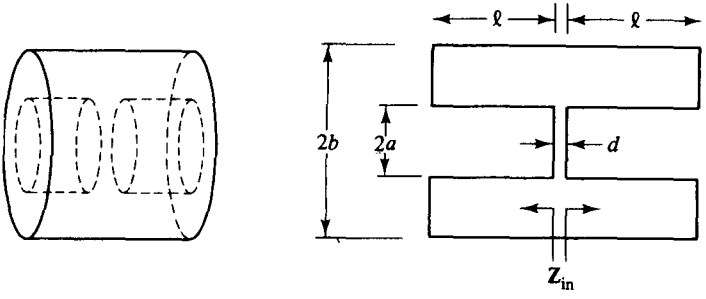

(a) Coaxial cavity

(b) Cross-section of coaxial cavity

Figure 9-2-4 Coaxial cavity and its equivalent.

The coaxial cavity is similar to a coaxial line shorted at two ends and joined at the center by a capacitor. The input impedance to each shorted coaxial line is given by

$$Z_{in} = jZ_0 \tan(\beta \ell) \tag{9-2-2}$$

where ℓ is the length of the coaxial line.

Substitution of Eq. (9-2-1) in (9-2-2) results in

$$Z_{in} = j\frac{1}{2\pi}\sqrt{\frac{\mu}{\epsilon}}\,\ell n\frac{b}{a}\tan(\beta \ell) \tag{9-2-3}$$

The inductance of the cavity is given by

$$L = \frac{2X_{in}}{\omega} = \frac{1}{\pi\omega}\sqrt{\frac{\mu}{\epsilon}}\,\ell n\frac{b}{a}\tan(\beta \ell) \tag{9-2-4}$$

and the capacitance of the gap by

$$C_g = \frac{\epsilon\pi a^2}{d} \tag{9-2-5}$$

At resonance the inductive reactance of the two shorted coaxial lines in series is equal in magnitude to the capacitive reactance of the gap. That is, $\omega L = 1/(\omega C_g)$. Thus

$$\tan(\beta \ell) = \frac{dv}{\omega a^2 \ell n(b/a)} \tag{9-2-6}$$

where $v = 1/\sqrt{\mu\epsilon}$ is the phase velocity in any medium.

The solution to this equation gives the resonant frequency of a coaxial cavity. Since Eq. (9-2-6) contains the tangent function, it has an infinite number of solutions with larger values of frequency. Therefore this type of reentrant cavity can support an infinite number of resonant frequencies or modes of oscillation. It can be shown that a shorted coaxial-line cavity stores more magnetic energy than electric energy. The balance of the electric stored energy appears in the gap, for at resonance the magnetic and electric stored energies are equal.

The radial reentrant cavity shown in Fig. 9-2-5 is another commonly used reentrant resonator. The inductance and capacitance of a radial reentrant cavity is expressed by

$$L = \frac{\mu \ell}{2\pi} \ell n \frac{b}{a} \tag{9-2-7}$$

$$C = \epsilon_0 \left[\frac{\pi a^2}{d} - 4a \ell n \frac{0.765}{\sqrt{\ell^2 + (b-a)^2}} \right] \tag{9-2-8}$$

The resonant frequency [1] is given by

$$f_r = \frac{c}{2\pi \sqrt{\epsilon_r}} \left\{ a\ell \left[\frac{a}{2d} - \frac{2}{\ell} \ell n \frac{0.765}{\sqrt{\ell^2 + (b-a)^2}} \right] \ell n \frac{b}{a} \right\}^{-1/2} \tag{9-2-9}$$

where $c = 3 \times 10^8$ m/s is the velocity of light in a vacuum.

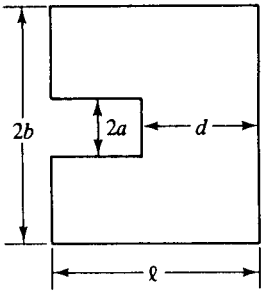

Figure 9-2-5 Radial reentrant cavity.

9-2-2 Velocity-Modulation Process

When electrons are first accelerated by the high dc voltage V_0 before entering the buncher grids, their velocity is uniform:

$$v_0 = \sqrt{\frac{2eV_0}{m}} = 0.593 \times 10^6 \sqrt{V_0} \quad \text{m/s} \tag{9-2-10}$$

In Eq. (9-2-10) it is assumed that electrons leave the cathode with zero velocity. When a microwave signal is applied to the input terminal, the gap voltage between the buncher grids appears as

$$V_s = V_1 \sin(\omega t) \tag{9-2-11}$$

where V_1 is the amplitude of the signal and $V_1 \ll V_0$ is assumed.

In order to find the modulated velocity in the buncher cavity in terms of either the entering time t_0 or the exiting time t_1 and the gap transit angle θ_g as shown in Fig. 9-2-2 it is necessary to determine the average microwave voltage in the buncher gap as indicated in Fig. 9-2-6.

Since $V_1 \ll V_0$, the average transit time through the buncher gap distance d is

$$\tau \approx \frac{d}{v_0} = t_1 - t_0 \tag{9-2-12}$$

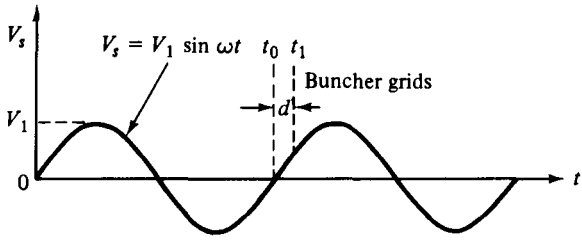

Figure 9-2-6 Signal voltage in the buncher gap.

The average gap transit angle can be expressed as

$$\theta_g = \omega\tau = \omega(t_1 - t_0) = \frac{\omega d}{v_0} \tag{9-2-13}$$

The average microwave voltage in the buncher gap can be found in the following way:

$$\langle V_s \rangle = \frac{1}{\tau}\int_{t_0}^{t_1} V_1 \sin(\omega t)dt = -\frac{V_1}{\omega\tau}[\cos(\omega t_1) - \cos(\omega t_0)]$$
$$= \frac{V_1}{\omega\tau}\left[\cos(\omega t_0) - \cos\left(\omega_0 + \frac{\omega d}{v_0}\right)\right] \tag{9-2-14}$$

Let

$$\omega t_0 + \frac{\omega d}{2v_0} = \omega t_0 + \frac{\theta_g}{2} = A$$

and

$$\frac{\omega d}{2v_0} = \frac{\theta_g}{2} = B$$

Then using the trigonometric identity that $\cos(A - B) - \cos(A + B) = 2 \sin A \sin B$, Eq. (9-2-14) becomes

$$\langle V_s \rangle = V_1 \frac{\sin[\omega d/2v_0)]}{\omega d/(2v_0)} \sin\left(\omega t_0 + \frac{\omega d}{2v_0}\right) = V_1 \frac{\sin(\theta_g/2)}{\theta_g/2} \sin\left(\omega t_0 + \frac{\theta_g}{2}\right) \tag{9-2-15}$$

It is defined as

$$\beta_i \equiv \frac{\sin[\omega d/(2v_0)]}{\omega d/(2v_0)} = \frac{\sin(\theta_g/2)}{\theta_g/2} \tag{9-2-16}$$

Note that β_i is known as the *beam-coupling coefficient* of the input cavity gap (see Fig. 9-2-7).

It can be seen that increasing the gap transit angle θ_g decreases the coupling between the electron beam and the buncher cavity; that is, the velocity modulation

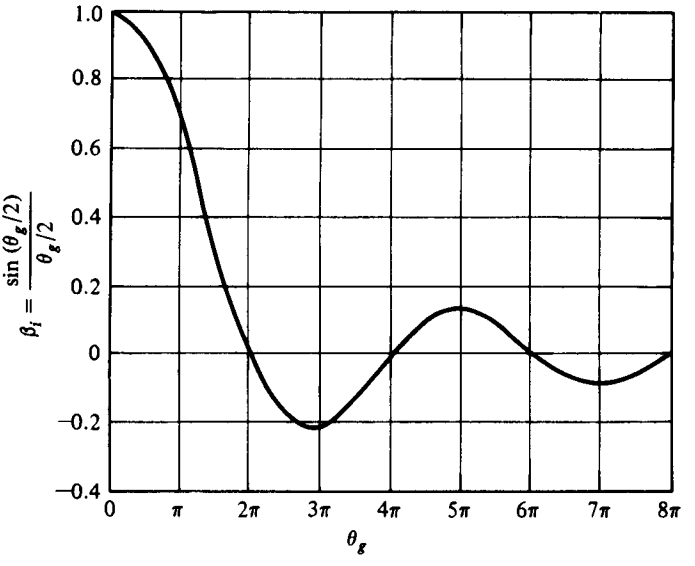

Figure 9-2-7 Beam-coupling coefficient versus gap transit angle.

of the beam for a given microwave signal is decreased. Immediately after velocity modulation, the exit velocity from the buncher gap is given by

$$v(t_1) = \sqrt{\frac{2e}{m}\left[V_0 + \beta_i V_1 \sin\left(\omega t_0 + \frac{\theta_g}{2}\right)\right]}$$
$$= \sqrt{\frac{2e}{m} V_0\left[1 + \frac{\beta_i V_1}{V_0} \sin\left(\omega t_0 + \frac{\theta_g}{2}\right)\right]} \tag{9-2-17}$$

where the factor $\beta_i V_1/V_0$ is called the *depth of velocity modulation.*

Using binomial expansion under the assumption of

$$\beta_i V_1 \ll V_0 \tag{9-2-18}$$

Eq. (9-2-17) becomes

$$v(t_1) = v_0\left[1 + \frac{\beta_i V_1}{2V_0} \sin\left(\omega t_0 + \frac{\theta_g}{2}\right)\right] \tag{9-2-19}$$

Equation (9-2-19) is the equation of velocity modulation. Alternatively, the equation of velocity modulation can be given by

$$v(t_1) = v_0\left[1 + \frac{\beta_i V_1}{2V_0} \sin\left(\omega t_1 - \frac{\theta_g}{2}\right)\right] \tag{9-2-20}$$

9-2-3 Bunching Process

Once the electrons leave the buncher cavity, they drift with a velocity given by Eq. (9-2-19) or (9-2-20) along in the field-free space between the two cavities. The effect of velocity modulation produces bunching of the electron beam—or current modulation. The electrons that pass the buncher at $V_s = 0$ travel through with unchanged velocity v_0 and become the bunching center. Those electrons that pass the buncher cavity during the positive half cycles of the microwave input voltage V_s travel faster than the electrons that passed the gap when $V_s = 0$. Those electrons that pass the buncher cavity during the negative half cycles of the voltage V_s travel slower than the electrons that passed the gap when $V_s = 0$. At a distance of ΔL along the beam from the buncher cavity, the beam electrons have drifted into dense clusters. Figure 9-2-8 shows the trajectories of minimum, zero, and maximum electron acceleration.

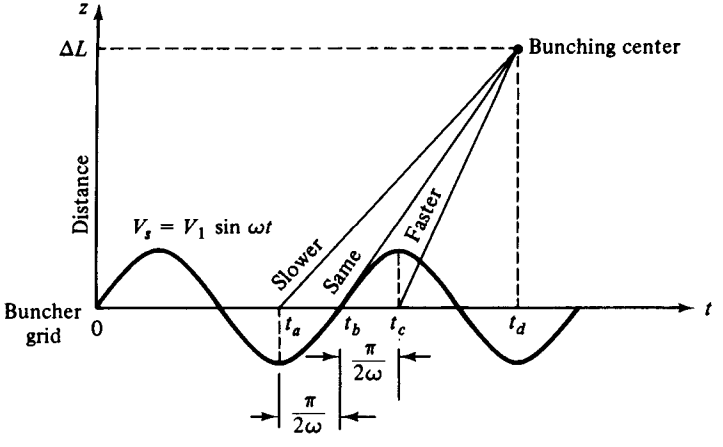

Figure 9-2-8 Bunching distance.

The distance from the buncher grid to the location of dense electron bunching for the electron at t_b is

$$\Delta L = v_0(t_d - t_b) \tag{9-2-21}$$

Similarly, the distances for the electrons at t_a and t_c are

$$\Delta L = v_{\min}(t_d - t_a) = v_{\min}\left(t_d - t_b + \frac{\pi}{2\omega}\right) \tag{9-2-22}$$

$$\Delta L = v_{\max}(t_d - t_c) = v_{\max}\left(t_d - t_b - \frac{\pi}{2\omega}\right) \tag{9-2-23}$$

From Eq. (9-2-19) or (9-2-20) the minimum and maximum velocities are

$$v_{\min} = v_0\left(1 - \frac{\beta_i V_1}{2V_0}\right) \tag{9-2-24}$$

$$v_{\max} = v_0\left(1 + \frac{\beta_i V_1}{2V_0}\right) \tag{9-2-25}$$

Substitution of Eqs. (9-2-24) and (9-2-25) in Eqs. (9-2-22) and (9-2-23), respectively, yields the distance

$$\Delta L = v_0(t_d - t_b) + \left[v_0\frac{\pi}{2\omega} - v_0\frac{\beta_i V_1}{2V_0}(t_d - t_b) - v_0\frac{\beta_i V_1}{2V_0}\frac{\pi}{2\omega}\right] \tag{9-2-26}$$

and

$$\Delta L = v_0(t_d - t_b) + \left[-v_0\frac{\pi}{2\omega} + v_0\frac{\beta_i V_1}{2V_0}(t_d - t_b) + v_0\frac{\beta_i V_1}{2V_0}\frac{\pi}{2\omega}\right] \tag{9-2-27}$$

The necessary condition for those electrons at t_a, t_b, and t_c to meet at the same distance ΔL is

$$v_0\frac{\pi}{2\omega} - v_0\frac{\beta_i V_1}{2V_0}(t_d - t_b) - v_0\frac{\beta_i V_1}{2V_0}\frac{\pi}{2\omega} = 0 \tag{9-2-28}$$

and

$$-v_0\frac{\pi}{2\omega} + v_0\frac{\beta_i V_1}{2V_0}(t_d - t_b) + v_0\frac{\beta_i V_1}{2V_0}\frac{\pi}{2\omega} = 0 \tag{9-2-29}$$

Consequently,

$$t_d - t_b \approx \frac{\pi V_0}{\omega\beta_i V_1} \tag{9-2-30}$$

and

$$\Delta L = v_0\frac{\pi V_0}{\omega\beta_i V_1} \tag{9-2-31}$$

It should be noted that the mutual repulsion of the space charge is neglected, but the qualitative results are similar to the preceding representation when the effects of repulsion are included. Furthermore, the distance given by Eq. (9-2-31) is not the one for a maximum degree of bunching. Figure 9-2-9 shows the distance-time plot or Applegate diagram.

What should the spacing be between the buncher and catcher cavities in order to achieve a maximum degree of bunching? Since the drift region is field free, the transit time for an electron to travel a distance of L as shown in Fig. 9-2-2 is given by

$$T = t_2 - t_1 = \frac{L}{v(t_1)} = T_0\left[1 - \frac{\beta_i V_1}{2V_0}\sin\left(\omega t_1 - \frac{\theta_g}{2}\right)\right] \tag{9-2-32}$$

where the binomial expansion of $(1 + x)^{-1}$ for $|x| \ll 1$ has been replaced and $T_0 = L/v_0$ is the dc transit time. In terms of radians the preceding expression can be written

$$\omega T = \omega t_2 - \omega t_1 = \theta_0 - X\sin\left(\omega t_1 - \frac{\theta_g}{2}\right) \tag{9-2-33}$$

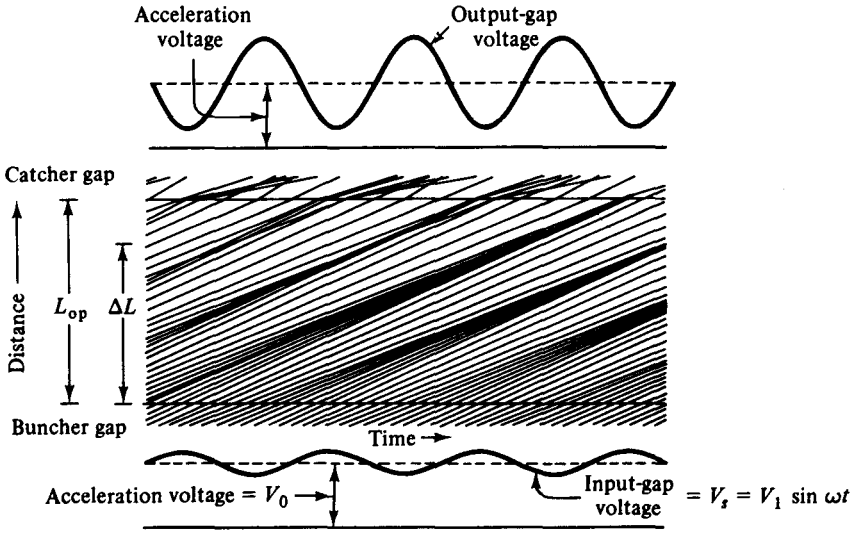

Figure 9-2-9 Applegate diagram.

where

$$\theta_0 = \frac{\omega L}{v_0} = 2\pi N \tag{9-2-34}$$

is the dc transit angle between cavities, N is the number of electron transit cycles in the drift space, and

$$X \equiv \frac{\beta_i V_1}{2V_0}\theta_0 \tag{9-2-35}$$

is defined as the *bunching parameter* of a klystron.

At the buncher gap a charge dQ_0 passing through at a time interval dt_0 is given by

$$dQ_0 = I_0 dt_0 \tag{9-2-36}$$

where I_0 is the dc current. From the principle of conservation of charges this same amount of charge dQ_0 also passes the catcher at a later time interval dt_2. Hence

$$I_0|dt_0| = i_2|dt_2| \tag{9-2-37}$$

where the absolute value signs are necessary because a negative value of the time ratio would indicate a negative current. Current i_2 is the current at the catcher gap. Rewriting Eq. (9-2-32) in terms of Eq. (9-2-19) yields

$$t_2 = t_0 + \tau + T_0\left[1 - \frac{\beta_i V_1}{2V_0}\sin\left(\omega t_0 + \frac{\theta_g}{2}\right)\right] \tag{9-2-38}$$

Alternatively,

$$\omega t_2 - \left(\theta_0 + \frac{\theta_g}{2}\right) = \left(\omega t_0 + \frac{\theta_g}{2}\right) - X\sin\left(\omega t_0 + \frac{\theta_g}{2}\right) \tag{9-2-39}$$

where $(\omega t_0 + \theta_g/2)$ is the buncher cavity departure angle and $\omega t_2 - (\theta_0 + \theta_g/2)$ is the catcher cavity arrival angle. Figure 9-2-10 shows the curves for the catcher cav-

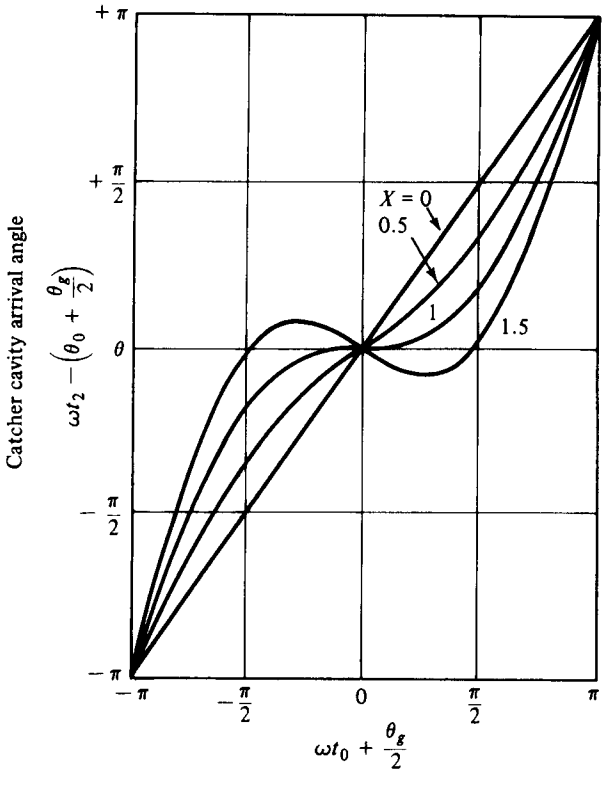

Figure 9-2-10 Catcher arrival angle versus buncher departure angle.

ity arrival angle as a function of the buncher cavity departure angle in terms of the bunching parameter X.

Differentiation of Eq. (9-2-38) with respect to t_0 results in

$$dt_2 = dt_0\left[1 - X\cos\left(\omega t_0 + \frac{\theta_g}{2}\right)\right] \tag{9-2-40}$$

The current arriving at the catcher cavity is then given as

$$i_2(t_0) = \frac{I_0}{1 - X\cos\left(\omega t_0 + \theta_g/2\right)} \tag{9-2-41}$$

In terms of t_2 the current is

$$i_2(t_2) = \frac{I_0}{1 - X\cos\left(\omega t_2 - \theta_0 - \theta_g/2\right)} \tag{9-2-42}$$

In Eq. (9-2-42) the relationsip of $t_2 = t_0 + \tau + T_0$ is used—namely, $\omega t_2 = \omega t_0 + \omega\tau + \omega T_0 = \omega t_0 + \theta_g + \theta_0$. Figure 9-2-11 shows curves of the beam current $i_2(t_2)$ as a function of the catcher arrival angle in terms of the bunching parameter X.

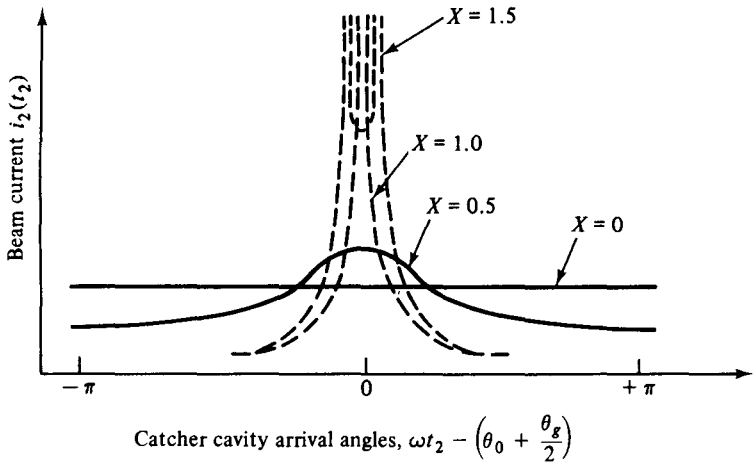

Figure 9-2-11 Beam current i_2 versus catcher cavity arrival angle.

The beam current at the catcher cavity is a periodic waveform of period $2\pi/\omega$ about dc current. Therefore the current i_2 can be expanded in a Fourier series and so

$$i_2 = a_0 + \sum_{n=1}^{\infty} [a_n \cos(n\omega t_2) + b_n \sin(n\omega t_2)] \tag{9-2-43}$$

where n is an integer, excluding zero. The series coefficients a_0, a_n, and b_n in Eq. (9-2-43) are given by the integrals

$$\begin{aligned} a_0 &= \frac{1}{2\pi}\int_{-\pi}^{\pi} i_2\, d(\omega t_2) \\ a_n &= \frac{1}{\pi}\int_{-\pi}^{\pi} \cos(n\omega t_2)\, d(\omega t_2) \\ b_n &= \frac{1}{\pi}\int_{-\pi}^{\pi} i_2 \sin(\mathrm{n}\omega \mathrm{t}_2)\, d(\omega t_2) \end{aligned} \tag{9-2-44}$$

Substitution of Eqs. (9-2-37) and (9-2-39) in Eq. (9-2-44) yields

$$a_0 = \frac{1}{2\pi}\int_{-\pi}^{\pi} I_0\, d(\omega t_0) = I_0 \tag{9-2-45}$$

$$a_n = \frac{1}{\pi}\int_{-\pi}^{\pi} I_0 \cos\left[(n\omega t_0 + n\theta_g + n\theta_0) + nX \sin\left(\omega t_0 + \frac{\theta_g}{2}\right)\right] d(\omega t_0) \tag{9-2-46}$$

$$b_n = \frac{1}{\pi}\int_{-\pi}^{\pi} I_0 \sin\left[(n\omega t_0 + n\theta_g + n\theta_0) + nX \sin\left(\omega t_0 + \frac{\theta_g}{2}\right)\right] d(\omega t_0) \tag{9-2-47}$$

By using the trigonometric functions

$$\cos(A \pm B) = \cos A \cos B \mp \sin A \sin B$$

and

$$\sin(A \pm B) = \sin A \cos B \pm \cos A \sin B$$

the two integrals shown in Eqs. (9-2-40) and (9-2-41) involve cosines and sines of a sine function. Each term of the integrand contains an infinite number of terms of Bessel functions. These are

$$\cos\left[nX\sin\left(\omega t_0+\frac{\theta_g}{2}\right)\right]=2J_0(nX)+2\left[J_2(nX)\cos 2\left(\omega t_0+\frac{\theta_g}{2}\right)\right]+2\left[J_4(nX)\cos 4\left(\omega t_0+\frac{\theta_g}{2}\right)\right]+\cdots \tag{9-2-48}$$

and

$$\sin\left[nX\sin\left(\omega t_0+\frac{\theta_g}{2}\right)\right]=2\left[J_1(nX)\sin\left(\omega t_0+\frac{\theta_g}{2}\right)\right]+2\left[J_3(nX)\sin 3\left(\omega t_0+\frac{\theta_g}{2}\right)\right]+\cdots \tag{9-2-49}$$

If these series are substituted into the integrands of Eqs. (9-2-46) and (9-2-47), respectively, the integrals are readily evaluated term by term and the series coefficients are

$$a_n=2I_0J_n(nX)\cos(n\theta_g+n\theta_0) \tag{9-2-50}$$

$$b_n=2I_0J_n(nX)\sin(n\theta_g+n\theta_0) \tag{9-2-51}$$

where $J_n(nX)$ is the nth-order Bessel function of the first kind (see Fig. 9-2-12).

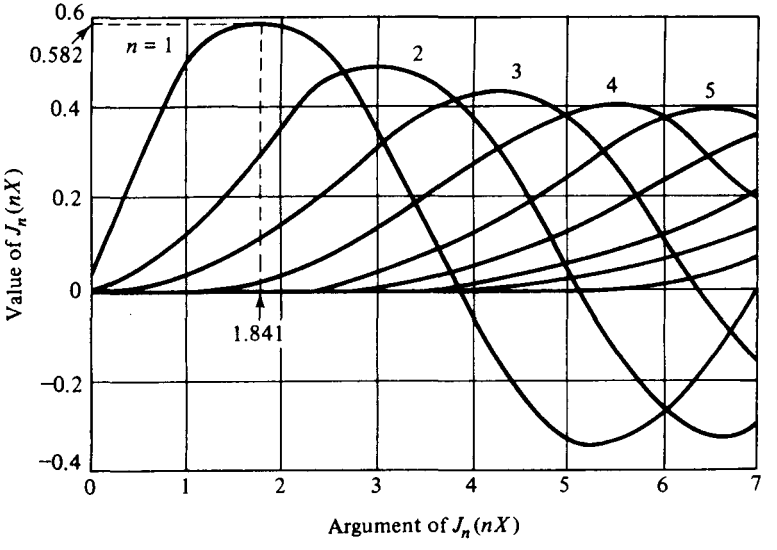

Figure 9-2-12 Bessel functions $J_n(nX)$.

Substitution of Eqs. (9-2-45), (9-2-50), and (9-2-51) in Eq. (9-2-43) yields the beam current i_2 as

$$i_2 = I_0 + \sum_{n=1}^{\infty} 2I_0 J_n(nX) \cos[n\omega(t_2 - \tau - T_0)] \tag{9-2-52}$$

The fundamental component of the beam current at the catcher cavity has a magnitude

$$I_f = 2I_0 J_1(X) \tag{9-2-53}$$

This fundamental component I_f has its maximum amplitude at

$$X = 1.841 \tag{9-2-54}$$

The optimum distance L at which the maximum fundamental component of current occurs is computed from Eqs. (9-2-34), (9-2-35), and (9-2-54) as

$$L_{\text{optimum}} = \frac{3.682 v_0 V_0}{\omega \beta_i V_1} \tag{9-2-55}$$

It is interesting to note that the distance given by Eq. (9-2-31) is approximately 15% less than the result of Eq. (9-2-55). The discrepancy is due in part to the approximations made in deriving Eq. (9-2-31) and to the fact that the maximum fundamental component of current will not coincide with the maximun electron density along the beam because the harmonic components exist in the beam.

9-2-4 Output Power and Beam Loading

The maximum bunching should occur approximately midway between the catcher grids. The phase of the catcher gap voltage must be maintained in such a way that the bunched electrons, as they pass through the grids, encounter a retarding phase. When the bunched electron beam passes through the retarding phase, its kinetic energy is transferred to the field of the catcher cavity. When the electrons emerge from the catcher grids, they have reduced velocity and are finally collected by the collector.

The induced current in the catcher cavity. Since the current induced by the electron beam in the walls of the catcher cavity is directly proportional to the amplitude of the microwave input voltage V_1, the fundamental component of the induced microwave current in the catcher is given by

$$i_{2\text{ind}} = \beta_0 i_2 = \beta_0 2I_0 J_1(X) \cos[\omega(t_2 - \tau - T_0)] \tag{9-2-56}$$

where β_0 is the beam coupling coefficient of the catcher gap. If the buncher and catcher cavities are identical, then $\beta_i = \beta_0$. The fundamental component of current induced in the catcher cavity then has a magnitude

$$I_{2\text{ind}} = \beta_0 I_2 = \beta_0 2I_0 J_1(X) \tag{9-2-57}$$

Figure 9-2-13 shows an output equivalent circuit in which R_{sho} represents the wall resistance of catcher cavity, R_B the beam loading resistance, R_L the external load resistance, and R_{sh} the effective shunt resistance.

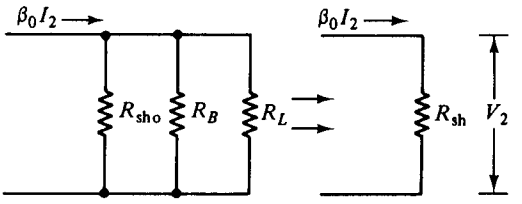

Figure 9-2-13 Output equivalent circuit.

The output power delivered to the catcher cavity and the load is given as

$$P_{out} = \frac{(\beta_0 I_2)^2}{2} R_{sh} = \frac{\beta_0 I_2 V_2}{2} \tag{9-2-58}$$

where R_{sh} is the total equivalent shunt resistance of the catcher circuit, including the load, and V_2 is the fundamental component of the catcher gap voltage.

Efficiency of klystron. The electronic efficiency of the klystron amplifier is defined as the ratio of the output power to the input power:

$$\text{Efficiency} \equiv \frac{P_{out}}{P_{in}} = \frac{\beta_0 I_2 V_2}{2 I_0 V_0} \tag{9-2-59}$$

in which the power losses to the beam loading and cavity walls are included.

If the coupling is perfect, $\beta_0 = 1$, the maximum beam current approaches $I_{2max} = 2I_0(0.582)$, and the voltage V_2 is equal to V_0. Then the maximum electronic efficiency is about 58%. In practice, the electronic efficiency of a klystron amplifier is in the range of 15 to 30%. Since the efficiency is a function of the catcher gap transit angle θ_g, Fig. 9-2-14 shows the maximum efficiency of a klystron as a function of catcher transit angle.

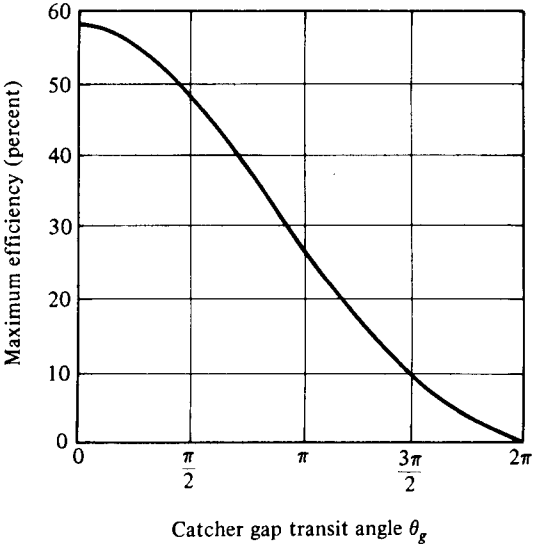

Figure 9-2-14 Maximum efficiency of klystron versus transit angle.

Mutual conductance of a klystron amplifier. The equivalent mutual conductance of the klystron amplifier can be defined as the ratio of the induced output current to input voltage. That is

$$|G_m| \equiv \frac{i_{2\,\text{ind}}}{V_1} = \frac{2\beta_0 I_0 J_1(X)}{V_1} \tag{9-2-60}$$

From Eq. (9-2-35) the input voltage V_1 can be expressed in terms of the bunching parameter X as

$$V_1 = \frac{2V_0}{\beta_0 \theta_0} X \tag{9-2-61}$$

In Eq. (9-2-61) it is assumed that $\beta_0 = \beta_i$. Substitution of Eq. (9-2-61) in Eq. (9-2-60) yields the normalized mutual conductance as

$$\frac{|G_m|}{G_0} = \beta_0^2 \theta_0 \frac{J_1(X)}{X} \tag{9-2-62}$$

where $G_0 = I_0/V_0$ is the dc beam conductance. The mutual conductance is not a constant but decreases as the bunching parameter X increases. Figure 9-2-15 shows the curves of normalized transconductance as a function of X.

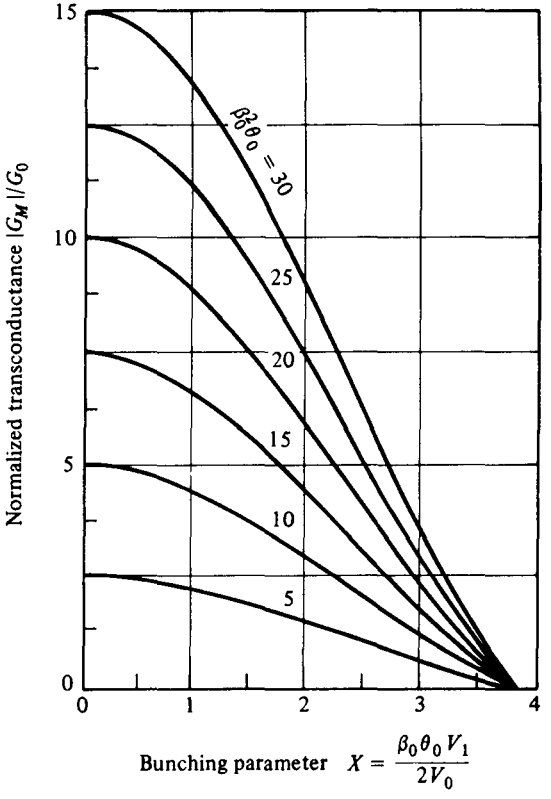

Figure 9-2-15 Normalized transconductance versus bunching parameter.

It can be seen from the curves that, for a small signal, the normalized transconductance is maximum. That is,

$$\frac{|G_m|}{G_0} = \frac{\beta_0^2 U_0}{2} \tag{9-2-63}$$

For a maximum output at $X = 1.841$, the normalized mutual conductance is

$$\frac{|G_m|}{G_0} = 0.316\beta_0^2\theta_0 \tag{9-2-64}$$

The voltage gain of a klystron amplifier is defined as

$$A_v \equiv \frac{|V_2|}{|V_1|} = \frac{\beta_0 I_2 R_{sh}}{V_1} = \frac{\beta_0^2\theta_0}{R_0}\frac{J_1(X)}{X}R_{sh} \tag{9-2-65}$$

where $R_0 = V_0/I_0$ is the dc beam resistance. Substitution of Eqs. (9-2-57) and (9-2-61) in Eq. (9-2-65) results in

$$A_v = G_m R_{sh} \tag{9-2-66}$$

Power required to bunch the electron beam. As described earlier, the bunching action takes place in the buncher cavity. When the buncher gap transit angle is small, the average energy of electrons leaving the buncher cavity over a cycle is nearly equal to the energy with which they enter. When the buncher gap transit angle is large, however, the electrons that leave the buncher gap have greater average energy than when they enter. The difference between the average exit energy and the entrance energy must be supplied by the buncher cavity to bunch the electron beam. It is difficult to calculate the power required to produce the bunching action. Feenberg did some extensive work on beam loading [6]. The ratio of the power required to produce bunching action over the dc power required to perform the electron beam is given by Feenberg as

$$\frac{P_B}{P_0} = \frac{V_1^2}{2V_0^2}\left[\frac{1}{2}\beta_i^2 - \frac{1}{2}\beta_i \cos\left(\frac{\theta_g}{2}\right)\right] = \frac{V_1^2}{2V_0^2}F(\theta_g) \tag{9-2-67}$$

where

$$F(\theta_g) = \frac{1}{2}\left[\beta_i^2 - \beta_i \cos\left(\frac{\theta_g}{2}\right)\right]$$

The dc power is

$$P_0 = V_0^2 G_0 \tag{9-2-68}$$

where $G_0 = I_0/V_0$ is the equivalent electron beam conductance. The power given by the buncher cavity to produce beam bunching is

$$P_B = \frac{V_1^2}{2}G_B \tag{9-2-69}$$

where G_B is the equivalent bunching conductance. Substitution of Eqs. (9-2-68) and (9-2-69) in Eq. (9-2-67) yields the normalized electronic conductance as

$$\frac{G_B}{G_0} = \frac{R_0}{R_B} = F(\theta_g) \tag{9-2-70}$$

Figure 9-2-16 shows the normalized electronic conductance as a function of the buncher gap transit angle. It can be seen that there is a critical buncher gap transit angle for a minimum equivalent bunching resistance. When the transit angle θ_g is 3.5 rad, the equivalent bunching resistance is about five times the electron beam resistance. The power delivered by the electron beam to the catcher cavity can be expressed as

$$\frac{V_2^2}{2R_{sh}} = \frac{V_2^2}{2R_{sho}} + \frac{V_2^2}{2R_B} + \frac{V_2^2}{2R_L} \tag{9-2-71}$$

As a result, the effective impedance of the catcher cavity is

$$\frac{1}{R_{sh}} = \frac{1}{R_{sho}} + \frac{1}{R_B} + \frac{1}{R_L} \tag{9-2-72}$$

Finally, the loaded quality factor of the catcher cavity circuit at the resonant frequency can be written

$$\frac{1}{Q_L} = \frac{1}{Q_0} + \frac{1}{Q_B} + \frac{1}{Q_{ext}} \tag{9-2-73}$$

where Q_L = loaded quality factor of the whole catcher circuit
Q_0 = quality factor of the catcher walls
Q_B = quality factor of the beam loading
Q_{ext} = quality factor of the external load

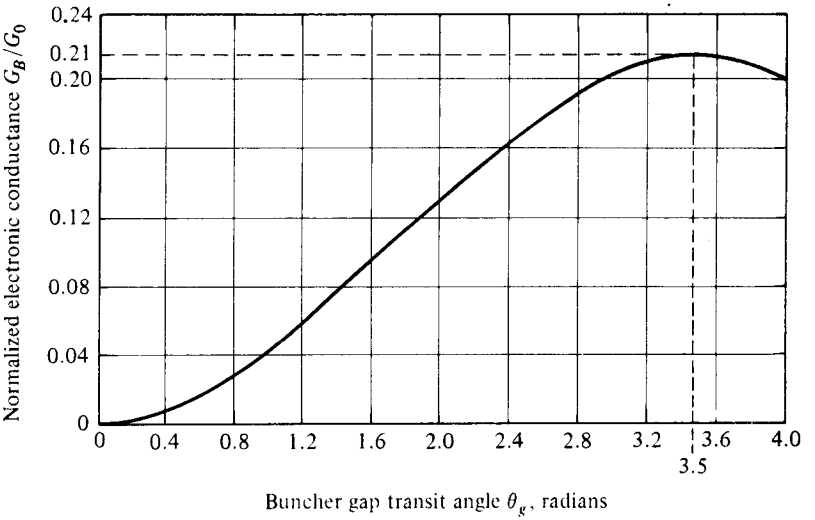

Figure 9-2-16 Normalized electronic conductance versus buncher gap transit angle.

Example 9-2-1: Klystron Amplifier

A two-cavity klystron amplifier has the following parameters:

$$V_0 = 1000 \text{ V} \qquad R_0 = 40 \text{ k}\Omega$$

$$I_0 = 25 \text{ mA} \qquad f = 3 \text{ GHz}$$

Gap spacing in either cavity: $d = 1$ mm
Spacing between the two cavities: $L = 4$ cm
Effective shunt impedance, excluding beam loading: $R_{sh} = 30 \text{ k}\Omega$

a. Find the input gap voltage to give maximum voltage V_2.
b. Find the voltage gain, neglecting the beam loading in the output cavity.
c. Find the efficiency of the amplifier, neglecting beam loading.
d. Calculate the beam loading conductance and show that neglecting it was justified in the preceding calculations.

Solution

a. For maximum V_2, $J_1(X)$ must be maximum. This means $J_1(X) = 0.582$ at $X = 1.841$. The electron velocity just leaving the cathode is

$$v_0 = (0.593 \times 10^6)\sqrt{V_0} = (0.593 \times 10^6)\sqrt{10^3} = 1.88 \times 10^7 \text{ m/s}$$

The gap transit angle is

$$\theta_g = \omega\frac{d}{v_0} = 2\pi(3 \times 10^9)\frac{10^{-3}}{1.88 \times 10^7} = 1 \text{ rad}$$

The beam-coupling coefficient is

$$\beta_i = \beta_0 = \frac{\sin(\theta_g/2)}{\theta_g/2} = \frac{\sin(1/2)}{1/2} = 0.952$$

The dc transit angle between the cavities is

$$\theta_0 = \omega T_0 = \omega\frac{L}{v_0} = 2\pi(3 \times 10^9)\frac{4 \times 10^{-2}}{1.88 \times 10^7} = 40 \text{ rad}$$

The maximum input voltage V_1 is then given by

$$V_{1\,max} = \frac{2V_0X}{\beta_i\theta_0} = \frac{2(10^3)(1.841)}{(0.952)(40)} = 96.5 \text{ V}$$

b. The voltage gain is found as

$$A_v = \frac{\beta_0^2\theta_0}{R_0}\frac{J_1(X)}{X}R_{sh} = \frac{(0.952)^2(40)(0.582)(30 \times 10^3)}{4 \times 10^4 \times 1.841} = 8.595$$

c. The efficiency can be found as follows:

$$I_2 = 2I_0J_1(X) = 2 \times 25 \times 10^{-3} \times 0.582 = 29.1 \times 10^{-3} \text{ A}$$

$$V_2 = \beta_0I_2R_{sh} = (0.952)(29.1 \times 10^{-3})(30 \times 10^3) = 831 \text{ V}$$

$$\text{Efficiency} = \frac{\beta_0I_2V_2}{2I_0V_0} = \frac{(0.952)(29.1 \times 10^{-3})(831)}{2(25 \times 10^{-3})(10^3)} = 46.2\%$$

d. Calculate the beam loading conductance (refer to Fig. 9-2-13). The beam loading conductance G_B is

$$G_B = \frac{G_0}{2}\left(\beta_0^2 - \beta_0 \cos\frac{\theta_g}{2}\right) = \frac{25 \times 10^{-6}}{2}[(0.952)^2 - (0.952)\cos(28.6°)]$$

$$= 8.8 \times 10^{-7} \text{ mho}$$

Then the beam loading resistance R_B is

$$R_B = \frac{1}{G_B} = 1.14 \times 10^6\ \Omega$$

In comparison with R_L and R_{sho} or the effective shunt resistance R_{sh}, the beam loading resistance is like an open circuit and thus can be neglected in the preceding calculations.

9-2-5 State of the Art

Extended Interaction. The most common form of extended interaction has been attained recently by coupling two or more adjacent klystron cavities. Figure 9-2-17 shows schematically a five-section extended-interaction cavity as compared to a single-gap klystron cavity.

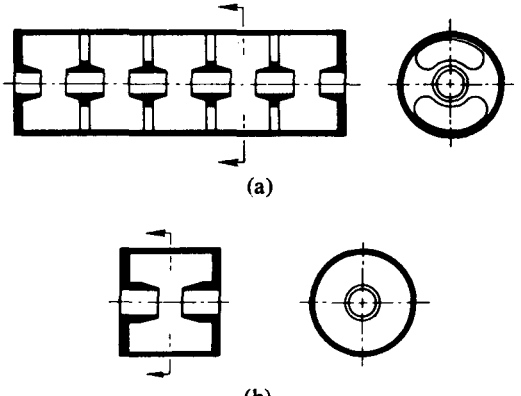

Figure 9-2-17 Comparison of a five-gap extended interaction cavity with a single-gap klystron cavity. (a) Five-gap coupled cavity resonator. (b)Single-gap klystron cavity. (*After A. Staprans et al. [7]; reprinted by permission of IEEE.*)

High efficiency and large power. In the 1960s much effort was devoted to improving the efficiency of klystrons. For instance, a 50-kW experimental tube has demonstrated 75% efficiency in the industrial heating band [8]. The VA-884D klystron is a five-cavity amplifier whose operating characteristics are listed in Table 9-2-1.

One of the better-known high-peak-power klystrons is the tube developed specifically for use in the 2-mile Stanford Linear Accelerator [9] at Palo Alto, California. A cutaway view of the tube is shown in Fig. 9-2-18. The operating characteristics of this tube are listed in Table 9-2-2.

The Varian CW superpower klystron amplifier VKC-8269A as shown in Fig. 9-2-19 has an output power of 500 kW (CW) at frequency of 2.114 GHz. Its power

TABLE 9-2-1 VA-884D OPERATING CHARACTERISTICS

Frequency	5.9–6.45 GHz
Power output	14 kW
Gain	52 dB
Efficiency	36%
Electronic bandwidth (1 dB)	75 MHz
Beam voltage	16.5 kV
Beam current	2.4 A

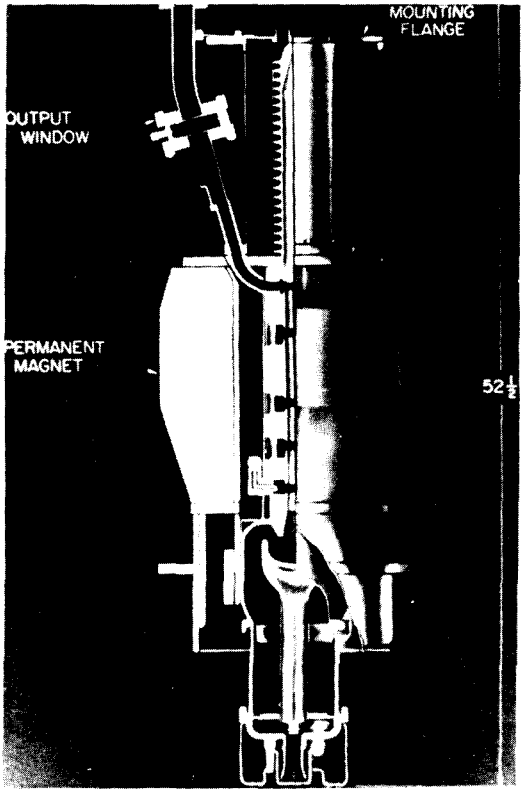

Figure 9-2-18 Cutaway of 24-MW S-band permanent-magnet-focused klystron. (*Courtesy of Stanford Linear Accelerator Center.*)

TABLE 9-2-2 OPERATING CHARACTERISTICS OF THE STANFORD LINEAR ACCELERATOR CENTER HIGH-POWER KLYSTRON [9]

Frequency	2.856	GHz
RF pulse width	2.5	μs
Pulse repetition rate	60 to 360	pps
Peak power output	24	MW
Beam voltage	250	kV
Beam current	250	A
Gain	50 to 55	dB
Efficiency	about 36	%
Weight of permanent (focusing) magnet	363	kg
Electronic bandwidth (1 dB)	20	MHz

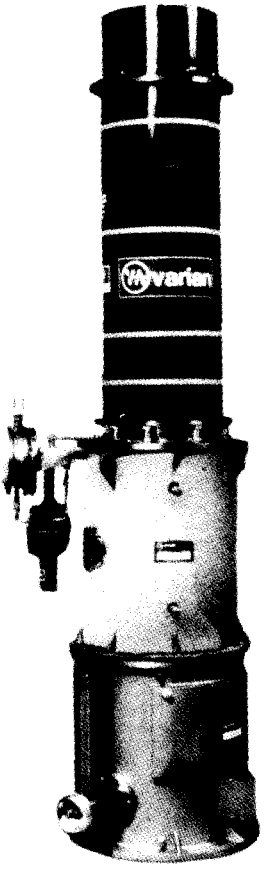

Figure 9-2-19 Photograph of Varian VKC-8269A CW super-power klystron amplifier. (*Courtesy of Varian Associates, Inc.*)

gain is 56 dB and efficiency is 50 percent. The beam voltage is 62 V (dc) and the beam current is 16.50 A (dc).

Long-life improvement. A new long-life klystron amplifier tube with a design life in excess of ten years, three times the current design life, has been developed by the Electron Dynamics Division of the Hughes Aircraft Company. Key to the long-life klystron was the development of a method of reducing the operating temperature of the tube's cathode. The cathode is made of porous tungsten impregnated with barium, calcium, and aluminum oxides. The new cathode is coated with a layer of osmium ruthenium alloy that lowers its work function, which is the temperature necessary for electrons to be emitted. This temperature reduction cuts evaporation of barium 10-fold and extends the life of the cathode.

9-3 MULTICAVITY KLYSTRON AMPLIFIERS

The typical power gain of a two-cavity klystron amplifier is about 30 dB. In order to achieve higher overall gain, one way is to connect several two-cavity tubes in cascade, feeding the output of each of the tubes to the input of the following one. Be-

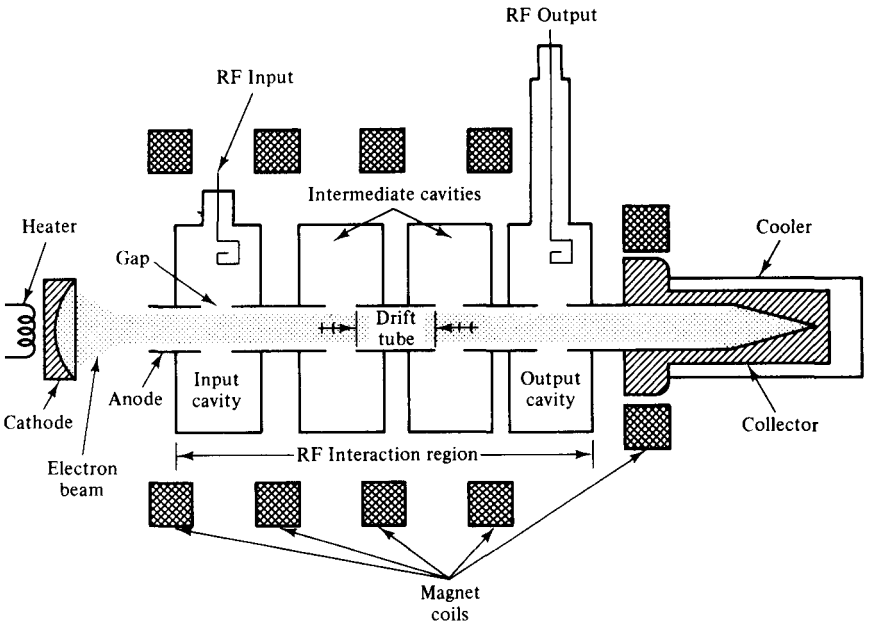

Figure 9-3-1 Schematic diagram of a four-cavity klystron amplifier. (*Courtesy of Varian Associates, Inc.*)

sides using the multistage techniques, the tube manufacturers have designed and produced multicavity klystron to serve the high-gain requirement as shown in Fig. 9-3-1.

In a multicavity klystron each of the intermediate cavities, placed at a distance of the bunching parameter X of 1.841 away from the previous cavity, acts as a buncher with the passing electron beam inducing a more enhanced RF voltage than the previous cavity, which in turn sets up an increased velocity modulation. The spacing between the consecutive cavities would therefore diminish because of the requirement of X being 1.841 and an increasing velocity modulating RF voltage as the beam progresses through the various cavities. Keeping the intercavity distance constant, an increasing beam voltage V_0 could be used in the subsequent cavities. Figure 9-3-2 shows the photograph of a four-cavity klystron amplifier.

9-3-1 Beam-Current Density

When the two-cavity klystron amplifier was discussed in Section 9-2, it was assumed that the space-charge effect was negligible, and it was not considered because of the assumed small density of electrons in the beam for low-power amplifier. However, when high-power klystron tubes are analyzed the electron density of the beam is large and the forces of mutual repulsion of the electrons must be considered. When the elecrons perturbate in the electron beam, the electron density consists of a dc part plus an RF perturbation caused by the electron bunches. The space-charge forces within electron bunches vary with the size and shape of an electron beam. In

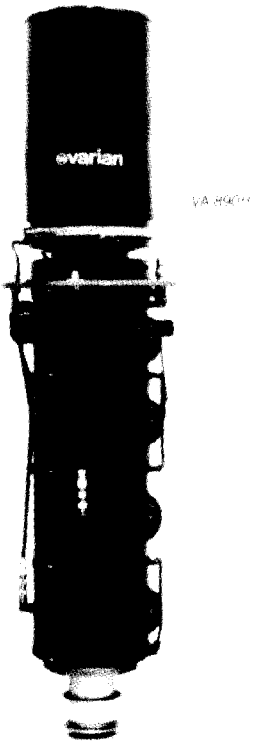

Figure 9-3-2 Photograph of a four-cavity klystron amplifier VA-890H. (*Courtesy of Varian Associates, Inc.*)

an infinitely wide beam, the electric fields (and, thus, the space-charge forces) are constrained to act only in the axial direction. In a finite beam, the electric fields are radial as well as axial with the result that the axial component is reduced in comparison to the infinite beam. With reduced axial space-charge force, the plasma frequency is reduced and the plasma wavelength is increased.

Mathematically, let the charge-density and velocity perturbations be simple sinusoidal variations in both time and position. They are

$$\text{Charge density:} \qquad \rho = B \cos(\beta_e z) \cos(\omega_q t + \theta) \tag{9-3-1}$$

$$\text{Velocity perturbation:} \qquad \mathcal{V} = -C \sin(\beta_e z) \sin(\omega_q t + \theta) \tag{9-3-2}$$

where B = constant of charge-density perturbation
C = constant of velocity perturbation
$\beta_e = \dfrac{\omega}{\mathcal{V}_0}$ is the dc phase constant of the electron beam
$\omega_q = R\omega_p$ is the pertubation frequency or reduced plasma frequency
$R = \omega_q/\omega_p$ is the space-charge reduction factor and varies from 0 to 1
$\omega_p = \sqrt{\dfrac{e\rho_0}{m\epsilon_0}}$ is the plasma frequency and is a function of the electron-beam density
θ = phase angle of oscillation

The electron plasma frequency is the frequency at which the electrons will oscillate in the electron beam. This plasma frequency applies only to a beam of infinite diameter. Practical beams of finite diameter are characterized by plasma frequency that is less than ω_p. This lower plasma frequency is called the *reduced plasma frequency* and is designated ω_q. The space-charge reduction factor R is a function of the beam radius r and the ratio n of the beam-tunnel radius to the beam radius as shown in Fig. 9-3-3 [10].

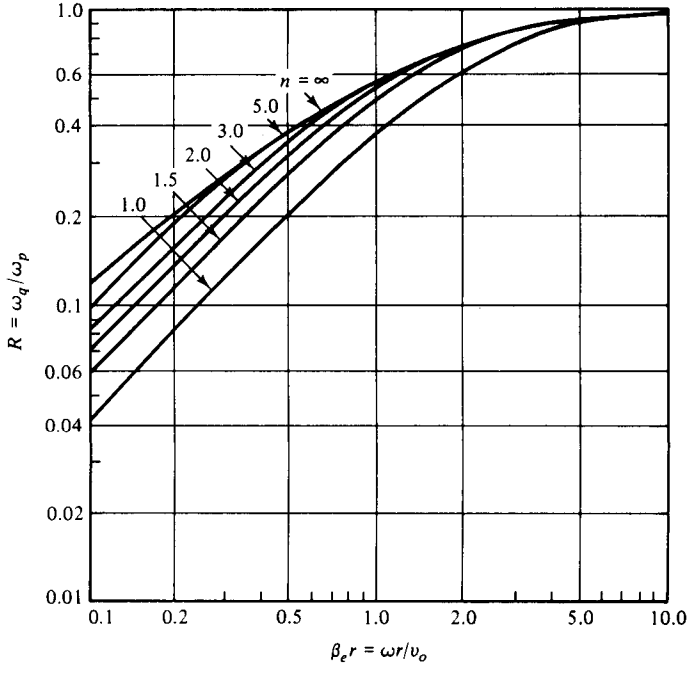

Figure 9-3-3 Plasma-frequency reduction factor R [10] (*Reprinted by permission of Pergamon Press.*)

As an example of the effect of the reduced space-charge forces, if $\beta_e r = \omega r/\mathcal{V}_0 = 0.85$ and $n = 2$, the reduced factor is $R = 0.5$. Therefore, $\omega_q = 2\omega_p$, which means that in a klystron the cavities would be placed twice as far apart as would be indicated by infinite-beam calculation. The total charge density and electron velocity are given by

$$\rho_{\text{tot}} = -\rho_0 + \rho \tag{9-3-3}$$

$$\mathcal{V}_{\text{tot}} = \mathcal{V}_0 + \mathcal{V} \tag{9-3-4}$$

where ρ_0 = dc electron charge density
ρ = instantaneous RF charge density
$\mathcal{V}_0$ = dc electron velocity
$\mathcal{V}$ = instantaneous electron velocity perturbation

The total electron beam-current density can be written as

$$J_{\text{tot}} = -J_0 + J \tag{9-3-5}$$

where J_0 = dc beam-current density
J = instantaneous RF beam-current perturbation

The instantaneous convection beam-current density at any point in the beam is expressed as

$$\begin{aligned} J_{\text{tot}} &= \rho_{\text{tot}} \mathcal{V}_{\text{tot}} = (-\rho_0 + \rho)(\mathcal{V}_0 + \mathcal{V}) \\ &= -\rho_0 \mathcal{V}_0 - \rho_0 \mathcal{V} + \rho \mathcal{V}_0 + \rho \mathcal{V} \\ &= -J_0 + J \end{aligned} \tag{9-3-6}$$

where $J = \rho \mathcal{V}_0 - \rho_0 \mathcal{V}$ (9-3-7)
$J_0 = \rho_0 \mathcal{V}_0$ is replaced
$\rho \mathcal{V}$ = very small is ignored

In accordance with the law of conservation of electric charge, the continuity equation can be written as

$$\nabla \cdot \mathbf{J} = -\frac{\partial \rho}{\partial t} \tag{9-3-8}$$

where $J = \rho \mathcal{V}_0 - \rho_0 \mathcal{V}$ is in positive z direction only. From

$$\begin{aligned} \frac{\partial J}{\partial z} = &-\omega B \sin(\beta_e z - \omega t) \cos(\omega_q t + \theta) \\ &+ \beta_e \rho_0 C \cos(\beta_e z - \omega t) \sin(\omega_q t + \theta) \end{aligned} \tag{9-3-9}$$

and

$$\begin{aligned} -\frac{\partial \rho}{\partial t} = &-\omega B \sin(\beta_e z - \omega t) \cos(\omega_q t + \theta) \\ &+ \omega_q B \cos(\beta_e z - \omega t) \sin(\omega_q t + \theta) \end{aligned} \tag{9-3-10}$$

then we have

$$\omega_q B = \beta_e \rho_0 C \tag{9-3-11}$$

The beam-current density and the modulated velocity are expressed as [10]

$$\begin{aligned} J = &\mathcal{V}_0 B \cos(\beta_e z - \omega t) \cos(\omega_q t + \theta) \\ &+ \frac{\omega_q}{\omega} \mathcal{V}_0 B \sin(\beta_e z - \omega t) \sin(\omega_q t + \theta) \end{aligned} \tag{9-3-12}$$

and

$$\mathcal{V} = -\mathcal{V}_0 \frac{\beta_i V_1}{2V_0} \cos(\beta_q z) \sin(\beta_e z - \omega t) \tag{9-3-13}$$

In practical microwave tubes, the ratio of ω_q/ω is much smaller than unity and the second term in Eq. (9-3-12) may be neglected in comparison with the first. Then we obtain

$$J = \mathcal{V}_0 B \cos(\beta_e z - \omega t) \cos(\omega_q t + \theta) \tag{9-3-14}$$

Example 9-3-1: Four-Cavity Klystron

A four-cavity klystron VA-828 has the following parameters:

Beam voltage:	$V_0 = 14.5$ kV
Beam current:	$I_0 = 1.4$ A
Operating frequency:	$f = 10$ GHz
dc electron charge density:	$\rho_0 = 10^{-6}$ C/m^3
RF charge density:	$\rho = 10^{-8}$ C/m^3
Velocity perturbation:	$\mathcal{V} = 10^5$ m/s

Compute:

a. The dc electron velocity
b. The dc phase constant
c. The plasma frequency
d. The reduced plasma frequency for $R = 0.4$
e. The dc beam current density
f. The instantaneous beam current density

Solution

a. The dc electron velocity is

$$\mathcal{V}_0 = 0.593 \times 10^6 \sqrt{14.5 \times 10^3} = 0.714 \times 10^8 \text{ m/s}$$

b. The dc phase constant is

$$\beta_e = \frac{2\pi \times 10^{10}}{0.714 \times 10^8} = 8.80 \times 10^2 \text{ rads/m}$$

c. The plasma frequency is

$$\omega_p = \left(1.759 \times 10^{11} \times \frac{10^{-6}}{8.854 \times 10^{-12}}\right)^{1/2} = 1.41 \times 10^8 \text{ rad/s}$$

d. The reduced plasma frequency for $R = 0.4$ is

$$\omega_q = 0.4 \times 1.41 \times 10^8 = 0.564 \times 10^8 \text{ rad/s}$$

e. The dc beam current density is

$$J_0 = 10^{-6} \times 0.714 \times 10^8 = 71.4 \text{ A/m}^2$$

f. The instantaneous beam current density is

$$J = 10^{-8} \times 0.714 \times 10^8 - 10^{-6} \times 10^5 = 0.614 \text{ A/m}^2$$

The electrons leaving the input gap of a klystron amplifier have a velocity given by Eq. (9-2-17) at the exit grid as

$$\mathcal{V}(t_1) = \mathcal{V}_0\left[1 + \frac{\beta_i V_1}{2V_0} \sin(\omega\tau)\right] \tag{9-3-15}$$

where V_1 = magnitude of the input signal voltage

$\tau = \dfrac{d}{\mathcal{V}_0} = t_1 - t_0$ is the transit time

d = gap distance

Since the electrons under the influence of the space-charge forces exhibit simple harmonic motion, the velocity at a later time t is given by

$$\mathcal{V}_{to\ell} = \mathcal{V}_0\left[1 + \frac{\beta_i V_1}{2V_0} \sin(\omega\tau) \cos(\omega_p t - \omega_p \tau)\right] \tag{9-3-16}$$

where ω_p = plasma frequency. The current-density equation may be obtained from Eq. (9-3-14) as

$$J = -\frac{1}{2}\frac{J_0\omega}{V_0\omega_q}\beta_i V_1 \sin(\beta_q z) \cos(\beta_e z - \omega t) \tag{9-3-17}$$

where $\beta_q = \dfrac{\omega_q}{\mathcal{V}_0}$ is the plasma phase constant.

Example 9-3-2: Operation of a Four-Cavity Klystron

A four-cavity CW klystron amplifier VA-864 has the following parameters:

Beam voltage:	$V_0 = 18$ kV
Beam current:	$I_0 = 2.25$ A
Gap distance:	$d = 1$ cm
Operating frequency:	$f = 10$ GHz
Signal voltage:	$V_1 = 10$ V (rms)
Beam coupling coefficient:	$\beta_0 = \beta_i = 1$
dc electron beam current density:	$\rho_0 = 10^{-8}$ C/m^3

Determine:

a. The dc electron velocity
b. The dc electron phase constant
c. The plasma frequency
d. The reduced plasma frequency for $R = 0.5$
e. The reduced plasma phase constant
f. The transit time across the input gap
g. The electron velocity leaving the input gap

Solution

a. The dc electron velocity is

$$\mathcal{V}_0 = 0.593 \times 10^6\sqrt{18 \times 10^3} = 0.796 \times 10^8 \text{ m/s}$$

b. The dc electron phase constant is

$$\beta_e = 2\pi \times 10^{10}/(0.796 \times 10^8) = 7.89 \times 10^2 \text{ rad/m}$$

c. The plasma frequency is

$$\omega_p = [1.759 \times 10^{11} \times 10^{-8}/(8.854 \times 10^{-12})]^{1/2} = 1.41 \times 10^7 \text{ rad/s}$$

d. The reduced plasma frequency is

$$\omega_q = 0.5 \times 1.41 \times 10^7 = 0.705 \times 10^7 \text{ rad/s}$$

e. The reduced plasma phase constant is

$$\beta_q = 0.705 \times 10^7/(0.796 \times 10^8) = 0.088 \text{ rad/m}$$

f. The transit time across the gap is

$$\tau = 10^{-2}/(0.796 \times 10^8) = 0.1256 \text{ ns}$$

g. The electron velocity leaving the input gap is

$$\mathcal{V}(t_1) = 0.796 \times 10^8[1 + 1 \times 10/(2 \times 18 \times 10^3) \sin (2\pi \times 10^{10} \times 1.256 \times 10^{-10})]$$
$$= 0.796 \times 10^8 + 2.21 \times 10^4 \text{ m/s}$$

9-3-2 Output Current and Output Power of Two-Cavity Klystron

If the two cavities of a two-cavity klystron amplifier are assumed to be identical and are placed at the point where the RF current modulation is a maximum, the magnitude of the RF convection current at the output cavity for a two-cavity klystron can be written from Eq. (9-3-17) as

$$|i_2| = \frac{1}{2}\frac{I_0\omega}{V_0\omega_q}\beta_i|V_1| \tag{9-3-18}$$

where V_1 = magnitude of the input signal voltage. Then the magnitudes of the induced current and voltage in the output cavity are equal to

$$|I_2| = \beta_0|i_2| = \frac{1}{2}\frac{I_0\omega}{V_0\omega_q}\beta_0^2|V_1| \tag{9-3-19}$$

and

$$|V_2| = |I_2|R_{shl} = \frac{1}{2}\frac{I_0\omega}{V_0\omega_q}\beta_0^2|V_1|R_{shl} \tag{9-3-20}$$

where $\beta_0 = \beta_i$ is the beam coupling coefficient
R_{shl} = total shunt resistance of the output cavity in a two-cavity klystron amplifier including the external load

The output power delivered to the load in a two-cavity klystron amplifier is given by

$$P_{\text{out}} = |I_2|^2 R_{shl} = \frac{1}{4}\left(\frac{I_0\omega}{V_0\omega_q}\right)^2 \beta_0^4 |V_1|^2 R_{shl} \tag{9-3-21}$$

The power gain of a two-cavity klystron amplifier is then expressed by

$$\text{Power gain} = \frac{P_{\text{out}}}{P_{\text{in}}} = \frac{P_{\text{out}}}{|V_1|^2/R_{sh}} = \frac{1}{4}\left(\frac{I_0\omega}{V_0\omega_q}\right)^2 \beta_0^4 R_{sh} \cdot R_{shl} \tag{9-3-22}$$

where R_{sh} = total shunt resistance of the input cavity. The electronic efficiency of a two-cavity klystron amplifier is

$$\eta = \frac{P_{\text{out}}}{P_{\text{in}}} = \frac{P_{\text{out}}}{I_0 V_0} = \frac{1}{4}\left(\frac{I_0}{V_0}\right)\left(\frac{|V_1|\omega}{V_0\omega_q}\right)^2 \beta_0^4 R_{shl} \tag{9-3-23}$$

Example 9-3-3: Characteristics of Two-Cavity Klystron

A two-cavity klystron has the following parameters:

Beam voltage:	$V_0 = 20$ kV
Beam current:	$I_0 = 2$ A
Operating frequency:	$f = 8$ GHz
Beam coupling coefficient:	$\beta_i = \beta_0 = 1$
dc electron beam current density:	$\rho_0 = 10^{-6}$ C/m^3
Signal voltage:	$V_1 = 10$ V (rms)
Shunt resistance of the cavity:	$R_{sh} = 10$ kΩ
Total shunt resistance including load:	$R = 30$ kΩ

Calculate:

a. The plasma frequency
b. The reduced plasma frequency for $R = 0.5$
c. The induced current in the output cavity
d. The induced voltage in the output cavity
e. The output power delivered to the load
f. The power gain
g. The electronic efficiency

Solution

a. The plasma frequency is

$$\omega_p = [1.759 \times 10^{11} \times 10^{-6}/(8.854 \times 10^{-12})]^{1/2} = 1.41 \times 10^8 \text{ rad/s}$$

b. The reduced plasma frequency is

$$\omega_q = 0.5 \times 1.41 \times 10^8 = 0.705 \times 10^8 \text{ rad/s}$$

$$\omega/\omega_q = 2\pi \times 8 \times 10^9/(0.705 \times 10^8) = 713$$

c. The induced current in the output cavity is

$$|I_2| = \frac{1}{2}\frac{2}{20 \times 10^3} \times 713 \times 1^2 \times |10| = 0.3565 \text{ A}$$

d. The induced voltage in the output cavity is

$$|V_2| = |I_2| R_{shl} = 0.357 \times 30 \times 10^3 = 10.71 \text{ kV}$$

e. The output power delivered to the load is

$$P_{\text{out}} = |I_2|^2 R_{shl} = 0.357^2 \times 30 \times 10^3 = 3.82 \text{ kW}$$

f. The power gain is

$$\text{Gain} = 1/4[2/(20 \times 10^3) \times 713]^2 \times 1^4 \times 10 \times 10^3 \times 30 \times 10^3$$

$$= 3.83 \times 10^5 = 55.8 \text{ dB}$$

g. The electronic efficiency is

$$\eta = \frac{P_{\text{out}}}{P_{\text{in}}} = \frac{3.82 \times 10^3}{2 \times 20 \times 10^3} = 9.6\%$$

9-3-3 Output Power of Four-Cavity Klystron

High power may be obtained by adding additional intermediate cavities in a two-cavity klystron. Multicavity klystrons with as many as seven cavities are commercially available, although the most frequently used number of cavities is four. Each of the intermediate cavities functions in the same manner as in the two-cavity klystron amplifier.

Let us carry out a simplified analysis of the four-cavity klystron amplifier. The four cavities are assumed to be identical and they have same unloaded Q and beam coupling coefficient $\beta_i = \beta_0$. The two intermediate cavities are not externally loaded, but the input and output cavities are matched to their transmission lines. If V_1 is the magnitude of the input cavity-gap voltage, the magnitude of the RF convection current density injected into the first intermediate cavity gap is given by Eq. (9-3-17). The induced current and voltage in the first intermediate cavity are given by Eqs. (9-3-19) and (9-3-20). This gap voltage of the first intermediate cavity produces a velocity modulation on the beam in the second intermediate cavity. The RF convection current in the second intermediate cavity can be written with $|V_1|$ replaced by $|V_2|$. That is,

$$\begin{aligned} |i_3| &= \frac{1}{2}\frac{I_0\omega}{V_0\omega_q}\beta_0|V_2| \\ &= \frac{1}{4}\left(\frac{I_0\omega}{V_0\omega_q}\right)^2 \beta_0^3 |V_1| R_{sh} \end{aligned} \tag{9-3-24}$$

The output voltage of the second intermediate cavity is then given by

$$\begin{aligned} |V_3| &= \beta_0 |i_3| R_{sh} \\ &= \frac{1}{4}\left(\frac{I_0\omega}{V_0\omega_q}\right)^2 \beta_0^4 |V_1| R_{sh}^2 \end{aligned} \tag{9-3-25}$$

This voltage produces a velocity modulation again and is converted into an RF convection current at the output cavity for four-cavity klystron as

$$\begin{aligned} |i_4| &= \frac{1}{2}\frac{I_0\omega}{V_0\omega_q}\beta_i |V_3| \\ &= \frac{1}{8}\left(\frac{I_0\omega}{V_0\omega_q}\right)^3 \beta_0^5 |V_1| R_{sh}^2 \end{aligned} \tag{9-3-26}$$

and

$$|I_4| = \beta_0 |i_4| = \frac{1}{8}\left(\frac{I_0\omega}{V_0\omega_q}\right)^3 \beta_0^6 |V_1| R_{sh}^2 \tag{9-3-27}$$

The output voltage is then

$$|V_4| = |I_4| R_{shl} = \frac{1}{8}\left(\frac{I_0\omega}{V_0\omega_q}\right)^3 \beta_0^6 |V_1| R_{sh}^2 R_{shl} \tag{9-3-28}$$

The output power from the output cavity in a four-cavity klystron amplifier can be expressed as

$$P_{\text{out}} = |I_4|^2 R_{shl} = \frac{1}{64}\left(\frac{I_0\omega}{V_0\omega_q}\right)^6 \beta_0^{12} |V_1|^2 R_{sh}^4 R_{shl}^2 \tag{9-3-29}$$

where R_{shl} = total shunt resistance of the output cavity including the external load.

The multicavity klystrons are often operated with their cavities stagger-tuned so as to obtain a greater bandwidth at some reduction in gain. In high-power klystrons, the cavity grids are omitted, because they would burn up during beam interception. High-power klystron amplifiers with a power gain of 40 to 50 dB and a bandwidth of several percent are commercially available.

Example 9-3-4: Output Power of Four-Cavity Klystron

A four-cavity klystron has the following parameters:

Beam voltage:	$V_0 = 10$ kV
Beam current:	$I_0 = 0.7$ A
Operating frequency:	$f = 4$ GHz
Beam coupling coefficient:	$\beta_i = \beta_0 = 1$
dc electron beam current density:	$\rho_0 = 5 \times 10^{-5}$ C/m^3
Signal voltage:	$V_1 = 2$ V (rms)
Shunt resistance of cavity:	$R_{sh} = 10$ kΩ
Total shunt resistance including load:	$R_{shl} = 5$ kΩ

Determine:

a. The plasma frequency
b. The reduced plasma frequency for $R = 0.6$
c. The induced current in the output cavity
d. The induced voltage in the output cavity
e. The output power delivered to the load

Solution

a. The plasma frequency is

$$\omega_p = \left[1.759 \times 10^{11} \times \frac{5 \times 10^{-5}}{8.854 \times 10^{-12}}\right]^{1/2} = 0.997 \times 10^9 \text{ rad/s}$$

b. The reduced plasma frequency is

$$\omega_q = 0.6 \times 0.997 \times 10^9 = 0.598 \times 10^9 \text{ rad/s}$$

$$\omega/\omega_q = 2\pi \times 4 \times 10^9/(0.598 \times 10^9) = 42.03$$

c. The induced current in the output cavity is

$$|I_4| = \frac{1}{8}\left(\frac{0.7}{10^4} \times 42.03\right)^3 \times 1^6 \times |2| \times (10 \times 10^3)^2$$

$$= 0.6365 \text{ A}$$

d. The induced voltage in the output cavity is

$$|V_4| = |I_4|R_{shl} = |0.6365| \times 5 \times 10^3$$

$$= 3.18 \text{ kV}$$

e. The output power is

$$P_{\text{out}} = |I_4|^2 R_{shl} = |0.6365|^2 \times 5 \times 10^3 = 2.03 \text{ kW}$$

9-4 REFLEX KLYSTRONS

If a fraction of the output power is fed back to the input cavity and if the loop gain has a magnitude of unity with a phase shift of multiple 2π, the klystron will oscillate. However, a two-cavity klystron oscillator is usually not constructed because, when the oscillation frequency is varied, the resonant frequency of each cavity and the feedback path phase shift must be readjusted for a positive feedback. The reflex klystron is a single-cavity klystron that overcomes the disadvantages of the two-cavity klystron oscillator. It is a low-power generator of 10 to 500-mW output at a frequency range of 1 to 25 GHz. The efficiency is about 20 to 30%. This type is widely used in the laboratory for microwave measurements and in microwave receivers as local oscillators in commercial, military, and airborne Doppler radars as well as missiles. The theory of the two-cavity klystron can be applied to the analysis of

the reflex klystron with slight modification. A schematic diagram of the reflex klystron is shown in Fig. 9-4-1.

The electron beam injected from the cathode is first velocity-modulated by the cavity-gap voltage. Some electrons accelerated by the accelerating field enter the repeller space with greater velocity than those with unchanged velocity. Some electrons decelerated by the retarding field enter the repeller region with less velocity. All electrons turned around by the repeller voltage then pass through the cavity gap in bunches that occur once per cycle. On their return journey the bunched electrons pass through the gap during the retarding phase of the alternating field and give up their kinetic energy to the electromagnetic energy of the field in the cavity. Oscillator output energy is then taken from the cavity. The electrons are finally collected by the walls of the cavity or other grounded metal parts of the tube. Figure 9-4-2 shows an Applegate diagram for the $1\frac{3}{4}$ mode of a reflex klystron.

9-4-1 Velocity Modulation

The analysis of a reflex klystron is similar to that of a two-cavity klystron. For simplicity, the effect of space-charge forces on the electron motion will again be neglected. The electron entering the cavity gap from the cathode at $z = 0$ and time t_0 is assumed to have uniform velocity

$$v_0 = 0.593 \times 10^6 \sqrt{V_0} \tag{9-4-1}$$

The same electron leaves the cavity gap at $z = d$ at time t_1 with velocity

$$v(t_1) = v_0\left[1 + \frac{\beta_1 V_1}{2V_0} \sin\left(\omega t_1 - \frac{\theta_g}{2}\right)\right] \tag{9-4-2}$$

This expression is identical to Eq. (9-2-17), for the problems up to this point are identical to those of a two-cavity klystron amplifier. The same electron is forced back to the cavity $z = d$ and time t_2 by the retarding electric field E, which is given by

$$E = \frac{V_r + V_0 + V_1 \sin(\omega t)}{L} \tag{9-4-3}$$

This retarding field E is assumed to be constant in the z direction. The force equation for one electron in the repeller region is

$$m\frac{d^2z}{dt^2} = -eE = -e\frac{V_r + V_0}{L} \tag{9-4-4}$$

where $\mathbf{E} = -\nabla V$ is used in the z direction only, V_r is the magnitude of the repeller voltage, and $|V_1 \sin \omega t| \ll (V_r + V_0)$ is assumed.

Integration of Eq. (9-4-4) twice yields

$$\frac{dz}{dt} = \frac{-e(V_r + V_0)}{mL}\int_{t_1}^{t} dt = \frac{-e(V_r + V_0)}{mL}(t - t_1) + K_1 \tag{9-4-5}$$

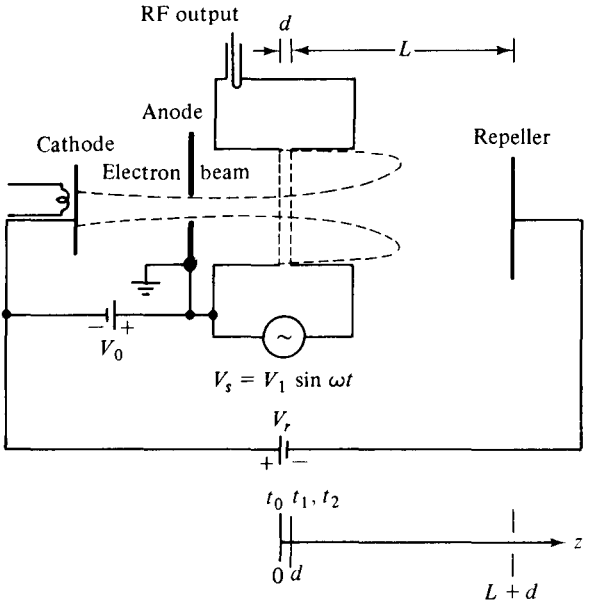

t_0 = time for electron entering cavity gap at $z = 0$
t_1 = time for same electron leaving cavity gap at $z = d$
t_2 = time for same electron returned by retarding field $z = d$ and collected on walls of cavity

Figure 9-4-1 Schematic diagram of a reflex klystron.

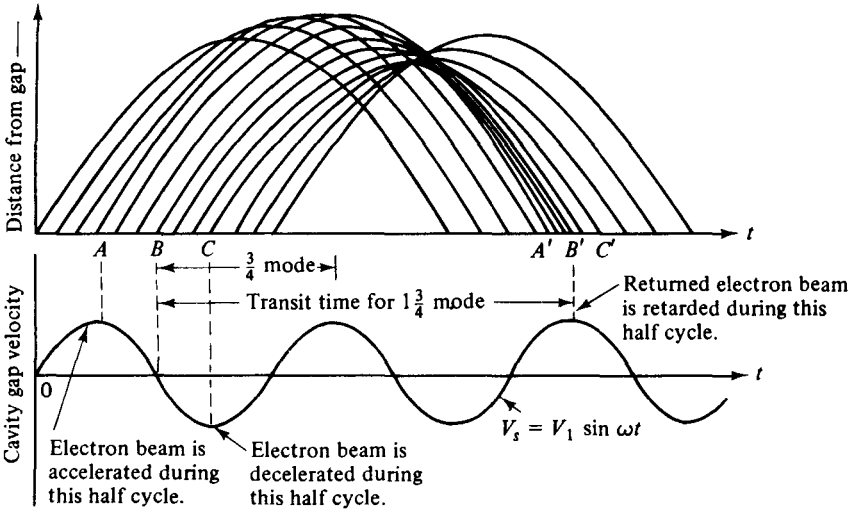

Figure 9-4-2 Applegate diagram with gap voltage for a reflex klystron.

at $t = t_1$, $dz/dt = v(t_1) = K_1$; then

$$z = \frac{-e(V_r + V_0)}{mL} \int_{t_1}^{t} (t - t_1)\, dt + v(t_1) \int_{t_1}^{t} dt$$

$$z = \frac{-e(V_r + V_0)}{2mL}(t - t_1)^2 + v(t_1)(t - t_1) + K_2$$

at $t = t_1$, $z = d = K_2$; then

$$z = \frac{-e(V_r + V_0)}{2mL}(t - t_1)^2 + v(t_1)(t - t_1) + d \tag{9-4-6}$$

On the assumption that the electron leaves the cavity gap at $z = d$ and time t_1 with a velocity of $v(t_1)$ and returns to the gap at $z = d$ and time t_2, then, at $t = t_2$, $z = d$,

$$0 = \frac{-e(V_r + V_0)}{2mL}(t_2 - t_1)^2 + v(t_1)(t_2 - t_1)$$

The round-trip transit time in the repeller region is given by

$$T' = t_2 - t_1 = \frac{2mL}{e(V_r + V_0)} v(t_1) = T_0' \left[1 + \frac{\beta_i V_1}{2V_0} \sin\left(\omega t_1 - \frac{\theta_g}{2}\right)\right] \tag{9-4-7}$$

where

$$T_0' = \frac{2mLv_0}{e(V_r + V_0)} \tag{9-4-8}$$

is the round-trip dc transit time of the center-of-the-bunch electron.

Multiplication of Eq. (9-4-7) through by a radian frequency results in

$$\omega(t_2 - t_1) = \theta_0' + X' \sin\left(\omega t_1 - \frac{\theta_g}{2}\right) \tag{9-4-9}$$

where

$$\theta_0' = \omega T_0' \tag{9-4-10}$$

is the round-trip dc transit angle of the center-of-the-bunch electron and

$$X' \equiv \frac{\beta_i V_1}{2V_0} \theta_0' \tag{9-4-11}$$

is the bunching parameter of the reflex klystron oscillator.

9-4-2 Power Output and Efficiency

In order for the electron beam to generate a maximum amount of energy to the oscillation, the returning electron beam must cross the cavity gap when the gap field is maximum retarding. In this way, a maximum amount of kinetic energy can be transferred from the returning electrons to the cavity walls. It can be seen from Fig.

9-4-2 that for a maximum energy transfer, the round-trip transit angle, referring to the center of the bunch, must be given by

$$\omega(t_2 - t_1) = \omega T_0' = \left(n - \frac{1}{4}\right)2\pi = N\,2\pi = 2\pi n - \frac{\pi}{2} \tag{9-4-12}$$

where $V_1 \ll V_0$ is assumed, n = any positive integer for cycle number, and $N = n - \frac{1}{4}$ is the number of modes.

The current modulation of the electron beam as it reenters the cavity from the repeller region can be determined in the same manner as in Section 9-2 for a two-cavity klystron amplifier. It can be seen from Eqs. (9-2-30) and (9-4-9) that the bunching parameter X' of a reflex klystron oscillator has a negative sign with respect to the bunching parameter X of a two-cavity klystron amplifier. Furthermore, the beam current injected into the cavity gap from the repeller region flows in the negative z direction. Consequently, the beam current of a reflex klystron oscillator can be written

$$i_{2t} = -I_0 - \sum_{n=1}^{\infty} 2I_0 J_n(nX') \cos\left[n(\omega t_2 - \theta_0' - \theta_g)\right] \tag{9-4-13}$$

The fundamental component of the current induced in the cavity by the modulated electron beam is given by

$$i_2 = -\beta_i I_2 = 2I_0\beta_i J_1(X') \cos(\omega t_2 - \theta_0') \tag{9-4-14}$$

in which θ_g has been neglected as a small quantity compared with θ_0'. The magnitude of the fundamental component is

$$I_2 = 2I_0\beta_i J_1(X') \tag{9-4-15}$$

The dc power supplied by the beam voltage V_0 is

$$P_{dc} = V_0 I_0 \tag{9-4-16}$$

and the ac power delivered to the load is given by

$$P_{ac} = \frac{V_1 I_2}{2} = V_1 I_0 \beta_i J_1(X') \tag{9-4-17}$$

From Eqs.(9-4-10), (9-4-11), and (9-4-12) the ratio of V_1 over V_0 is expressed by

$$\frac{V_1}{V_0} = \frac{2X'}{\beta_i(2\pi n - \pi/2)} \tag{9-4-18}$$

Substitution of Eq. (9-4-18) in Eq. (9-4-17) yields the power output as

$$P_{ac} = \frac{2V_0 I_0 X' J_1(X')}{2\pi n - \pi/2} \tag{9-4-19}$$

Therefore the electronic efficiency of a reflex klystron oscillator is defined as

$$\text{Efficiency} \equiv \frac{P_{ac}}{P_{dc}} = \frac{2X' J_1(X')}{2\pi n - \pi/2} \tag{9-4-20}$$

The factor $X'J_1(X')$ reaches a maximum value of 1.25 at $X' = 2.408$ and $J_1(X') = 0.52$. In practice, the mode of $n = 2$ has the most power output. If $n = 2$ or $1\frac{3}{4}$ mode, the maximum electronic efficiency becomes

$$\text{Efficiency}_{\max} = \frac{2(2.408)J_1(2.408)}{2\pi(2) - \pi/2} = 22.7\% \tag{9-4-21}$$

The maximum theoretical efficiency of a reflex klystron oscillator ranges from 20 to 30%. Figure 9-4-3 shows a curve of $X'J_1(X')$ versus X'.

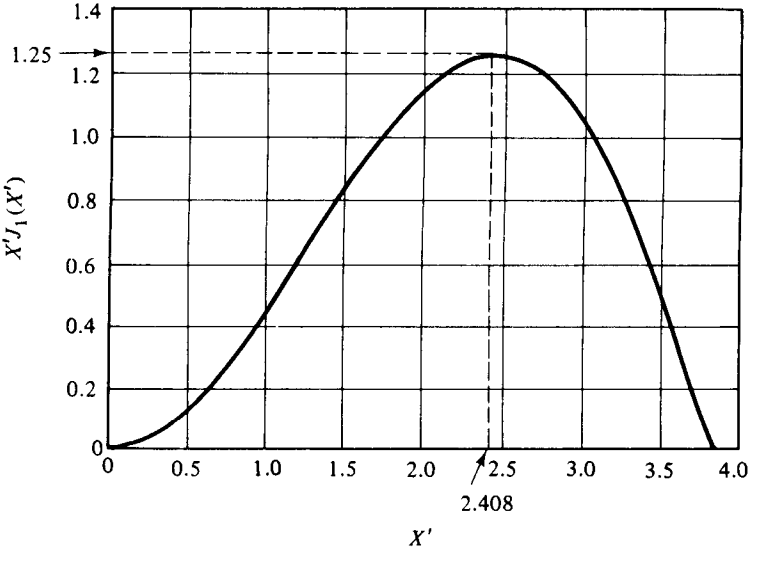

Figure 9-4-3 $X'J_1(X')$ versus X'.

For a given beam voltage V_0, the relationship between the repeller voltage and cycle number n required for oscillation is found by inserting Eqs. (9-4-12) and (9-4-1) into Eq. (9-4-8):

$$\frac{V_0}{(V_r + V_0)^2} = \frac{(2\pi n - \pi/2)^2}{8\omega^2 L^2}\frac{e}{m} \tag{9-4-22}$$

The power output can be expressed in terms of the repeller voltage V_r. That is,

$$P_{ac} = \frac{V_0 I_0 X' J_1(X')(V_r + V_0)}{\omega L}\sqrt{\frac{e}{2mV_o}} \tag{9-4-23}$$

It can be seen from Eq. (9-4-22) that, for a given beam voltage V_0 and cycle number n or mode number N, the center repeller voltage V_r can be determined in terms of the center frequency. Then the power output at the center frequency can be calculated from Eq. (9-4-23). When the frequency varies from the center frequency and the repeller voltage about the center voltage, the power output will vary accordingly, assuming a bell shape (see Fig. 9-4-4).

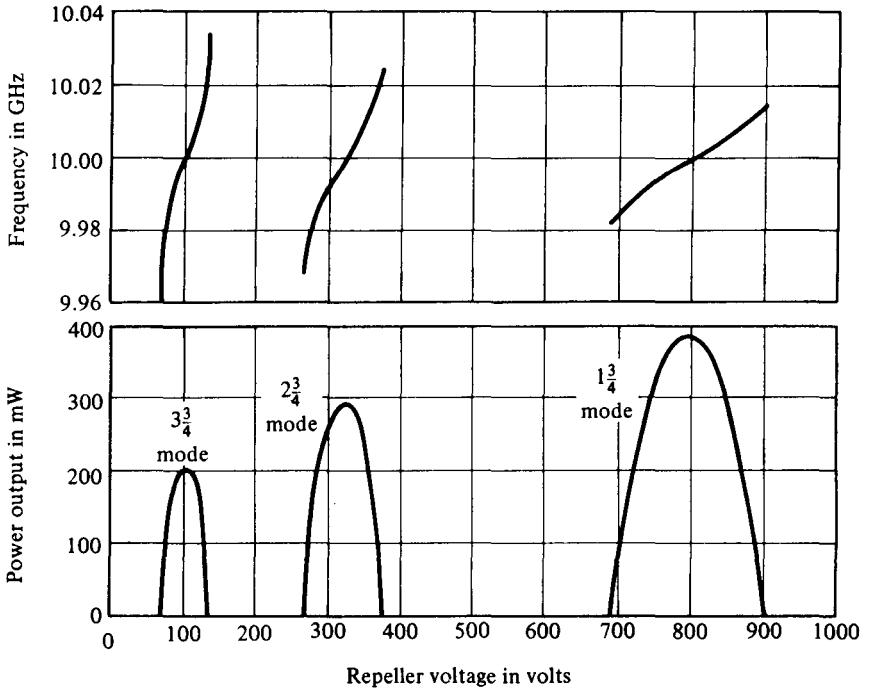

Figure 9-4-4 Power output and frequency characteristics of a reflex klystron.

9-4-3 Electronic Admittance

From Eq. (9-4-14) the induced current can be written in phasor form as

$$i_2 = 2I_0\beta_i J_1(X')e^{-j\theta_0'} \tag{9-4-24}$$

The voltage across the gap at time t_2 can also be written in phasor form:

$$V_2 = V_1 e^{-j\pi/2} \tag{9-4-25}$$

The ratio of i_2 to V_2 is defined as the electronic admittance of the reflex klystron. That is,

$$Y_e = \frac{I_0}{V_0}\frac{\beta_i^2\,\theta_0'}{2}\frac{2J_1(X')}{X'}e^{j(\pi/2-\theta_0')} \tag{9-4-26}$$

The amplitude of the phasor admittance indicates that the electronic admittance is a function of the dc beam admittance, the dc transit angle, and the second transit of the electron beam through the cavity gap. It is evident that the electronic admittance is nonlinear, since it is proportional to the factor $2J_1(X')/X'$, and X' is proportional to the signal voltage. This factor of proportionality is shown in Fig. 9-4-5. When the signal voltage goes to zero, the factor approaches unity.

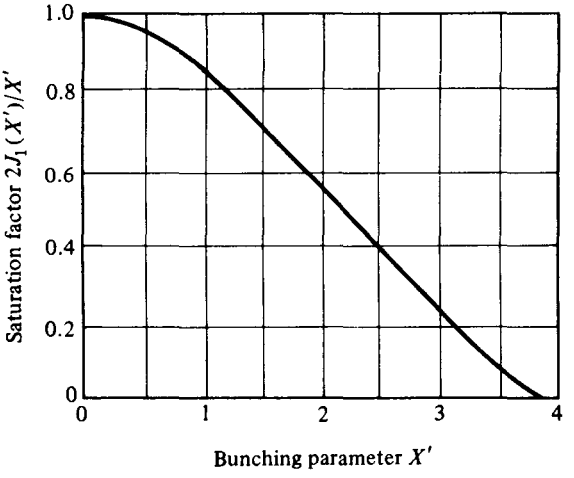

Figure 9-4-5 Reflex klystron saturation factor.

The equivalent ciruit of a reflex klystron is shown in Fig. 9-4-6. In this circuit L and C are the energy storage elements of the cavity; G_c represents the copper losses of the cavity, G_b the beam loading conductance, and G_ℓ the load conductance.

The necessary condition for oscillations is that the magnitude of the negative real part of the electronic admittance as given by Eq. (9-4-26) not be less than the total conductance of the cavity circuit. That is,

$$|-G_e| \geq G \tag{9-4-27}$$

where $G = G_c + G_b + G_\ell = 1/R_{sh}$ and R_{sh} is the effective shunt resistance.

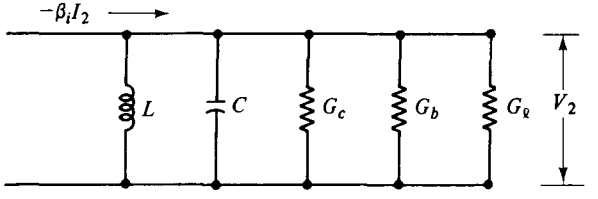

Figure 9-4-6 Equivalent circuit of a reflex klystron.

Equation (9-4-26) can be rewritten in rectangular form:

$$Y_e = G_e + jB_e \tag{9-4-28}$$

Since the electronic admittance shown in Eq. (9-4-26) is in exponential form, its phase is $\pi/2$ when θ_0' is zero. The rectangular plot of the electron admittance Y_e is a spiral (see Fig. 9-4-7). Any value of θ_0' for which the spiral lies in the area to the left of line $(-G - jB)$ will yield oscillation. That is,

$$\theta_0' = \left(n - \frac{1}{4}\right)2\pi = N\,2\pi \tag{9-4-29}$$

where N is the mode number as indicated in the plot, the phenomenon verifies the early analysis.

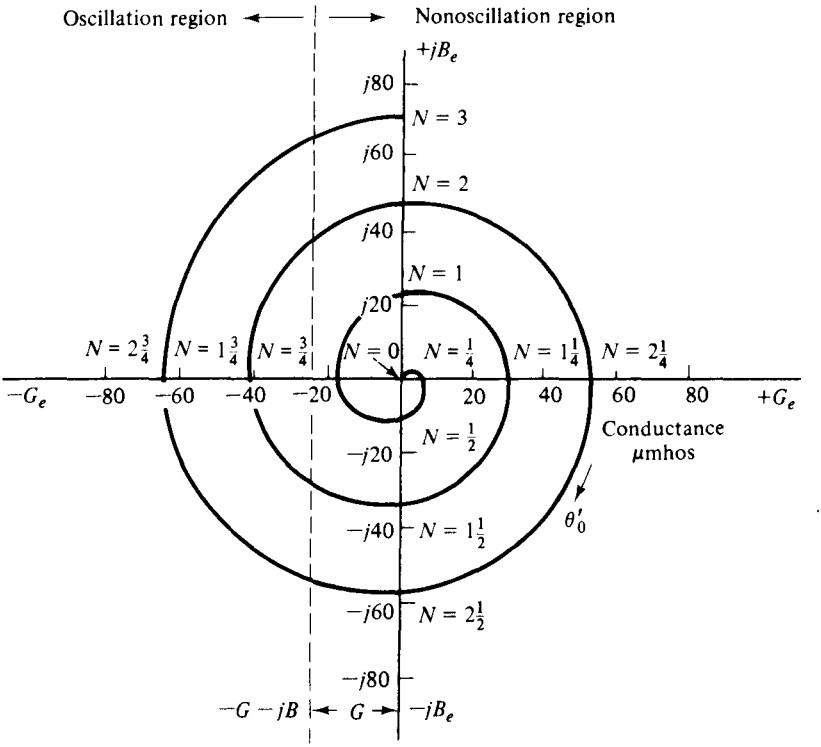

Figure 9-4-7 Electronic admittance spiral of a reflex klystron.

Example 9-4-1: Reflex Klystron

A reflex klystron operates under the following conditions:

$$V_0 = 600 \text{ V} \qquad L = 1 \text{ mm}$$

$$R_{sh} = 15\text{k}\Omega \qquad \frac{e}{m} = 1.759 \times 10^{11} \text{ (MKS system)}$$

$$f_r = 9 \text{ GHz}$$

The tube is oscillating at f_r at the peak of the $n = 2$ mode or $1\frac{3}{4}$ mode. Assume that the transit time through the gap and beam loading can be neglected.

a. Find the value of the repeller voltage V_r.

b. Find the direct current necessary to give a microwave gap voltage of 200 V.

c. What is the electronic efficiency under this condition?

Solution

a. From Eq. (9-4-22) we obtain

$$\frac{V_0}{(V_r + V_0)^2} = \left(\frac{e}{m}\right)\frac{(2\pi n - \pi/2)^2}{8\omega^2 L^2}$$

$$= (1.759 \times 10^{11})\frac{(2\pi 2 - \pi/2)^2}{8(2\pi \times 9 \times 10^9)^2(10^{-3})^2} = 0.832 \times 10^{-3}$$

$$(V_r + V_0)^2 = \frac{600}{0.832 \times 10^{-3}} = 0.721 \times 10^6$$

$$V_r = 250 \text{ V}$$

b. Assume that $\beta_0 = 1$. Since

$$V_2 = I_2 R_{sh} = 2I_0 J_1(X')R_{sh}$$

the direct current I_0 is

$$I_0 = \frac{V_2}{2J_1(X')R_{sh}} = \frac{200}{2(0.582)(15 \times 10^3)} = 11.45 \text{ mA}$$

c. From Eqs. (9-4-11), (9-4-12), and (9-4-20) the electronic efficiency is

$$\text{Efficiency} = \frac{2X'J_1(X')}{2\pi n - \pi/2} = \frac{2(1.841)(0.582)}{2\pi(2) - \pi/2} = 19.49\%$$

9-5 HELIX TRAVELING-WAVE TUBES (TWTs)

Since Kompfner invented the helix traveling-wave tube (TWT) in 1944 [11], its basic circuit has changed little. For broadband applications, the helix TWTs are almost exclusively used, whereas for high-average-power purposes, such as radar transmitters, the coupled-cavity TWTs are commonly used.

In previous sections klystrons and reflex klystrons were analyzed in some detail. Before starting to describe the TWT, it seems appropriate to compare the basic operating principles of both the TWT and the klystron. In the case of the TWT, the microwave circuit is nonresonant and the wave propagates with the same speed as the electrons in the beam. The initial effect on the beam is a small amount of velocity modulation caused by the weak electric fields associated with the traveling wave. Just as in the klystron, this velocity modulation later translates to current modulation, which then induces an RF current in the circuit, causing amplification. However, there are some major differences between the TWT and the klystron:

1. The interaction of electron beam and RF field in the TWT is continuous over the entire length of the circuit, but the interaction in the klystron occurs only at the gaps of a few resonant cavities.
2. The wave in the TWT is a propagating wave; the wave in the klystron is not.
3. In the coupled-cavity TWT there is a coupling effect between the cavities, whereas each cavity in the klystron operates independently.

A helix traveling-wave tube consists of an electron beam and a slow-wave structure. The electron beam is focused by a constant magnetic field along the electron beam and the slow-wave structure. This is termed an O-type traveling-wave tube. The slow-wave structure is either the helical type or folded-back line. The applied signal propagates around the turns of the helix and produces an electric field at the

center of the helix, directed along the helix axis. The axial electric field progresses with a velocity that is very close to the velocity of light multiplied by the ratio of helix pitch to helix circumference. When the electrons enter the helix tube, an interaction takes place between the moving axial electric field and the moving electrons. On the average, the electrons transfer energy to the wave on the helix. This interaction causes the signal wave on the helix to become larger. The electrons entering the helix at zero field are not affected by the signal wave; those electrons entering the helix at the accelerating field are accelerated, and those at the retarding field are decelerated. As the electrons travel further along the helix, they bunch at the collector end. The bunching shifts the phase by $\pi/2$. Each electron in the bunch encounters a stronger retarding field. Then the microwave energy of the electrons is delivered by the electron bunch to the wave on the helix. The amplification of the signal wave is accomplished. The characteristics of the traveling-wave tube are:

Frequency range: 3 GHz and higher
Bandwidth: about 0.8 GHz
Efficiency: 20 to 40%
Power output: up to 10 kW average
Power gain: up to 60 dB

The present state of the art for U.S. high-power TWTs is shown in Fig. 9-5-1.

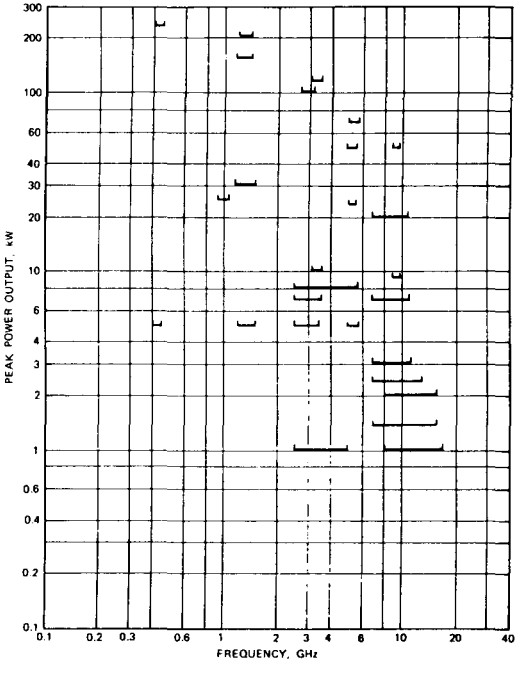

Figure 9-5-1 State of the art for U.S. high-power TWTs.

9-5-1 Slow-Wave Structures

As the operating frequency is increased, both the inductance and capacitance of the resonant circuit must be decreased in order to maintain resonance at the operating frequency. Because the gain-bandwidth product is limited by the resonant circuit, the ordinary resonator cannot generate a large output. Several nonresonant periodic circuits or slow-wave structures (see Fig. 9-5-2) are designed for producing large gain over a wide bandwidth.

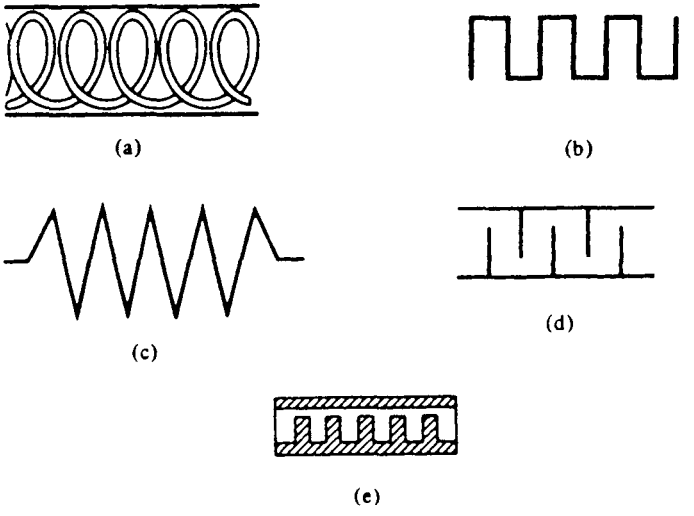

Figure 9-5-2 Slow-wave structures. (a) Helical line. (b) Folded-back line. (c) Zigzag line. (d) Interdigital line. (e) Corrugated waveguide.

Slow-wave structures are special circuits that are used in microwave tubes to reduce the wave velocity in a certain direction so that the electron beam and the signal wave can interact. The phase velocity of a wave in ordinary waveguides is greater than the velocity of light in a vacuum. In the operation of traveling-wave and magnetron-type devices, the electron beam must keep in step with the microwave signal. Since the electron beam can be accelerated only to velocities that are about a fraction of the velocity of light, a slow-wave structure must be incorporated in the microwave devices so that the phase velocity of the microwave signal can keep pace with that of the electron beam for effective interactions. Several types of slow-wave structures are shown in Fig. 9-5-2.

The commonly used slow-wave structure is a helical coil with a concentric conducting cylinder (see Fig. 9-5-3).

It can be shown that the ratio of the phase velocity v_p along the pitch to the phase velocity along the coil is given by

$$\frac{v_p}{c} = \frac{p}{\sqrt{p^2 + (\pi d)^2}} = \sin \psi \tag{9-5-1}$$

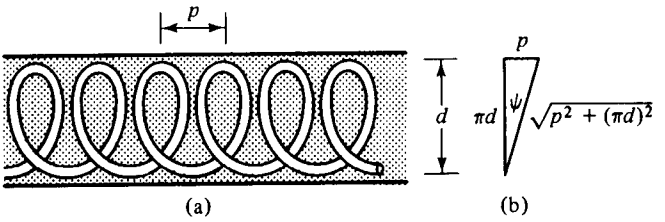

Figure 9-5-3 Helical slow-wave structure. (a) Helical coil. (b) One turn of helix.

where $c = 3 \times 10^8$ m/s is the velocity of light in free space
p = helix pitch
d = diameter of the helix
ψ = pitch angle

In general, the helical coil may be within a dielectric-filled cylinder. The phase velocity in the axial direction is expressed as

$$v_{p\epsilon} = \frac{p}{\sqrt{\mu\epsilon[p^2 + (\pi d)^2]}} \tag{9-5-2}$$

If the dielectric constant is too large, however, the slow-wave structure may introduce considerable loss to the microwave devices, thereby reducing their efficiency. For a very small pitch angle, the phase velocity along the coil in free space is approximately represented by

$$v_p \approx \frac{pc}{\pi d} = \frac{\omega}{\beta} \tag{9-5-3}$$

Figure 9-5-4 shows the ω-β (or Brillouin) diagram for a helical slow-wave structure. The helix ω-β diagram is very useful in designing a helix slow-wave structure. Once β is found, v_p can be computed from Eq. (9-5-3) for a given dimension of the helix. Furthermore, the group velocity of the wave is merely the slope of the curve as given by

$$v_{gr} = \frac{\partial\omega}{\partial\beta} \tag{9-5-4}$$

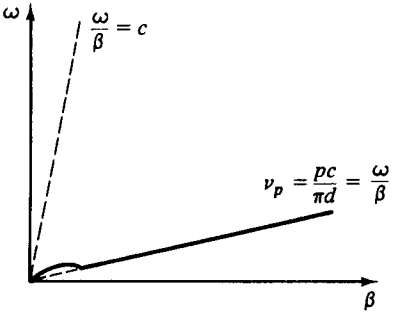

Figure 9-5-4 ω-β diagram for a helical structure.

In order for a circuit to be a slow-wave structure, it must have the property of periodicity in the axial direction. The phase velocity of some of the spatial harmonics in the axial direction obtained by Fourier analysis of the waveguide field may be smaller than the velocity of light. In the helical slow-wave structure a translation back or forth through a distance of one pitch length results in identically the same structure again. Thus the period of a helical slow-wave structure is its pitch.

In general, the field of the slow-wave structure must be distributed according to Floquet's theorem for periodic boundaries. Floquet's periodicity theorem states that:

> The steady-state solutions for the electromagnetic fields of a single propagating mode in a periodic structure have the property that fields in adjacent cells are related by a complex constant.

Mathematically, the theorem can be stated

$$E(x, y, z - L) = E(x, y, z)e^{j\beta_0 L} \tag{9-5-5}$$

where $E(x, y, z)$ is a periodic function of z with period$L$. Since β_0 is the phase constant in the axial direction, in a slow-wave structure β_0 is the phase constant of average electron velocity.

It is postulated that the solution to Maxwell's equations in a periodic structure can be written

$$E(x, y, z) = f(x, y, z)e^{-j\beta_0 Z} \tag{9-5-6}$$

where $f(x, y, z)$ is a periodic function of z with period L that is the period of the slow-wave structure.

For a periodic structure, Eq. (9-5-6) can be rewritten with z replaced by $z - L$:

$$E(x, y, z - L) = f(x, y, z - L)e^{-j\beta_0(z-L)} \tag{9-5-7}$$

Since $f(x, y, z - L)$ is a periodic function with period L, then

$$f(x, y, z - L) = f(x, y, z) \tag{9-5-8}$$

Substitution of Eq. (9-5-8) in (9-5-7) results in

$$E(x, y, z - L) = f(x, y, z)e^{-j\beta_0 z}e^{j\beta_0 L} \tag{9-5-9}$$

and substitution of Eq. (9-5-6) in (9-5-9) gives

$$E(x, y, z - L) = E(x, y, z)e^{j\beta_0 L} \tag{9-5-10}$$

This expression is the mathematical statement of Floquet's theorem, Eq. (9-5-5). Therefore Eq. (9-5-6) does indeed satisfy Floquet's theorem.

From the theory of Fourier series, any function that is periodic, single-valued, finite, and continuous may be represented by a Fourier series. Hence the field distribution function $E(x, y, z)$ may be expanded into a Fourier series of fundamental period L as

$$E(x, y, z) = \sum_{n=-\infty}^{\infty} E_n(x, y)e^{-j(2\pi n/L)z}e^{-j\beta_0 Z} = \sum_{n=-\infty}^{\infty} E_n(x, y)e^{-j\beta_n Z} \tag{9-5-11}$$

where

$$E_n(x, y) = \frac{1}{L}\int_0^L E(x, y, z)e^{j(2\pi n/L)Z}\,dz \tag{9-5-12}$$

are the amplitudes of n harmonics and

$$\beta_n = \mathrm{B}_0 + \frac{2\pi n}{L} \tag{4-5-13}$$

is the phase constant of the nth modes, where $n = -\infty, \ldots, -2, -1, 0, 1, 2, 3, \ldots, \infty$.

The quantities $E_n(x, y)e^{-j\beta_n Z}$ are known as spatial harmonics by analogy with time-domain Fourier series. The question is whether Eq. (9-5-11) can satisfy the electric wave equation, Eq. (2-1-20). Substitution of Eq. (9-5-11) into the wave equation results in

$$\nabla^2\left[\sum_{n=-\infty}^{\infty} E_n(x, y)e^{-j\beta_n Z}\right] - \gamma^2\left[\sum_{n=-\infty}^{\infty} E_n(x, y)e^{-j\beta_n Z}\right] = 0 \tag{9-5-14}$$

Since the wave equation is linear, Eq. (9-5-14) can be rewritten as

$$\sum_{n=-\infty}^{\infty} [\nabla^2 E_n(x, y)e^{-j\beta_n Z} - \gamma^2 E_n(x, y)e^{-j\beta_n Z)}] = 0 \tag{9-5-15}$$

It is evident from the preceding equation that if each spatial harmonic is itself a solution of the wave equation for each value of n, the summation of space harmonics also satisfies the wave equation of Eq. (9-5-14). This means that only the complete solution of Eq. (9-5-14) can satisfy the boundary conditions of a periodic structure.

Furthermore, Eq. (9-5-11) shows that the field in a periodic structure can be expanded as an infinite series of waves, all at the same frequency but with different phase velocities v_{pn}. That is

$$v_{pn} = \frac{\omega}{\beta_n} \equiv \frac{\omega}{\beta_0 + (2\pi n/L)} \tag{9-5-16}$$

The group velocity v_{gr}, defined by $v_{gr} = \partial\omega/\partial\beta$, is then given as

$$v_{gr} = \left[\frac{d(\beta_0 + 2\pi n/L)}{d\omega}\right]^{-1} = \frac{\partial\omega}{\partial\beta_0} \tag{9-5-17}$$

which is independent of n.

It is important to note that the phase velocity v_{pn} in the axial direction decreases for higher values of positive n and β_0. So it appears possible for a microwave of suitable n to have a phase velocity less than the velocity of light. It follows that interactions between the electron beam and microwave signal are possible and thus the amplification of active microwave devices can be achieved.

Figure 9-5-5 shows the ω-β (or Brillouin) diagram for a helix with several spatial harmonics. This ω-β diagram demonstrates some important properties needing more explanation. First, the second quadrant of the ω-β diagram indicates the negative phase velocity that corresponds to the negative n. This means that the electron beam moves in the positive z direction while the beam velocity coincides with

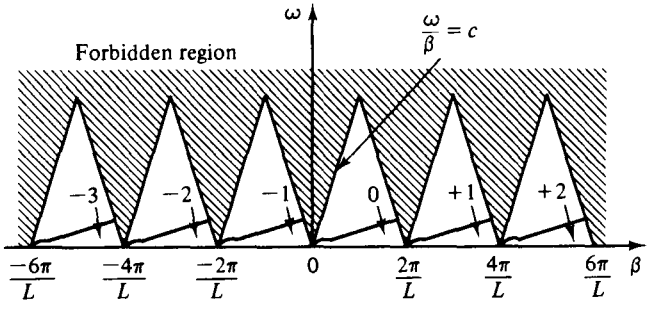

Figure 9-5-5 ω-β diagram of spatial harmonics for helical structure.

the negative spatial harmonic's phase velocity. This type of tube is called a *backward-wave oscillator*. Second, the shaded areas are the forbidden regions for propagation. This situation occurs because if the axial phase velocity of any spatial harmonic exceeds the velocity of light, the structure radiates energy. This property has been verified by experiments [10].

9-5-2 Amplification Process

A schematic diagram of a helix-type traveling-wave tube is shown in Fig. 9-5-6.

The slow-wave structure of the helix is characterized by the Brillouin diagram shown in Fig. 9-5-5. The phase shift per period of the fundamental wave on the structure is given by

$$\theta_1 = \beta_0 L \tag{9-5-18}$$

where $\beta_0 = \omega/v_0$ is the phase constant of the average beam velocity and L is the period or pitch.

Since the dc transit time of an electron is given by

$$T_0 = \frac{L}{v_o} \tag{9-5-19}$$

the phase constant of the nth space harmonic is

$$\beta_n = \frac{\omega}{v_0} = \frac{\theta_1 + 2\pi n}{v_0 T_0} = \beta_0 + \frac{2\pi n}{L} \tag{9-5-20}$$

In Eq. (9-5-20) the axial space-harmonic phase velocity is assumed to be synchronized with the beam velocity for possible interactions between the electron beam and electric field. That is,

$$v_{np} = v_0 \tag{9-5-21}$$

Equation (9-5-20) is identical to Eq. (9-5-13). In practice, the dc velocity of the electrons is adjusted to be slightly greater than the axial velocity of the electromagnetic wave for energy transfer. When a signal voltage is coupled into the helix, the axial electric field exerts a force on the electrons as a result of the following relationships:

$$\mathbf{F} = -e\mathbf{E} \qquad \text{and} \qquad \mathbf{E} = -\nabla V \tag{9-5-22}$$

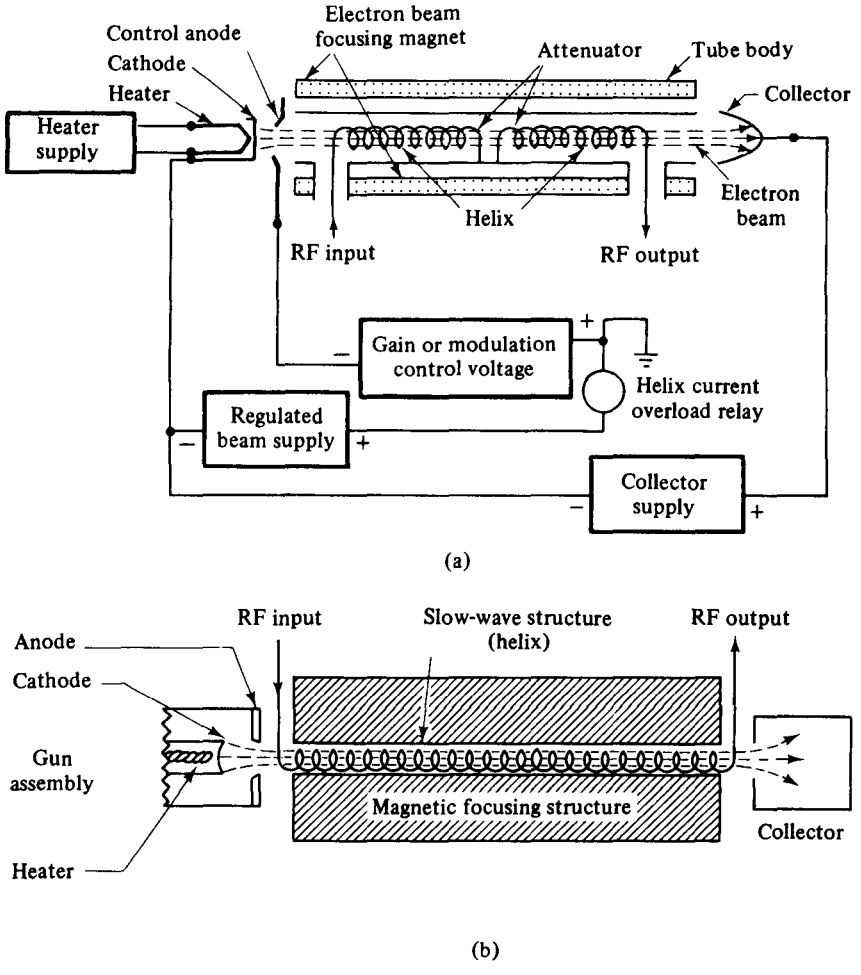

Figure 9-5-6 Diagram of helix traveling-wave tube: (a) schematic diagram of helix traveling-wave tube; (b) simplified circuit.

The electrons entering the retarding field are decelerated and those in the accelerating field are accelerated. They begin forming a bunch centered about those electrons that enter the helix during the zero field. This process is shown in Fig. 9-5-7.

Since the dc velocity of the electrons is slightly greater than the axial wave velocity, more electrons are in the retarding field than in the accelerating field, and a great amount of energy is transferred from the beam to the electromagnetic field. The microwave signal voltage is, in turn, amplified by the amplified field. The bunch continues to become more compact, and a larger amplification of the signal voltage occurs at the end of the helix. The magnet produces an axial magnetic field to prevent spreading of the electron beam as it travels down the tube. An attenuator placed near the center of the helix reduces all the waves traveling along the helix to nearly zero so that the reflected waves from the mismatched loads can be prevented from reaching the input and causing oscillation. The bunched electrons emerging

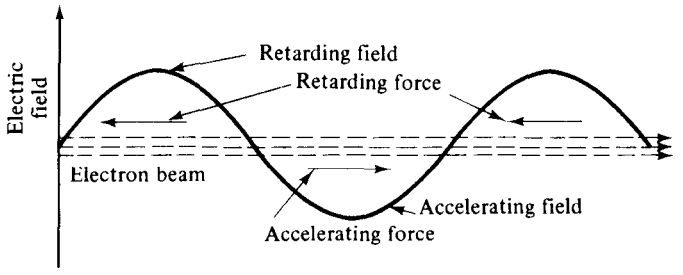

Figure 9-5-7 Interactions between electron beam and electric field.

from the attenuator induce a new electric field with the same frequency. This field, in turn, induces a new amplified microwave signal on the helix.

The motion of electrons in the helix-type traveling-wave tube can be quantitatively analyzed in terms of the axial electric field. If the traveling wave is propagating in the z direction, the z component of the electric field can be expressed as

$$E_z = E_1 \sin (\omega t - \beta_p z) \tag{9-5-23}$$

where E_1 is the magnitude of the electric field in the z direction. If $t = t_0$ at $z = 0$, the electric field is assumed maximum. Note that $\beta_p = \omega/v_p$ is the axial phase constant of the microwave, and v_p is the axial phase velocity of the wave.

The equation of motion of the electron is given by

$$m \frac{dv}{dt} = -eE_1 \sin (\omega t - \beta_p z) \tag{9-5-24}$$

Assume that the velocity of the electron is

$$v = v_0 + v_e \cos (\omega_e t + \theta_e) \tag{9-5-25}$$

Then

$$\frac{dv}{dt} = -v_e \omega_e \sin (\omega_e t + \theta_e) \tag{9-5-26}$$

where v_0 = dc electron velocity
v_e = magnitude of velocity fluctuation in the velocity-modulated electron beam
ω_e = angular frequency of velocity fluctuation
θ_e = phase angle of the fluctuation

Substitution of Eq. (9-5-26) in Eq. (9-5-24) yields

$$m v_e \omega_e \sin (\omega_e t + \omega_e) = eE_1 \sin (\omega t - \beta_p z) \tag{9-5-27}$$

For interactions between the electrons and the electric field, the velocity of the velocity-modulated electron beam must be approximately equal to the dc electron velocity. This is

$$v \approx v_0 \tag{9-5-28}$$

Hence the distance z traveled by the electrons is

$$z = v_0(t - t_0) \tag{9-5-29}$$

and

$$mv_e\omega_e \sin(\omega_e t + \theta_e) = eE_1 \sin[\omega t - \beta_p v_0(t - t_0)] \tag{9-5-30}$$

Comparison of the left and right-hand sides of Eq. (9-5-30) shows that

$$v_e = \frac{eE_1}{m\omega_e} \tag{9-5-31}$$

$$\omega_e = \beta_p(v_p - v_0)$$

$$\theta_e = \beta_p v_0 t_0$$

It can be seen that the magnitude of the velocity fluctuation of the electron beam is directly proportional to the magnitude of the axial electric field.

9-5-3 Convection Current

In order to determine the relationship between the circuit and electron beam quantities, the convection current induced in the electron beam by the axial electric field and the microwave axial field produced by the beam must first be developed. When the space-charge effect is considered, the electron velocity, the charge density, the current density, and the axial electric field will perturbate about their averages or dc values. Mathematically, these quantities can be expressed as

$$v = v_0 + v_1 e^{j\omega t - \gamma z} \tag{9-5-32}$$

$$\rho = \rho_0 + \rho_1 e^{j\omega t - \gamma z} \tag{9-5-33}$$

$$J = -J_0 + J_1 e^{j\omega t - \gamma z} \tag{9-5-34}$$

$$E_z = E_1 e^{j\omega t - \gamma z} \tag{9-5-35}$$

where $\gamma = \alpha_e + j\beta_e$ is the propagation constant of the axial waves. The minus sign is attached to J_0 so that J_0 may be a positive in the negative z direction. For a small signal, the electron beam-current density can be written

$$J = \rho v \approx -J_0 + J_1 e^{j\omega t - \gamma z} \tag{9-5-36}$$

where $-J_0 = \rho_0 v_0$, $J_1 = \rho_1 v_0 + \rho_0 v_1$, and $\rho_1 v_1 \approx 0$ have been replaced. If an axial electric field exists in the structure, it will perturbate the electron velocity according to the force equation. Hence the force equation can be written

$$\frac{dv}{dt} = -\frac{e}{m}E_1 e^{j\omega t - \gamma z} = \left(\frac{\partial}{\partial t} + \frac{dz}{dt}\frac{\partial}{\partial z}\right)v = (j\omega - \gamma v_0)v_1 e^{j\omega t - \gamma z} \tag{9-5-37}$$

where dz/dt has been replaced by v_0. Thus

$$v_1 = \frac{-e/m}{j\omega - \gamma v_0}E_1 \tag{9-5-38}$$

In accordance with the law of conservation of electric charge, the continuity equation can be written

$$\nabla \cdot J + \frac{\partial \rho}{\partial t} = (-\gamma J_1 + j\omega\rho_1)e^{j\omega t - \gamma z} = 0 \tag{9-5-39}$$

It follows that

$$\rho_1 = -\frac{j\gamma J_1}{\omega} \tag{9-5-40}$$

Substitution Eqs. (9-5-38) and (9-5-40) in

$$J_1 = \rho_1 v_0 + \rho_0 v_1 \tag{9-5-44}$$

gives

$$J_1 = J\frac{\omega}{v_0}\frac{e}{m}\frac{J_0}{(j\omega - \gamma v_0)^2}E_1 \tag{9-5-42}$$

where $-J_0 = \rho_0 v_0$ has been replaced. If the magnitude of the axial electric field is uniform over the cross-sectional area of the electron beam, the spatial ac current i will be proportional to the dc current I_0 with the same proportionality constant for J_1 and J_0. Therefore the convection current in the electron beam is given by

$$i = j\frac{\beta_e I_0}{2V_0(j\beta_e - \gamma)^2}E_1 \tag{9-5-43}$$

where $\beta_e \equiv \omega/v_0$ is defined as the phase constant of the velocity-modulated electron beam and $v_0 = \sqrt{(2e/m)V_0}$ has been used. This equation is called the *electronic equation*, for it determines the convection current induced by the axial electric field. If the axial field and all parameters are known, the convection current can be found by means of Eq. (9-5-43).

9-5-4 Axial Electric Field

The convection current in the electron beam induces an electric field in the slow-wave circuit. This induced field adds to the field already present in the circuit and causes the circuit power to increase with distance. The coupling relationship between the electron beam and the slow-wave helix is shown in Fig. 9-5-8.

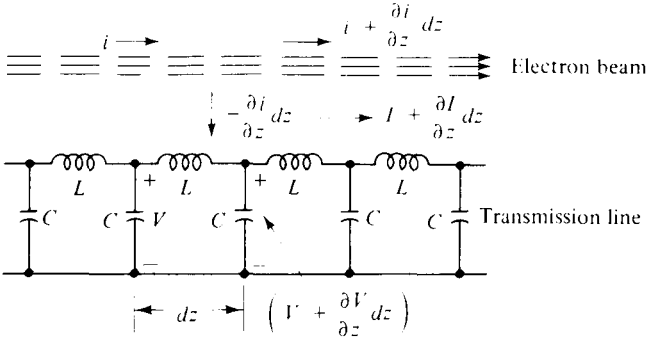

Figure 9-5-8 Electron beam coupled to equivalent circuit of a slow-wave helix.

For simplicity, the slow-wave helix is represented by a distributed lossless transmission line. The parameters are defined as follows:

L = inductance per unit length
C = capacitance per unit length
I = alternating current in transmission line
V = alternating voltage in transmission line
i = convection current

Since the transmission line is coupled to a convection-electron beam current, a current is then induced in the line. The current flowing into the left-end portion of the line of length dz is i, and the current flowing out of the right end of dz is $[i + (\partial i/\partial z)\, dz]$. Since the net change of current in the length dz must be zero, however, the current flowing out of the electron beam into the line must be $[-(\partial i/\partial z)\, dz]$. Application of transmission-line theory and Kirchhoff's current law to the electron beam results, after simplification, in

$$\frac{\partial I}{\partial z} = -C\frac{\partial V}{\partial t} - \frac{\partial i}{\partial z} \tag{9-5-44}$$

Then

$$-\gamma I = -j\omega CV + \gamma i \tag{9-5-45}$$

in which $\partial/\partial z = -\gamma$ and $\partial/\partial t = j\omega$ are replaced.

From Kirchhoff's voltage law the voltage equation, after simplification, is

$$\frac{\partial V}{\partial z} = -L\frac{\partial I}{\partial t} \tag{9-5-46}$$

Similarly,

$$-\gamma V = -j\omega LI \tag{9-5-47}$$

Elimination of the circuit current I from Eqs. (9-5-45) and (9-5-46) yields

$$\gamma^2 V = -V\omega^2 LC - \gamma i j\omega L \tag{9-5-48}$$

If the convection-elecron beam current is not present, Eq. (9-5-48) reduces to a typical wave equation of a transmission line. When $i = 0$, the propagation constant is defined from Eq. (9-5-48) as

$$\gamma_0 \equiv j\omega\sqrt{LC} \tag{9-5-49}$$

and the characteristic impedance of the line can be determined from Eqs. (9-5-45) and (9-5-47):

$$Z_0 = \sqrt{\frac{L}{C}} \tag{9-5-50}$$

When the electron beam current is present, Eq. (9-5-48) can be written in terms of Eqs. (9-5-49) and (9-5-50):

$$V = \frac{\gamma\gamma_0 Z_0}{\gamma^2 - \gamma_0^2} i \tag{9-5-51}$$

Since $E_z = -\nabla V = -(\partial V/\partial z) = \gamma V$, the axial electric field is given by

$$E_1 = -\frac{\gamma^2\gamma_0 Z_0}{\gamma^2 - \gamma_0^2} i \tag{9-5-52}$$

This equation is called the *circuit equation* because it determines how the axial electric field of the slow-wave helix is affected by the spatial ac electron beam current.

9-5-5 Wave Modes

The wave modes of a helix-type traveling-wave tube can be determined by solving the electronic and circuit equations simultaneously for the propagation constants. Each solution for the propagation constants represents a mode of traveling wave in the tube. It can be seen from Eqs. (9-5-43) and (9-5-52) that there are four distinct solutions for the propagation constants. This means that there are four modes of traveling wave in the O-type traveling-wave tube. Substitution of Eq. (9-5-43) in Eq. (9-5-52) yields

$$(\gamma^2 - \gamma_0^2)(j\beta_e - \gamma)^2 = -j\frac{\gamma^2\gamma_0 Z_0 \beta_e I_0}{2V_o} \tag{9-5-53}$$

Equation (9-5-53) is of fourth order in γ and thus has four roots. Its exact solutions can be obtained with numerical methods and a digital computer. However, the approximate solutions may be found by equating the dc electron beam velocity to the axial phase velocity of the traveling wave, which is equivalent to setting

$$\gamma_0 = j\beta_e \tag{9-5-54}$$

Then Eq. (9-5-53) reduces to

$$(\gamma - j\beta_e)^3(\gamma + j\beta_e) = 2C^3\beta_e^2\gamma^2 \tag{9-5-55}$$

where C is the traveling-wave tube gain parameter and is defined as

$$C \equiv \left(\frac{I_0 Z_0}{4V_0}\right)^{1/3} \tag{9-5-56}$$

It can be seen from Eq. (9-5-55) that there are three forward traveling waves corresponding to $e^{-j\beta_e z}$ and one backward traveling wave corresponding to $e^{+j\beta_e z}$. Let the propagation constant of the three forward traveling waves be

$$\gamma = j\beta_e - \beta_e C\delta \tag{9-5-57}$$

where it is assumed that $C\delta \ll 1$.

Substitution of Eq. (9-5-57) in Eq. (9-5-55) results in

$$(-\beta_e C\delta)^3(j2\beta_e - \beta_e C\delta) = 2C^3\beta_e^2(-\beta_e^2 - 2j\beta_e^2 C\delta + \beta_e^2 C^2\delta^2) \tag{9-5-58}$$

Since $C\delta \ll 1$, Eq. (9-5-58) is reduced to

$$\delta = (-j)^{1/3} \tag{9-5-59}$$

From the theory of complex variables the three roots of $(-j)$ can be plotted in Fig. 9-5-9.

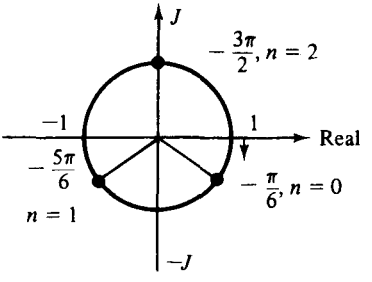

Figure 9-5-9 Three roots of $(-j)$.

Equation (9-5-59) can be written in exponential form as

$$\delta = (-j)^{1/3} = e^{-j[(\pi/2+2n\pi)/3]} \qquad (n = 0, 1, 2) \tag{9-5-60}$$

The first root δ_1 at $n = 0$ is

$$\delta_1 = e^{-j\pi/6} = \frac{\sqrt{3}}{2} - j\frac{1}{2} \tag{9-5-61}$$

The second root δ_2 at $n = 1$ is

$$\delta_2 = e^{-j5\pi/6} = -\frac{\sqrt{3}}{2} - j\frac{1}{2} \tag{9-5-62}$$

The third root δ_3 at $n = 2$ is

$$\delta_3 = e^{-j3\pi/2} = j \tag{9-5-63}$$

The fourth root δ_4 corresponding to the backward traveling wave can be obtained by setting

$$\gamma = -j\beta_e - \beta_e C\delta_4 \tag{9-5-64}$$

Similarly,

$$\delta_4 = -j\frac{C^2}{4} \tag{9-5-65}$$

Thus the values of the four propagation constants γ are given by

$$\gamma_1 = -\beta_e C\frac{\sqrt{3}}{2} + j\beta_e\left(1 + \frac{C}{2}\right) \tag{9-5-66}$$

$$\gamma_2 = \beta_e C\frac{\sqrt{3}}{2} + j\beta_e\left(1 + \frac{C}{2}\right) \tag{9-5-67}$$

$$\gamma_3 = j\beta_e(1 - C) \tag{9-5-68}$$

$$\gamma_4 = -j\beta_e\left(1 - \frac{C^3}{4}\right) \tag{9-5-69}$$

These four propagation constants represent four different modes of wave propagation in the O-type helical traveling-wave tube. It is concluded that the wave corresponding to γ_1 is a forward wave and that its amplitude grows exponentially with distance; the wave corresponding to γ_2 is also a forward wave, but its amplitude decays exponentially with distance; the wave corresponding to γ_3 is also a forward wave, but its amplitude remains constant; the fourth wave corresponding to γ_4 is a backward wave, and there is no change in amplitude. The growing wave propagates at a phase velocity slightly lower than the electron beam velocity, and the energy flows from the electron beam to the wave. The decaying wave propagates at the same velocity as that of the growing wave, but the energy flows from the wave to the electron beam. The constant-amplitude wave travels at a velocity slightly higher than the electron beam velocity, but no net energy exchange occurs between the wave and the electron beam. The backward wave progresses in the negative z direction with a velocity slightly higher than the velocity of the electron beam inasmuch as the typical value of C is about 0.02.

9-5-6 Gain Consideration

For simplicity, it is assumed that the structure is perfectly matched so that there is no backward traveling wave. Such is usually the case. Even though there is a reflected wave from the output end of the tube traveling backward toward the input end, the attenuator placed around the center of the tube subdues the reflected wave to a minimum or zero level. Thus the total circuit voltage is the sum of three forward voltages corresponding to the three forward traveling waves. This is equivalent to

$$V(z) = V_1 e^{-\gamma_1 z} + V_2 e^{-\gamma_2 z} + V_3 e^{-\gamma_3 z} = \sum_{n=1}^{3} V_n e^{-\gamma_n z} \tag{9-5-70}$$

The input current can be found from Eq. (9-5-43) as

$$i(z) = -\sum_{n=1}^{3} \frac{I_0}{2V_0 C^2} \frac{V_n}{\delta_n^2} e^{-\gamma_n z} \tag{9-5-71}$$

in which $C\delta \ll 1$, $E_1 = \gamma V$, and $\gamma = j\beta_e(1 - C\delta)$ have been used.

The input fluctuating component of velocity of the total wave may be found from Eq. (9-5-38) as

$$v_1(z) = \sum_{n=1}^{3} j \frac{v_0}{2V_0 C} \frac{V_n}{\delta_n} e^{-\gamma_n z} \tag{9-5-72}$$

where $E_1 = \gamma V$, $C\delta \ll 1$, $\beta_e v_0 = \omega$, and $v_0 = \sqrt{(2e/m)V_0}$ have been used.

To determine the amplification of the growing wave, the input reference point is set at $z = 0$ and the output reference point is taken at $z = \ell$. It follows that at $z = 0$ the voltage, current, and velocity at the input point are given by

$$V(0) = V_1 + V_2 + V_3 \tag{9-5-73}$$

$$i(0) = -\frac{I_0}{2V_0 C^2}\left(\frac{V_1}{\delta_1^2} + \frac{V_2}{\delta_2^2} + \frac{V_3}{\delta_3^2}\right) \tag{9-5-74}$$

$$v_1(0) = -j\frac{v_0}{2V_0C}\left(\frac{V_1}{\delta_1} + \frac{V_2}{\delta_2} + \frac{V_3}{\delta_3}\right) \tag{9-5-75}$$

The simultaneous solution of Eqs. (9-5-73), (9-5-74), and (9-5-75) with $i(0) = 0$ and $v_1(0) = 0$ is

$$V_1 = V_2 = V_3 = \frac{V(0)}{3} \tag{9-5-76}$$

Since the growing wave is increasing exponentially with distance, it will predominate over the total voltage along the circuit. When the length ℓ of the slow-wave structure is sufficiently large, the output voltage will be almost equal to the voltage of the growing wave. Substitution of Eqs. (9-5-66) and (9-5-76) in Eq. (9-5-70) yields the output voltage as

$$V(\ell) \approx \frac{V(0)}{3}\exp\left(\frac{\sqrt{3}}{2}\beta_e C\ell\right)\exp\left[-j\beta_e\left(1 + \frac{C}{2}\right)\ell\right] \tag{9-5-77}$$

The factor $\beta_e\ell$ is conventionally written $2\pi N$, where N is the circuit length in electronic wavelength—that is,

$$N = \frac{\ell}{\lambda_e} \qquad \text{and} \qquad \beta_e = \frac{2\pi}{\lambda_e} \tag{9-5-78}$$

The amplitude of the output voltage is then given by

$$V(\ell) = \frac{V(0)}{3}\exp\left(\sqrt{3}\,\pi NC\right) \tag{9-5-79}$$

The output power gain in decibels is defined as

$$A_p \equiv 10\log\left|\frac{V(\ell)}{V(0)}\right|^2 = -9.54 + 47.3NC \qquad \text{dB} \tag{9-5-80}$$

where NC is a numerical number.

The output power gain shown in Eq. (9-5-80) indicates an initial loss at the circuit input of 9.54 dB. This loss results from the fact that the input voltage splits into three waves of equal magnitude and the growing wave voltage is only one-third the total input voltage. It can also be seen that the power gain is proportional to the length N in electronic wavelength of the slow-wave structure and the gain parameter C of the circuit.

Example 9-5-1: Operation of Traveling-Wave Tube (TWT)

A traveling-wave tube (TWT) operates under the following parameters:

Beam voltage: $V_0 = 3$ kV
Beam current: $I_0 = 30$ mA
Characteristic impedance of helix: $Z_0 = 10\ \Omega$
Circuit length: $N = 50$
Frequency: $f = 10$ GHz

Determine: (**a**) the gain parameter C; (**b**) the output power gain A_p in decibels; and (**c**) all four propagation constants.

Solution

a. From Eq. (9-5-56) the gain parameter is

$$C = \left(\frac{I_0 Z_0}{4V_0}\right)^{1/3} = \left(\frac{30 \times 10^{-3} \times 10}{4 \times 3 \times 10^3}\right)^{1/3} = 2.92 \times 10^{-2}$$

b. From Eq. (9-5-80) the output power gain is

$$A_p = -9.54 + 4.73\,NC = -9.54 + 47.3 \times 50 \times 2.92 \times 10^{-2} = 59.52 \text{ dB}$$

c. The four propagation constants are

$$\beta_e = \frac{\omega}{v_0} = \left(\frac{2\pi \times 10^{10}}{0.593 \times 10^6 \sqrt{3} \times 10}\right) = 1.93 \times 10^3 \text{ rad/m}$$

$$\gamma_1 = -\beta_e C \frac{\sqrt{3}}{2} + j\beta_e\left(1 + \frac{C}{2}\right)$$

$$= -1.93 \times 10^3 \times 2.92 \times 10^{-2} \times 0.87 + j1.93 \times 10^3\left(1 + \frac{2.92 \times 10^{-2}}{2}\right)$$

$$= -49.03 + j1952$$

$$\gamma_2 = \beta_e C \frac{\sqrt{3}}{2} + j\beta_e\left(1 + \frac{C}{2}\right) = 49.03 + j1952$$

$$\gamma_3 = j\beta_e(1 - C) = j1.93 \times 10^3(1 - 2.92 \times 10^{-2})$$

$$= j1872.25$$

$$\gamma_4 = -j\beta_e\left(1 - \frac{C^3}{4}\right) = -j1.93 \times 10^3\left[1 - \frac{(2.92 \times 10^{-2})^3}{4}\right]$$

$$= -j1930$$

9-6 COUPLED-CAVITY TRAVELING-WAVE TUBES

Helix traveling-wave tubes (TWTs) produce at most up to several kilowatts of average power output. Here we describe coupled-cavity traveling-wave tubes, which are used for high-power applications.

9-6-1 Physical Description

The term *coupled cavity* means that a coupling is provided by a long slot that strongly couples the magnetic component of the field in adjacent cavities in such a manner that the passband of the circuit is mainly a function of this one variable. Figure 9-6-1 shows two coupled-cavity circuits that are principally used in traveling-wave tubes.

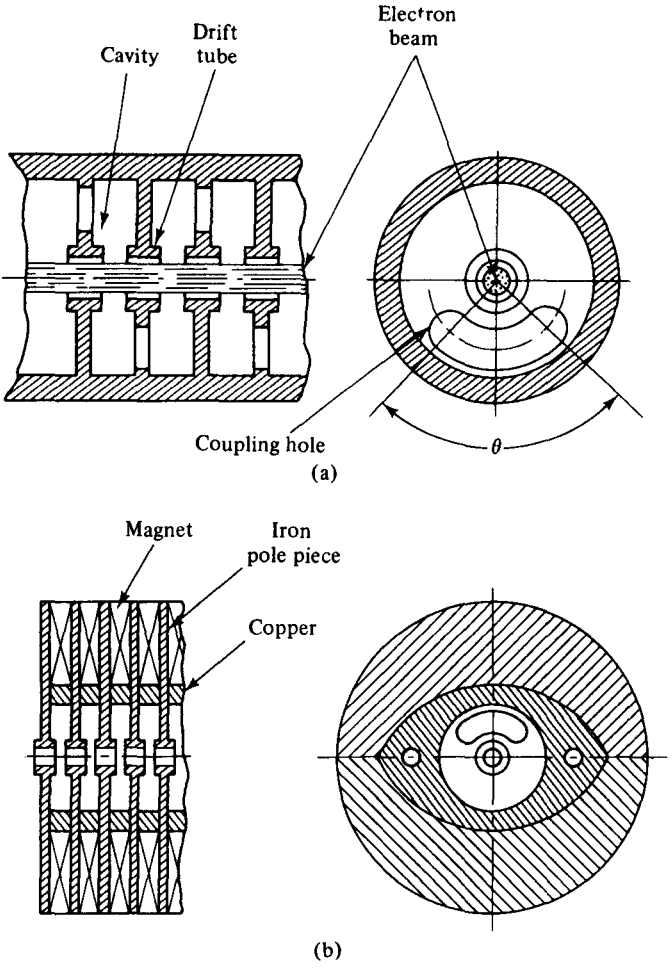

Figure 9-6-1 Coupled-cavity circuits in the TWTs. (a) Basic coupled-cavity circuit. (b) Coupled-cavity circuit with integral periodic-permanent-magnet (PPM) focusing. (*After J. T. Mendel [15]; reprinted by permission of IEEE.*)

As far as the coupling effect is concerned, there are two types of coupled-cavity circuits in traveling-wave tubes. The first type consists of the fundamentally forward-wave circuits that are normally used for pulse applications requiring at least half a megawatt of peak power. These coupled-cavity circuits exhibit negative mutual inductive coupling between the cavities and operate with the fundamental space harmonic. The cloverleaf [12] and centipede circuits [13] (see Fig. 9-6-2) belong to this type. The second type is the first space-harmonic circuit, which has positive mutual coupling between the cavities. These circuits operate with the first spatial harmonic and are commonly used for pulse or continuous wave (CW) applications from one to several hundred kilowatts of power output [14]. In addition, the long-slot circuit of the positive mutual coupling-cavity circuit operates at the fundamental spatial

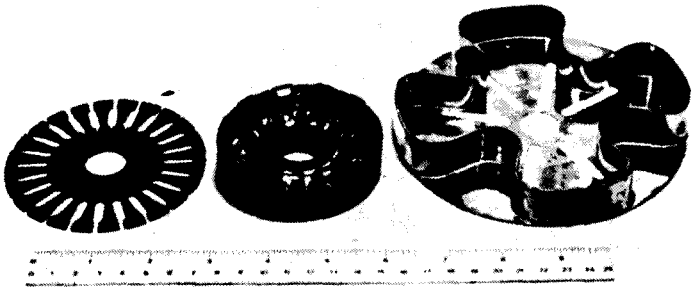

Figure 9-6-2 Centipede and cloverleaf coupled-cavity circuits. (*After A. Staprans et al. [7]; reprinted by permission of IEEE.*)

Figure 9-6-3 Space-harmonic coupled-cavity circuits. (*After A. Staprans et al. [7]; reprinted by permission of IEEE, Inc.*)

harmonic with a higher frequency mode. This circuit is suitable for megawatt power output. Figure 9-6-3 shows several space-harmonic coupled-cavity circuits.

9-6-2 Principles of Operation

Any repetitive series of lumped LC elements constitute a propagating filter-type circuit. The coupled cavities in the traveling-wave tube are usually highly over-coupled, resulting in a bandpass-filter-type characteristic. When the slot angle (θ) as shown in Fig. 9-6-1(a) is larger than 180°, the passband is close to its practical limits. The drift tube is formed by the reentrant part of the cavity, just as in the case of a klystron. During the interaction of the RF field and the electron beam in the traveling-wave tube a phase change occurs between the cavities as a function of frequency. A decreasing phase characteristic is reached if the mutual inductance of the coupling slot is positive, whereas an increasing phase characteristic is obtained if the mutual inductive coupling of the slot is negative [12].

The amplification of the traveling-wave tube interaction requires that the electron beam interact with a component of the circuit field that has an increasing phase characteristic with frequency. The circuit periodicity can give rise to field components that have phase characteristics [16] as shown in Fig. 9-6-4. In Fig. 9-6-4 the angular frequency (ω) is plotted as a function of the phase shift ($\beta \ell$) per cavity. The ratio of ω to β is equal to the phase velocity. For a circuit having positive mutual in-

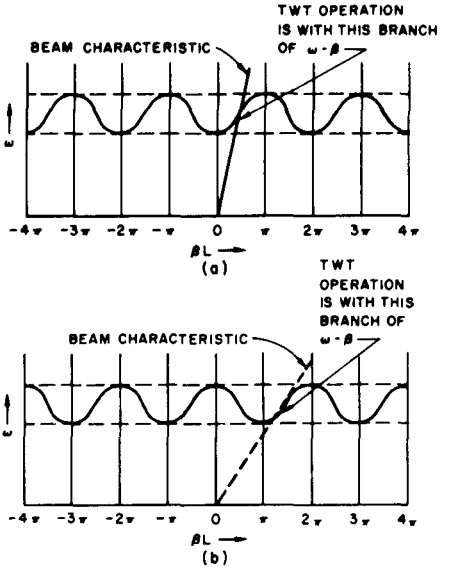

Figure 9-6-4 ω-β diagrams for coupled-cavity circuits. (a) Fundamental forward-wave circuit (negative mutual inductance coupling between cavities). (b) Fundamental backward-wave circuit (positive mutual inductive coupling between cavities). (*After A. Staprans et al. [7]; reprinted by permission of IEEE, Inc.*)

ductive coupling between the cavities, the electron beam velocity is adjusted to be approximately equal to the phase velocity of the first forward-wave spatial harmonic. For the circuits with negative mutual inductive coupling, the fundamental branch component of the circuit wave is suitable for synchronism with the electron beam and is normally used by the traveling-wave tube. The coupled-cavity equivalent circuit has been developed by Curnow [17] as shown in Fig. 9-6-5.

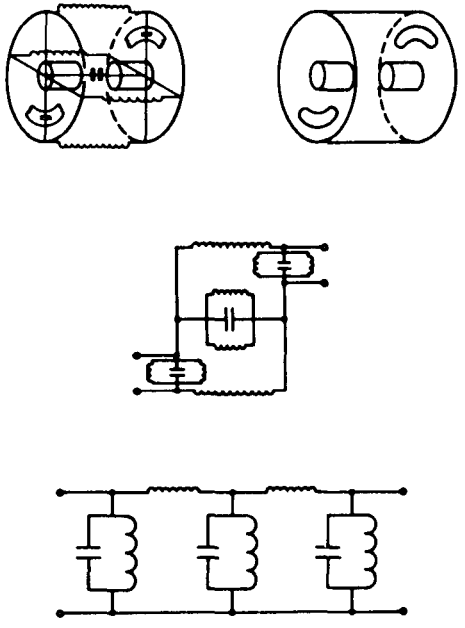

Figure 9-6-5 Equivalent circuits for a slot-coupled cavity. (*After A. Staprans et al. [7]; reprinted by permission of IEEE, Inc.*)

In Fig. 9-6-5 inductances are used to represent current flow and capacitors to represent the electric fields of the cavities. The circuit can be evolved into a fairly simple configuration. Loss in the cavities can be approximately calculated by adding resistance in series with the circuit inductance.

9-6-3 Microwave Characteristics

When discussing the power capability of traveling-wave tubes, it is important to make a clear distinction between the average and the peak power because these two figures are limited by totally different factors. The average power at a given frequency is almost always limited by thermal considerations relative to the RF propagating circuit. However, the peak RF power capability depends on the voltage for which the tube can be designed. The beam current varies as the three-half power of

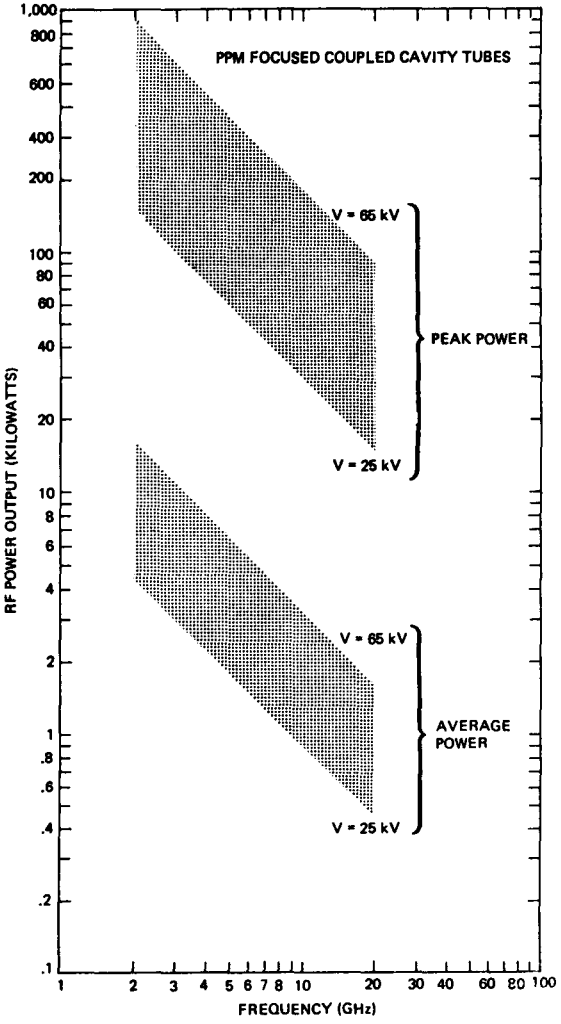

Figure 9-6-6 Peak and average power capability of typical TWTs in field use. (*After J. T. Mendel [15]; reprinted by permission of IEEE., Inc.*)

the voltage, and the product of the beam current and the voltage determines the total beam power. That is,

$$I_{\text{beam}} = KV_0^{3/2} \tag{9-6-1}$$

$$P_{\text{beam}} = KV_0^{5/2} \tag{9-6-2}$$

where V_0 is the beam voltage and K is the electron-gun perveance.

For a solid-beam electron gun with good optics, the perveance is generally considered to be between 1 to 2×10^{-6}. Once the perveance is fixed, the required voltage for a given peak beam power is then uniquely determined. Figures 9-6-6 and 9-6-7 demonstrate the difference between peak and average power capability and the difference between periodic-permanent-magnet (PPM) and solenoid-focused designs [15].

Coupled-cavity traveling-wave tubes are constructed with a limited amount of gain per section of cavities to ensure stability. Each cavity section is terminated by

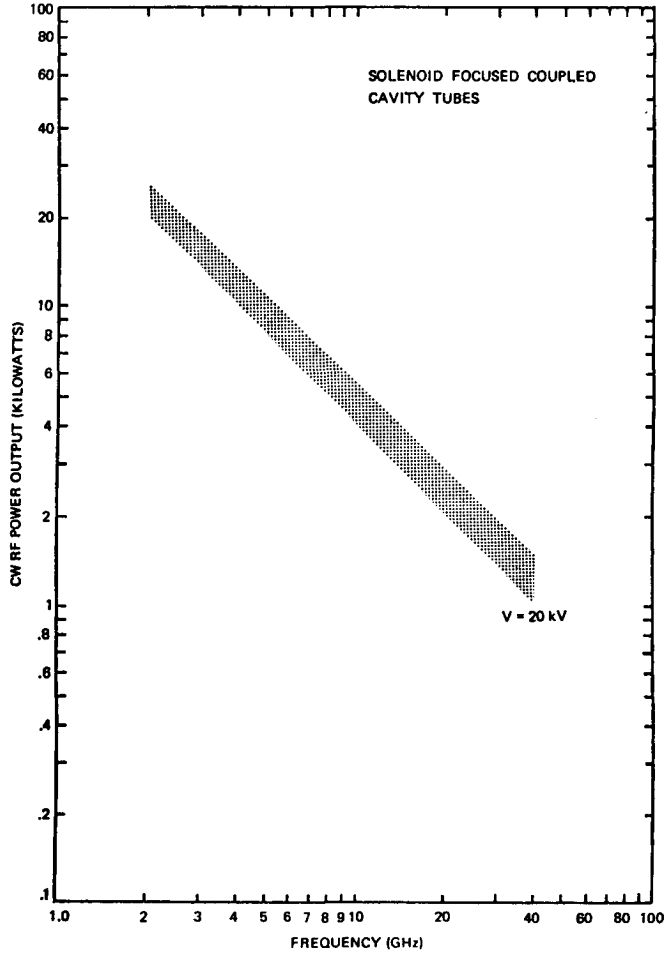

Figure 9-6-7 CW power capability of TWTs operating at nearly 20 kV. (*After J. T. Mendel [15]; reprinted by permission of IEEE., Inc.*)

either a matched load or an input or output line in order to reduce gain variations with frequency. Cavity sections are cascaded to achieve higher tube gain than can be tolerated in one section of cavities. Stable gain greater than 60 dB can be obtained over about 30% bandwidth by this method.

The overall efficiency of coupled-cavity traveling-wave tubes is determined by the amount of energy converted to RF energy and the energy dissipated by the collector. Interaction efficiencies from 10 to 40% have been achieved from coupled-cavity traveling-wave tubes. Overall efficiencies of 20 to 55% have been obtained [7].

9-7 HIGH-POWER AND GRIDDED-CONTROL TRAVELING-WAVE TUBES

Coupled-cavity traveling-wave tubes are the most versatile devices used for amplification at microwave frequencies with high gain, high power, high efficiency, and wide bandwidth. The present state of the art for U.S. high-power gridded tubes is shown in Fig. 9-7-1. High-power TWTs have four main sections: electron gun for electron emission, slow-wave structure for effective beam interaction, magnetic circuit for beam focusing, and collector structure for collecting electron beams and dissipating heat energy. Specifically, the physical components of a coupled-cavity traveling-wave tube consist of an electron emitter, a shadow grid, a control grid, a modulating anode, a coupled-cavity circuit, a solenoid magnetic circuit, and a collector depression structure (see Fig. 9-7-2).

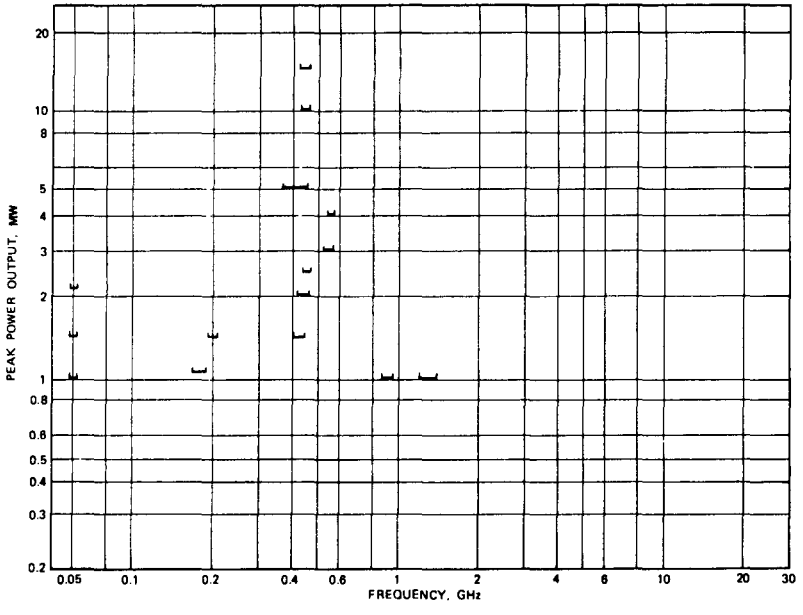

Figure 9-7-1 State of the art for U.S. high-power gridded tubes.

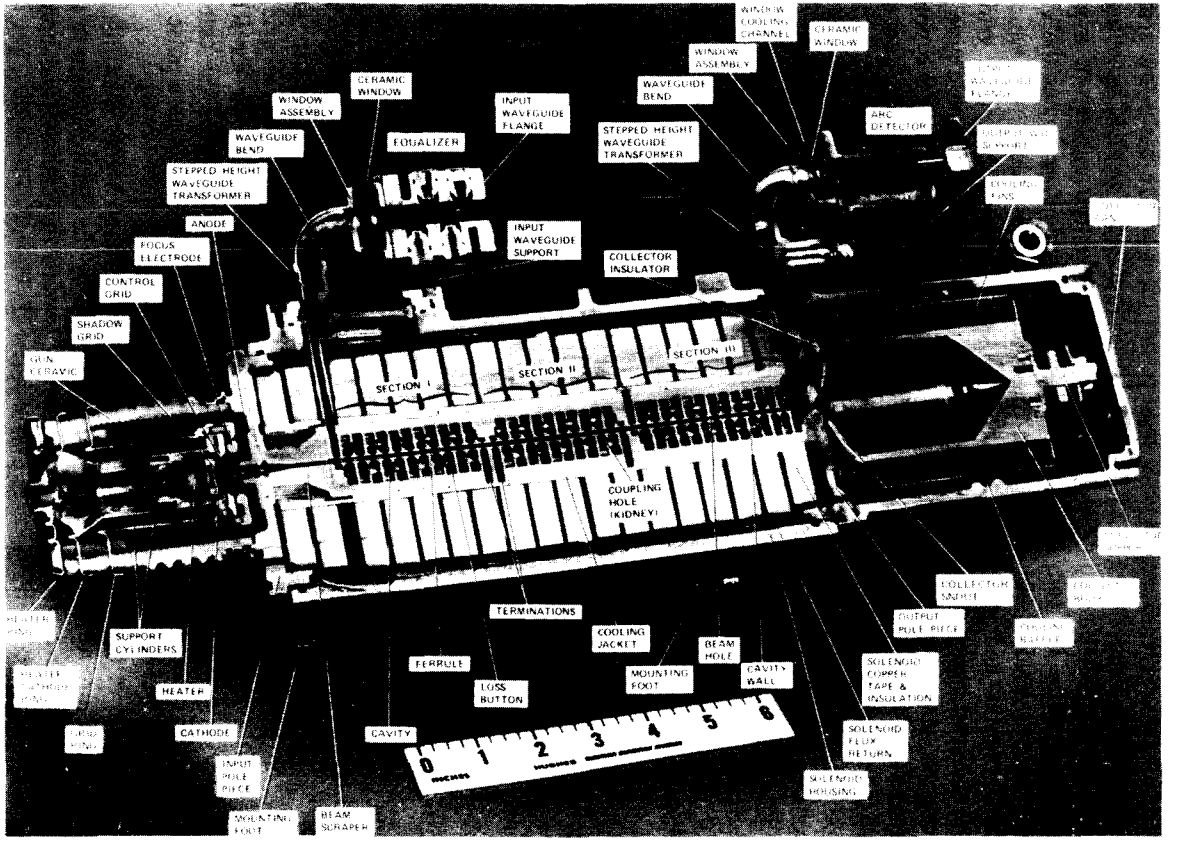

Figure 9-7-2 Cutaway of a coupled-cavity traveling-wave tube. (*Courtesy of Hughes Aircraft Company, Electron Dynamics Division.*)

After electrons are emitted from the cathode, the electron beam has a tendency to spread out because of the electron-repelling force. On the other hand, the electron beam must be small enough for effective interaction with the slow-wave circuit. Usually the diameter of the electron beam is smaller than one-tenth wavelength of the signal. Coupled-cavity traveling-wave high-power tubes utilize a shadow-grid technique to control the electron beam; so the device is called a *gridded traveling-wave tube* (GTWT). As shown in Fig. 9-7-3 [18], the electron emitter of a gridded traveling-wave tube has two control electrodes: one shadow grid near the cathode and one control grid slightly away from the cathode. The shadow grid, which is at cathode potential and interposed between the cathode and the control grid, suppresses electron emission from those portions of the cathode that would give rise to interception at the control grid. The control grid, which is at a positive potential, controls the electron beam. These grids can control far greater beam power than would otherwise be possible.

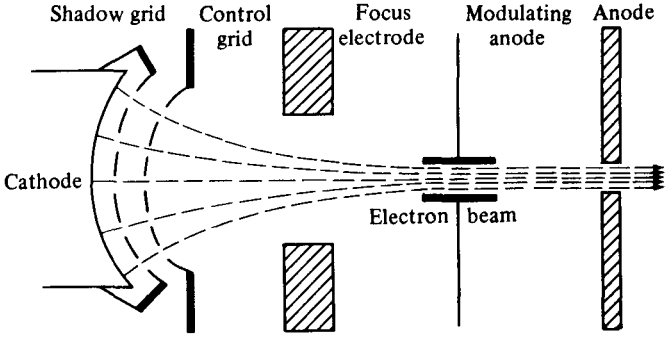

Figure 9-7-3 Electron emitter with control electrodes for gridded high-power TWT.

In general, an anode modulation technique is frequently used in traveling-wave tubes to eliminate voltage pulsing through the lower unstable beam voltage and to reduce modulator power requirements for high-power pulse output. In gridded traveling-wave tubes the modulator applies a highly regulated positive grid drive voltage with respect to the cathode to turn the electron beam on for RF amplification. An unregulated negative grid bias voltage with respect to the cathode is used to cut the electron beam off. Thus the anode modulator acts as a pulse switch for the electron beam of the gridded traveling-wave tube.

The anode of the electron gun is operated at a voltage higher than that of the slow-wave structure to prevent positive ions, formed by the electron beam in the region of the slow-wave structure, from draining toward the cathode and bombarding it.

9-7-1 High Efficiency and Collector Voltage Depression

After passing through the output cavity, the electron beam strikes a collector electrode. The function of the collector electrode could be performed by replacing the second grid of the output cavity with a solid piece of metal. However, using a sepa-

rate electrode may have two advantages. First, the collector can be made as large as desired in order to collect the electron beam at a lower density, thus minimizing localized heating. If the collector were part of the slow-wave circuit, its size would be limited by the maximum gap capacitance consistent with good high-frequency performance. Second, using a separate collector can reduce its potential considerably below the beam voltage in the RF interaction region, thereby reducing the power dissipated in the collector and increasing the overall efficiency of the device. Gridded traveling-wave high-power tubes have a separate collector that dissipates the electrons in the form of heat. A cooling mechanism absorbs the heat by thermal conduction to a cooler surface.

The efficiency of a gridded traveling-wave high-power tube is the ratio of the RF power output to the product of cathode voltage (beam voltage) and cathode current (beam current). It may be expressed in terms of the product of the electronic efficiency and the circuit efficiency. The electronic efficiency expresses the percentage of the dc or pulsed input power that is converted into RF power on the slow-wave structure. The circuit efficiency, on the other hand, determines the percentage of dc input power that is delivered to the load exterior to the tube. The electron beam does not extract energy from any dc power supply unless the electrons are actually collected by an electrode connected to that power supply. If a separate power supply is connected between cathode and collector and if the cavity grids intercept a negligible part of the electron beam, the power supply between the cathode and collector will be the only one supplying power to the tube. For a gridded traveling-wave tube, the collector voltage is normally operated at about 40% of the cathode voltage. Thus the overall efficiency of conversion of dc to RF power is almost twice the electronic efficiency. Under this condition the tube is operating with collector voltage depression.

9-7-2 Normal Depression and Overdepression of Collector Voltage

Most gridded traveling-wave tubes are very sensitive to variations of collector depression voltages below normal depression level, since the tubes operate close to the knee of the electron spent beam curves. Figure 9-7-4 [18] shows the spent beam curves for a typical gridded traveling-wave tube.

Under normal collector depression voltage V_c at -7.5 kV with full saturated power output, the spent beam electrons are collected by the collector and returned to the cathode. Thus the collector current I_c is about 2.09 A. A small amount of electrons intercepted by the beam scraper or slow-wave circuit contribute the tube body current for about 0.178 A. Very few electrons with lower kinetic energy reverse the direction of their velocity inside the collector and fall back onto the output pole piece. These returning electrons yield a current I_r of 0.041 A, which is only a small fraction of the body current I_b. These values are shown in Fig. 9-7-4.

When the collector voltage is overdepressed from the normal level of -7.5 kV to the worst case of about -11.5 kV, a greater number of the spent electrons inside the collector reverse the direction of their velocity by a highly negative collector voltage and fall back onto the grounded output pole piece because the potential of the pole piece is 11.5 kV higher than the collector voltage. It can be seen from Fig.

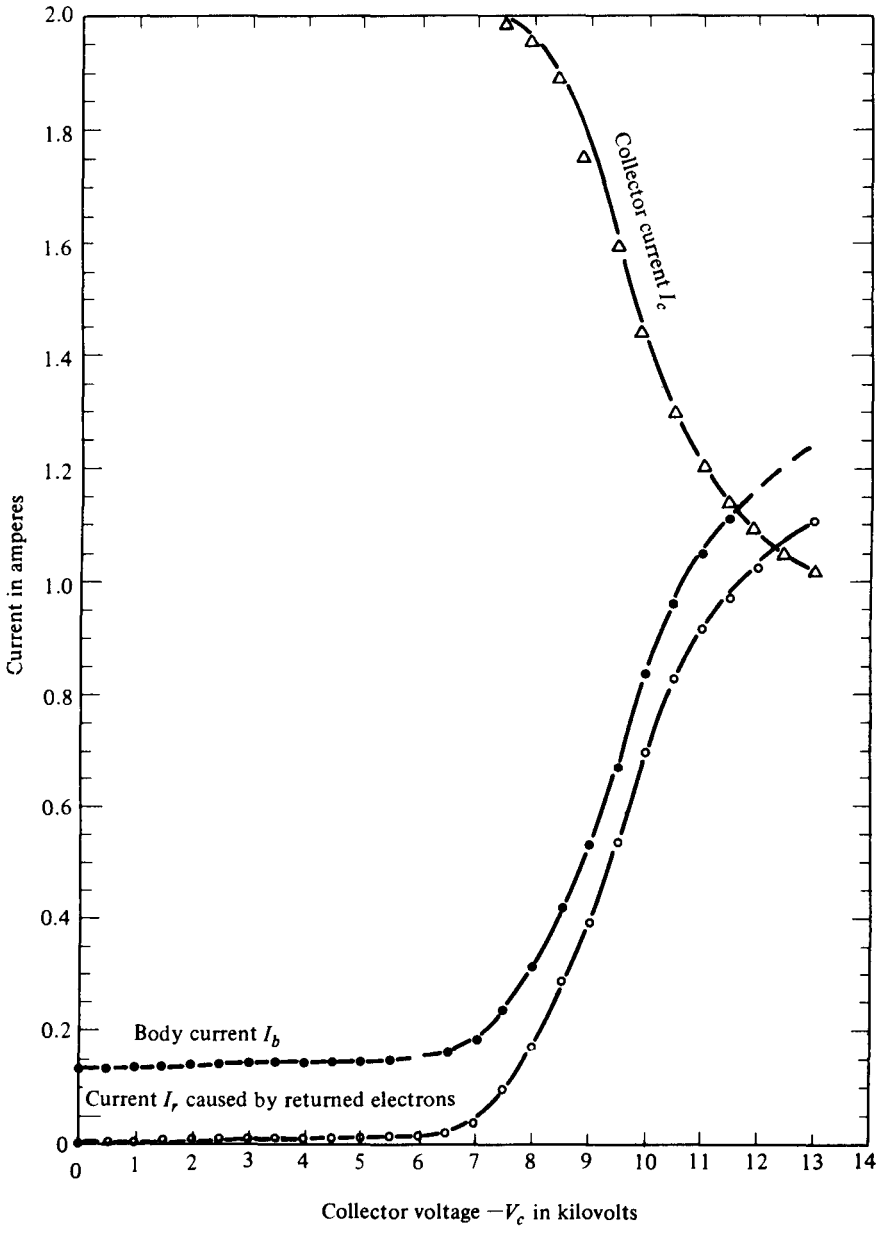

Figure 9-7-4 Spent beam curves for a typical gridded TWT.

9-7-4 that when the collector voltage is overdepressed from -7.5 to -11.5 kV, the collector current is decreased sharply from 2.01 to 1.14 A and the body current is increased rapidly from 0.237 to 1.110 A. The body current consists of two parts: One part is the current caused by the electrons intercepted by the circuit or the beam scrapers; another part is the current caused by the electrons returned by the overdepressed collector voltage. Figure 9-7-5 [18] shows the impact probability of returned electrons by certain overdepressed collector voltage.

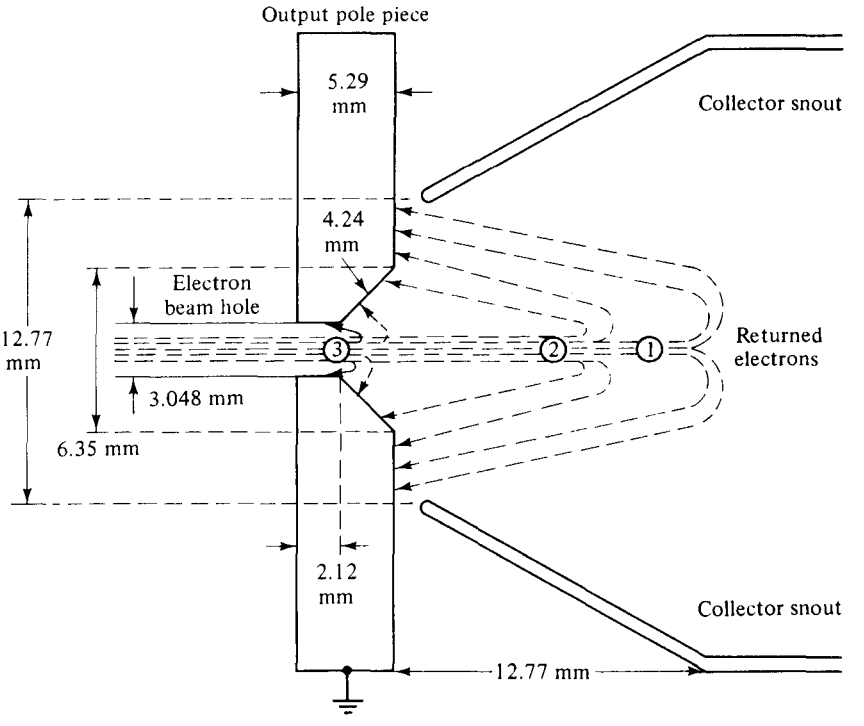

Figure 9-7-5 Impact probability of returned electrons by overdepressed collector voltage.

Example 9-7-1: Gridded Traveling-Wave Tube (GTWT)

A gridded traveling-wave tube is operated with overdepression of collector voltage as follows:

Overdepression collector voltage:	$V_c = -11$ kV
Returned current:	$I_r = 0.85$ A
Mass of heated iron pole piece:	mass = 250 mg
Specific heat H of iron at 20°C:	$H = 0.108$ calories/g-°C

Determine:

a. The number of electrons returned per second

b. The energy (in eV) associated with these returning electrons in 20 ms

c. The power in watts for the returning electrons

d. The heat in calories associated with the returning electrons (a factor for converting joules to calories is 0.238)

e. The temperature T in degrees Celsius for the output iron pole piece [*Hint:* $T = 0.238VIt/(\text{mass} \times \text{specific heat})$]

f. Whether the output iron pole piece is melted

Solution

a. The number of electrons returned per second is

$$I_r = \frac{0.85}{1.6 \times 10^{-19}} = 5.31 \times 10^{18} \text{ electrons per second}$$

b. The energy is

$$W = Pt = VI_r t = 11 \times 10^3 \times 5.31 \times 10^{18} \times 20 \times 10^{-3}$$
$$= 1.168 \times 10^{21} \text{ eV}$$

c. The power is

$$P = VI_r = 11 \times 10^3 \times 0.85 = 9.35 \text{ kW}$$

d. The created heat is

$$H(\text{heat}) = 0.238Pt = 0.238VI_r t$$
$$= 0.238 \times 11 \times 10^3 \times 0.85 \times 20 \times 10^{-3}$$
$$= 44.51 \text{ calories}$$

e. The temperature is

$$T = \frac{0.238VI_r t}{\text{mass} \times \text{specific heat}}$$
$$= \frac{44.51}{250 \times 10^{-3} \times 0.108} = 1648.52°C$$

f. The output iron pole piece is melted.

9-7-3 Two-Stage Collector Voltage Depression Technique

When the spent electron beam arrives in the collector, the kinetic energies of each electron are different. Under the normal operation at a collector voltage of about 40% of the cathode voltage, very few electrons will be returned by the negative collector voltage. Consequently, the tube body current is very small and negligible because the returned electrons are the only ones intercepted by the cavity grids and the slow-wave circuit. When the collector is more negative, however, more electrons with lower energy will reverse their direction of velocity and fall onto the output

pole piece. Thus the tube body current will increase sharply. Since electrons of various energy classes exist inside the collector, two-stage collector voltage depression may be utilized. Each stage is biased at a different voltage. Specifically, the main collector may be biased at 40% depression of the cathode voltage for normal operation, but the collector snout may be grounded to the output pole piece for overdepression operation. As a result, the returned electrons will be collected by the collector snout and returned to the cathode even though the collector voltage is overdepressed to be more negative. Since the collector is cooled by a cooling mechanism, the overheating problem for overdepression is eased. Figure 9-7-6 shows a structure of two-stage collector voltage depression, and Fig. 9-7-7 depicts a basic interconnection of a gridded traveling-wave tube with its power supplies [18].

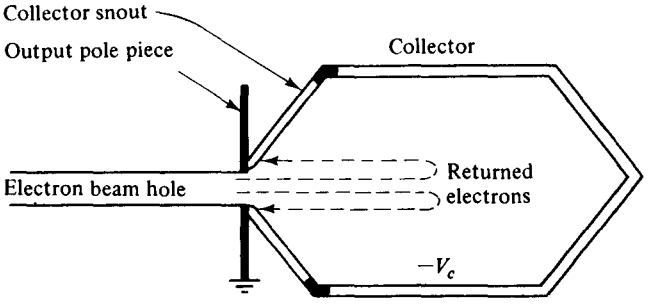

Figure 9-7-6 Diagram for two-stage collector depression.

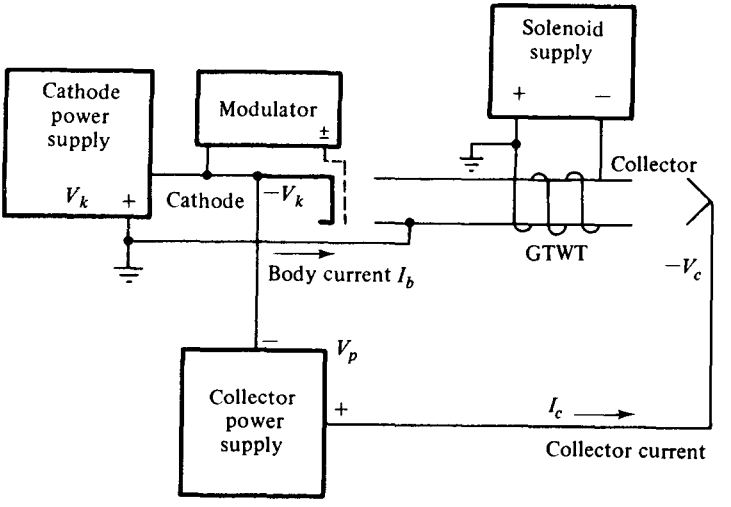

Figure 9-7-7 Basic interconnection of a gridded traveling-wave tube with its power supplies.

9-7-4 Stabilization of Cathode and Collector Voltages

The cathode voltage of a gridded traveling-wave tube is negative with respect to ground so that the electrons can be emitted from the cathode. In order to maintain a constant beam power for a uniform gain, the cathode voltage must be constant. In addition, the phase shift through the tube is directly related to the beam velocity; thus high resolution and low ripple are required in the cathode voltage power supply to avoid undesirable phase-shift variations. Consequently, the cathode power supply of the gridded traveling-wave high-power tube is usually regulated for better than 1% over line and load changes and is also well filtered because of the critical requirements on the cathode voltage with respect to ground. The cathode power supply provides the tube body current. Under normal operation the body current is very small in comparison with the collector current. Figure 9-7-8 shows a basic interconnection for a gridded traveling-wave tube with two regulated power supplies.

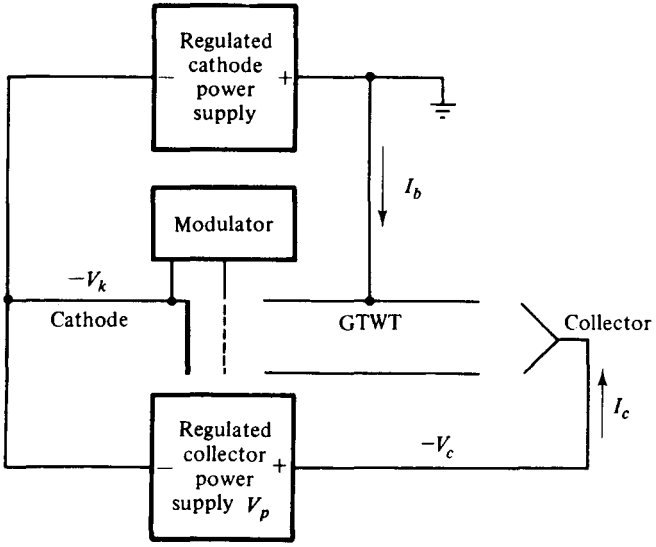

Figure 9-7-8 Interconnections for a gridded traveling-wave high-power tube.

Figure 9-7-9 illustrates a voltage-regulator circuit for a cathode power supply. The voltage regulator indicated in the circuit consists of two devices: one differential amplifier and one tetrode tube. The solid-state differential amplifier amplifies the difference between the preset reference voltage and the voltage that is one-thousandth of the output voltage. The reference voltage is adjustable to a preset level. The output voltage of the differential amplifier drives the control grid of the regulator tube between cutoff and saturation in order to nullify the difference voltage.

As shown in Fig. 9-7-8 the negative terminal of the collector power supply is connected to the cathode and the positive terminal to the collector electrode. The

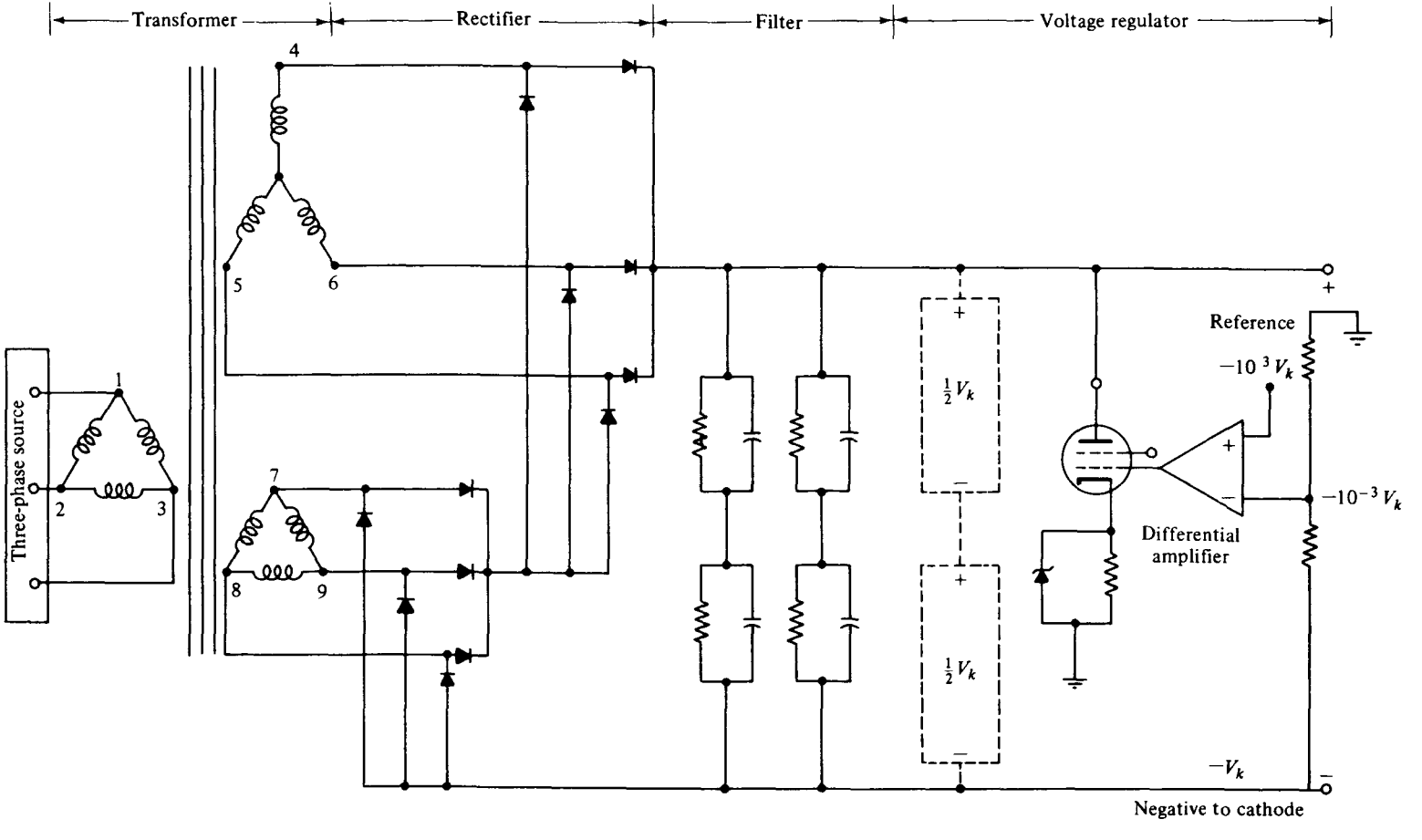

Figure 9-7-9 Voltage-regulator circuit for cathode power supply.

collector depression voltage is the difference of the two regulated supply voltages. The cathode supply provides the tube body current and the collector supply yields the collector current. The ratio of the collector current over the body current is about 10 for an operation of 40% voltage depression. Thus the power delivered to the tube by the collector supply is about four times larger than the power furnished by the cathode supply. An electrical transient may occur in the circuit when power supplies are just being switched on or off. The reasons for an electrical transient may be caused by two factors:

1. Load changes: When the load of a generator is suddenly increased, a larger current is needed. Since the generator cannot meet the demand instantaneously, the output voltage of the generator drops momentarily. Conversely, when the load of a generator is suddenly decreased, the output voltage drops accordingly.
2. Switching on or off: When the switch of a generator is just turned on or off, the armature current in the armature conductors produces armature reaction. The nature of armature reaction reduces the terminal voltage for lagging loads.

When an electrical transient is created in the circuit, the collector voltage is overdepressed. As a result, the spent electrons inside the collector reverse the direction of their velocity by the highly negative collector voltage and fall back onto the grounded output pole piece. The tube body current is sharply increased and the collector current is greatly decreased. When the returned electrons impact the output pole piece, the pole piece will be damaged by high heat. The damage of the output pole piece creates a mismatch in the interaction circuit and degrades the performance of the tube. In particular, the tube gain, efficiency, bandwidth, and power output are affected accordingly by the circuit mismatch when the collector voltage is overdepressed below the normal depression level. Furthermore, the large body current may burnout the solid-state differential amplifier of the cathode voltage regulator and vary the electron beam of the gridded tube. If the damage is beyond the tolerance of the gridded traveling-wave high-power tube, the tube may cease to function.

In order to maintain a constant collector depression voltage, the collector voltage must be regulated. There are three possible ways to do so [18]:

1. Regulator in series with the collector power supply: In this method a voltage regulator is incorporated in series with the collector supply as shown in Fig. 9-7-10 so that the output voltage of the collector supply may be regulated at a certain level with respect to ground. Since the output voltage of the cathode supply is highly regulated at a certain level, the difference between the two regulated voltages will produce a well-regulated voltage with respect to ground at the collector electrode.
2. Regulator in parallel with the collector supply: In this method a voltage regulator is inserted in parallel with the collector supply as shown in Fig. 9-7-11 so that a regulated voltage with respect to ground at normal depression may be achieved at the collector terminal.

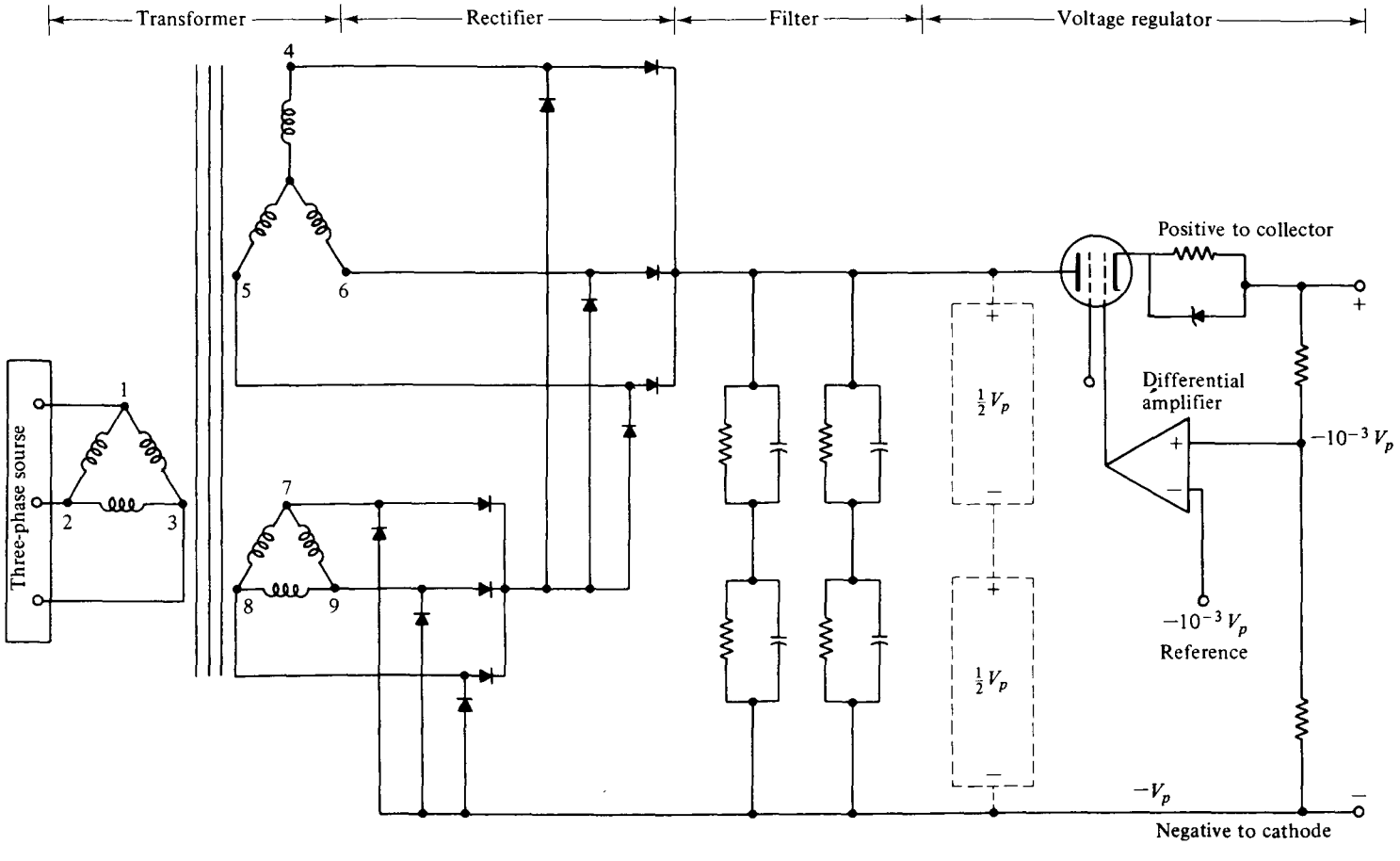

Figure 9-7-10 Regulator in series with collector supply.

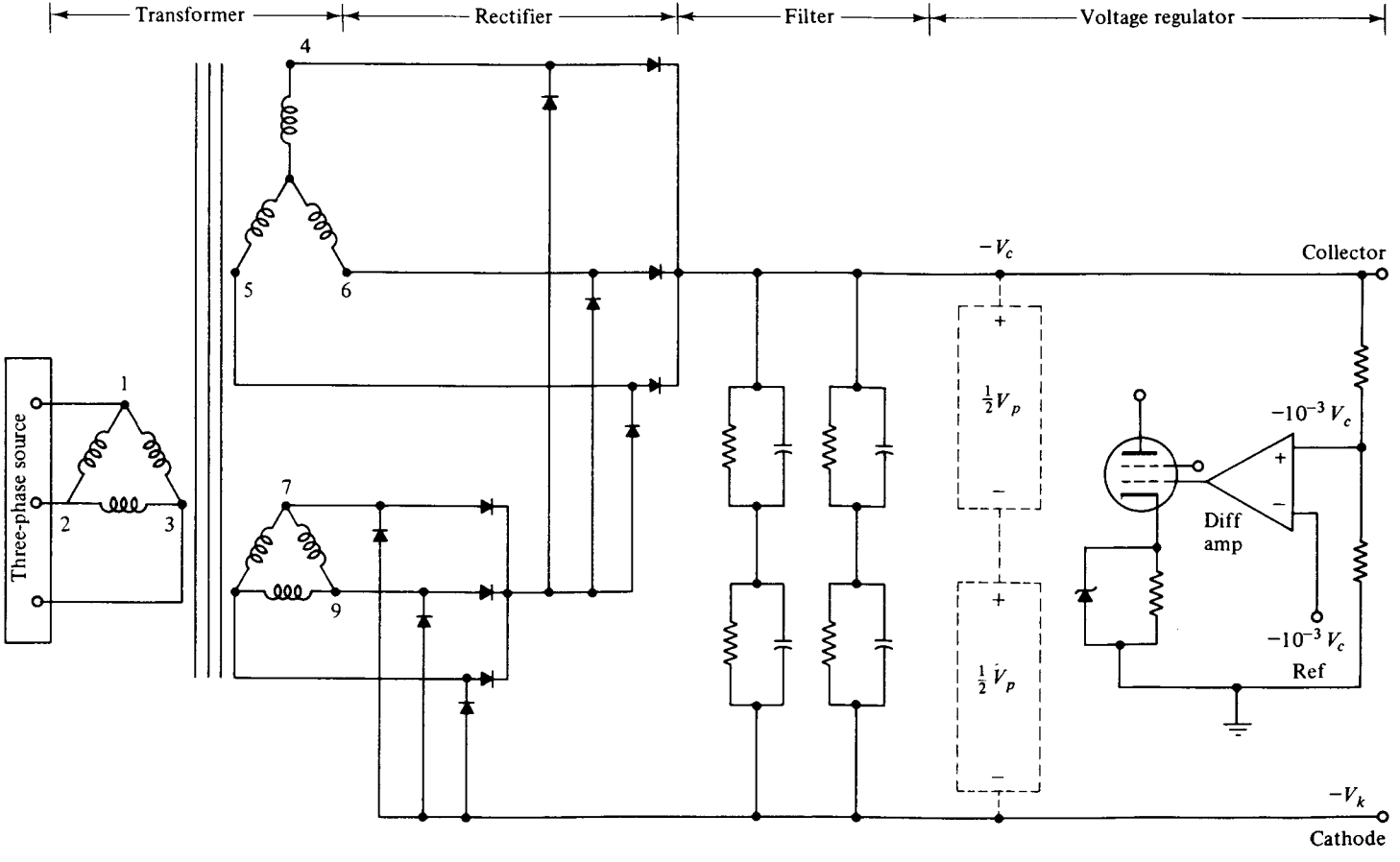

Figure 9-7-11 Regulator in parallel with collector supply.

3. Regulator between the cathode voltage and the collector voltage: In this method the collector depression voltage is regulated with respect to the cathode voltage as shown in Fig. 9-7-12. If the collector voltage is overdepressed above the normal depression value (absolute value), differential amplifier 2 tends to adjust the cathode voltage below its fixed level (absolute value). When the cathode voltage is dropped, the collector voltage is readjusted to its normal depression level with respect to ground.

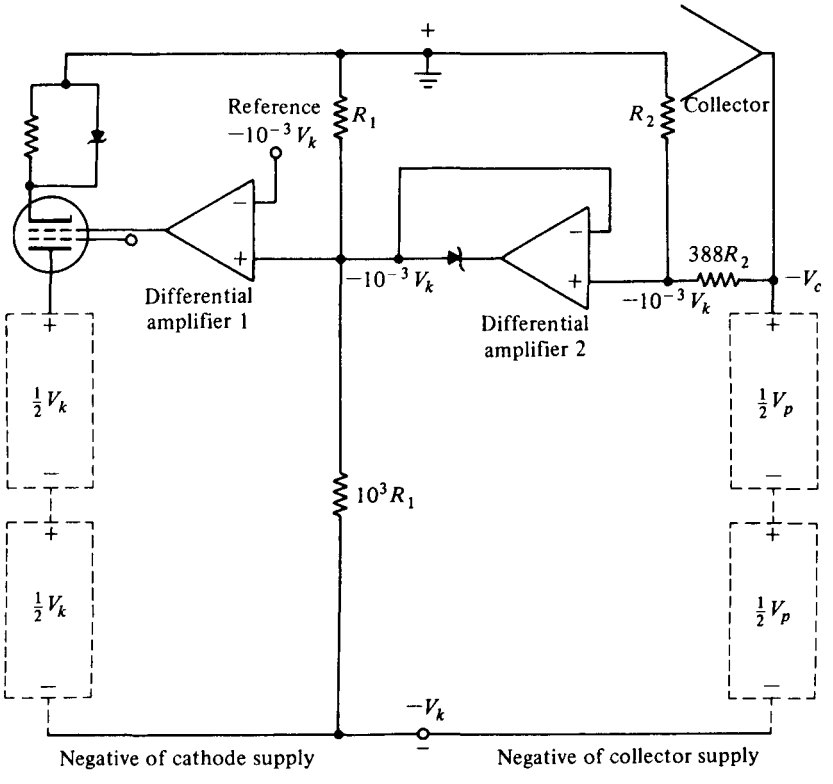

Figure 9-7-12 Regulator between cathode voltage and collector voltage.

REFERENCES

[1] WARNECKE, R. R., et al., Velocity modulated tubes. In *Advances in Electronics*, Vol. 3. Academic Press, New York, 1951.

[2] CHODOROW, M., and C. SUSSKIND, *Fundamentals of Microwave Electronics*. McGraw-Hill Book Company, New York, 1964.

[3] CHODOROW, M., and T. WESSEL-BERG, A high-efficiency klystron with distributed interaction. *IRE Trans. Electron Devices*, **ED-8,** 44–55, January 1961.

[4] LARUE, A. D., and R. R. RUBERT, Multi-Megawatt Hybrid TWT's at *S*-band and *C*-band. Presented to the IEEE Electron Devices Meeting, Washington, D.C., October 1964.

[5] HIESLMAIR, H., et al., State of the art of solid-state and tube transmitters. *Microwave J.*, **26,** No. 10, 46–48, October 1983.

[6] FEENBERG, E., Notes on velocity modulation. *Sperry Gyroscope Laboratories Report. 5521–1043,* Chapter I, 41–44.

[7] STAPRANS, A., et al., High-power linear beam tubes. *Proc. IEEE,* **61,** No. 3, 299–330. March 1973.

[8] LIEN, E. L., High efficiency klystron amplifier. In *Conv. Rec. MOGA 70* (8th Int. Conf., Amsterdam, September 1970).

[9] MERDINIAN, G., and J. V. LEBACQZ, High power, permanent magnet focused, *S*-band klystron for linear accelerator use. *Proc. 5th Int. Conf. of Hyper-frequency Tubes* (Paris, September 1964).

[10] BECK, A. H. W., Space charge wave and slow electromagnetic waves. p. 106, Pergamon Press, New York, 1985.

[11] KOMPFNER, R., The traveling-wave tube as amplifier at microwaves. *Proc. IRE,* **35,** 124–127, February 1947.

[12] CHODOROW, M., and R. A. CRAIG, Some new circuits for high-power traveling-wave tubes. *Proc. IRE,* **45,** 1106–1118, August 1957.

[13] ROUMBANIS, T., et al., A megawatt *X*-band TWT amplifier with 18% bandwidth. *Proc. High-Power Microwave Tubes Symp.*, Vol. 1 (The Hexagon, Fort Monmouth, N.J., September 25–26, 1962).

[14] RUETZ, A. J., and W. H. YOCOM, High-power traveling-wave tubes for radar systems. *IRE Trans. Mil. Electron.*, **MIL-5,** 39–45, April 1961.

[15] MENDEL, J. T., Helix and coupled-cavity traveling-wave tubes. *Proc. IEEE,* **61,** No. 3, 280–298, March 1973.

[16] BRILLOUIN, L., *Wave Propagation in Periodic Structures,* 2nd ed. Dover, New York, 1953.

[17] CURNOW, H. J., A general equivalent circuit for coupled-cavity slow-wave structures. *IEEE Trans. on Microwave Theory and Tech.*, **MTT-13,** 671–675, September 1965.

[18] LIAO, S. Y., The effect of collector voltage overdepression on tube performance of the gridded traveling-wave tubes. Report for Hughes Aircraft Company, El Segundo, Calif., August 1977.

SUGGESTED READINGS

COLLIN, R. E., *Foundations for Microwave Engineering,* Chapter 9. McGraw-Hill Book Company, New York, 1966.

GANDHI, O. P., *Microwave Engineering and Applications,* Chapters 9, 10, and 11. Pergamon Press, New York, 1981.

GEWARTOWSKI, J. W., and H. A. WATSON, *Principles of Electron Tubes,* Chapters 5, 6, and 10 to 13. D. Van Nostrand Company, Princeton, N.J., 1965.

GILMOUR, A. S., JR., *Microwave Tubes.* Artech House, Dedham, Mass., 1986.

IEEE Proceedings, **61,** No. 3, March 1973. Special issue on high-power microwave tubes.

LIAO, S. Y., *Microwave Electron Tubes.* Prentice-Hall, Inc., Englewood Cliffs, N.J., 1988.

PROBLEMS

Vacuum Tubes

9-1. A vacuum pentode tube has five grids: a cathode, a control grid, a screen grid, a suppressor grid, and an anode plate as shown in Fig. P9-1.

a. Sketch the equivalent circuit.

b. Derive an expression for the input impedance Z_{in} in terms of the angular frequency ω and the circuit parameters.

c. Determine the transit-angle effect.

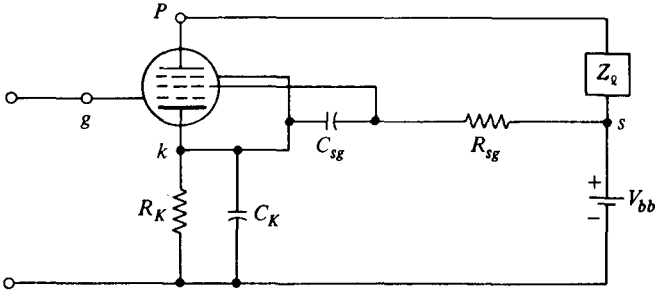

Figure P9-1

Klystrons

9-2. The parameters of a two-cavity amplifier klystron are as follows:

Beam voltage:	$V_0 = 1200$ V
Beam current:	$I_0 = 28$ mA
Frequency:	$f = 8$ GHz
Gap spacing in either cavity:	$d = 1$ mm
Spacing between the two cavities:	$L = 4$ cm
Effective shunt resistance:	$R_{sh} = 40$ kΩ (excluding beam loading)

a. Find the input microwave voltage V_1 in order to generate a maximum output voltage V_2 (including the finite transit-time effect through the cavities).

b. Determine the voltage gain (neglecting the beam loading in the output cavity).

c. Calculate the efficiency of the amplifier (neglecting the beam loading).

d. Compute the beam loading conductance and show that one may neglect it in the preceding calculations.

9-3. A two-cavity amplifier klystron has the following characteristics:

Voltage gain:	15 dB
Input power:	5 mW
Total shunt impedance of input cavity R_{sh}:	30 kΩ
Total shunt impedance of output cavity R_{sh}:	40 kΩ
Load impedance at output cavity R_ℓ:	40 kΩ

Determine:

a. The input voltage (rms)
b. The output voltage (rms)
c. The power delivered to the load in watts

9-4. A two-cavity amplifier klystron has the following parameters:

Beam voltage:	$V_0 = 900$ V
Beam current:	$I_0 = 30$ mA
Frequency:	$f = 8$ GHz
Gap spacing in either cavity:	$d = 1$ mm
Spacing between centers of cavities:	$L = 4$ cm
Effective shunt impedance:	$R_{sh} = 40$ kΩ

Determine:

a. The electron velocity
b. The dc electron transit time
c. The input voltage for maximum output voltage
d. The voltage gain in decibels

9-5. Derive Eq. (9-2-49).

Multicavity Klystrons

9-6. A four-cavity klystron amplifier has the following parameters:

Beam voltage:	$V_0 = 20$ kV
Beam current:	$I_0 = 2$ A
Operating frequency:	$f = 9$ GHz
dc charge density:	$\rho_0 = 10^{-6}$ C/m^3
RF charge density:	$\rho = 10^{-8}$ C/m^3
Velocity perturbation:	$\mathcal{V} = 10^5$ m/s

Determine:

a. The dc electron velocity
b. The dc phase constant
c. The plasma frequency
d. The reduced plasma frequency for $R = 0.5$
e. The beam current density
f. The instantaneous beam current density

9-7. A four-cavity CW klystron amplifier has the following parameters:

Beam voltage:	$V_0 = 30$ kV
Beam current:	$I_0 = 3$ A
Gap distance:	$d = 1$ cm
Operating frequency:	$f = 8$ GHz
Signal voltage:	$V_1 = 15$ V(rms)
Beam coupling coefficient:	$\beta_i = \beta_0 = 1$
dc electron charge density:	$\rho_0 = 10^{-7}$ C/m^3

Compute:

a. The dc electron velocity
b. The dc electron phase constant
c. The plasma frequency
d. The reduced plasma frequency for $R = 0.4$
e. The reduced plasma phase constant
f. The transit time across the input gap
g. The modulated electron velocity leaving the input gap

9-8. A two-cavity klystron amplifier has the following parameters:

Beam voltage:	$V_0 = 30$ kV
Beam current:	$I_0 = 3$ A
Operating frequency:	$f = 10$ GHz
Beam coupling coefficient:	$\beta_i = \beta_0 = 1$
dc electron charge density:	$\rho_0 = 10^{-7}$ C/m^3
Signal voltage:	$V_1 = 15$ V(rms)
Cavity shunt resistance:	$R_{sh} = 1$ kΩ
Total shunt resistance including load:	$R_{sht} = 10$ kΩ

Calculate:

a. The plasma frequency
b. The reduced plasma frequency for $R = 0.4$
c. The induced current in the output cavity
d. The induced voltage in the output cavity
e. The output power delivered to the load
f. The power gain
g. The electronic efficiency

9-9. A four-cavity klystron amplifier has the following parameters:

Beam voltage:	$V_0 = 20$ kV
Beam current:	$I_0 = 1.5$ A
Operating frequency:	$f = 2$ GHz
Beam coupling coefficient:	$\beta_i = \beta_0 = 1$
dc electron charge density:	$\rho_0 = 10^{-6}$ C/m^3
Signal voltage:	$V_1 = 2$ V(rms)
Cavity shunt resistance:	$R_{sh} = 2$ kΩ
Total shunt resistance including load:	$R_{sht} = 1$ kΩ

Determine:

a. The plasma frequency
b. The reduced plasma frequency for $R = 0.4$
c. The induced current in the output cavity
d. The induced voltage in the output cavity
e. The output power delivered to the load
f. The electronic efficiency

Reflex Klystrons

9-10. A reflex klystron operates at the peak mode of $n = 2$ with

Beam voltage:	$V_0 = 300$ V
Beam current:	$I_0 = 20$ mA
Signal voltage:	$V_1 = 40$ V

Determine:
a. The input power in watts
b. The output power in watts
c. The effficiency

9-11. A reflex klystron operates under the following conditions:

$V_0 = 500$ V
$R_{sh} = 20$ kΩ
$f_r = 8$ GHz
$L = 1$ mm is the spacing between repeller and cavity

The tube is oscillating at f_r at the peak of the $n = 2$ mode or $1\frac{3}{4}$ mode. Assume that the transit time through the gap and the beam loading effect can be neglected.
a. Find the value of repeller voltage V_r.
b. Find the direct current necessary to give microwave gap voltage of 200 V.
c. Calculate the electronic efficiency.

9-12. A reflex klystron operates at the peak of the $n = 2$ mode. The dc power input is 40 mW and $V_1/V_0 = 0.278$. If 20% of the power delivered by the beam is dissipated in the cavity walls, find the power delivered to the load.

9-13. A reflex klystron operates at the peak of the $n = 1$ or $\frac{3}{4}$ mode. The dc power input is 40 mW and the ratio of V_1 over V_0 is 0.278.
a. Determine the efficiency of the reflex klystron.
b. Find the total output power in milliwatts.
c. If 20% of the power delivered by the electron beam is dissipated in the cavity walls, find the power delivered to the load.

Traveling-Wave Tubes (TWTs)

9-14. A traveling-wave tube (TWT) has the following characteristics:

Beam voltage:	$V_0 = 2$ kV
Beam current:	$I_0 = 4$ mA
Frequency:	$f = 8$ GHz
Circuit length:	$N = 50$
Characteristic impedance:	$Z_0 = 20\ \Omega$

Determine:
a. The gain parameter C
b. The power gain in decibels

9-15. A TWT operates under the following parameters:

Beam current:	$I_0 = 50$ mA
Beam voltage:	$V_0 = 2.5$ kV
Characteristic impedance of helix:	$Z_0 = 6.75\ \Omega$
Circuit length:	$N = 45$
Frequency:	$f = 8$ GHz

Determine:

a. The gain parameter C

b. The output power gain A_p in decibels

c. All four propagation constants

d. The wave equations for all four modes in exponential form

9-16. An O-type traveling-wave tube operates at 2 GHz. The slow-wave structure has a pitch angle of 5.7°. Determine the propagation constant of the traveling wave in the tube. It is assumed that the tube is lossless.

9-17. An O-type helix traveling-wave tube operates at 8 GHz. The slow-wave structure has a pitch angle of 4.4° and an attenuation constant of 2 Np/m. Determine the propagation constant γ of the traveling wave in the tube.

9-18. In an O-type traveling-wave tube, the acceleration voltage (beam voltage) is 3000 V. The characteristic impedance is 10 Ω. The operating frequency is 10 GHz and the beam current is 20 mA. Determine the propagation constants of the four modes of the traveling waves.

9-19. Describe the structure of an O-type traveling-wave tube and its characteristics; then explain how it works.

9-20. In an O-type traveling-wave tube, the acceleration voltage is 4000 V and the magnitude of the axial electric field is 4 V/m. The phase velocity on the slow-wave structure is 1.10 times the average electron beam velocity. The operating frequency is 2 GHz. Determine the magnitude of velocity fluctuation.

Gridded Traveling-Wave Tubes (GTWTs)

9-21. The current I_r caused by the returning electrons at an overdepression voltage of -11.5 kV in a GTWT is about 0.973 A as shown by the spent beam curve in Fig. 9-7-4.

a. Calculate the number of electrons returned per second.

b. Determine the energy in electron volts associated with these returning electrons in 1 ms for part (a).

c. Find the power in watts for the returning electrons.

9-22. The output iron pole piece of a GTWT has the following characteristics:

1. The specific heat H at 20°C is 0.108 cal/g°C.
2. A factor for converting joules to calories is 0.238.
3. The mass of the heated iron pole piece is assumed to be 203.05 mg.
4. The duration time t of the collector depression transient voltage of -11.5 kV is 15 ms.
5. The melting point of iron is 1535°C.

Using these characteristics,

a. Calculate the heat in calories associated with the returning electrons at an overdepression voltage of -11.5 kV.

b. Compute the temperature T in degrees Celsius for the output iron pole piece. [*Hint:* $T = 0.238VIt/(\text{mass} \times \text{specific heat})$.]

c. Determine whether the output iron pole piece is melted.

9-23. The efficiency of a GTWT is expressed as

$$\eta = \frac{\text{RF}P_{\text{ac}}}{P_{\text{dc}}} = \frac{\text{RF}P_{\text{ac}}}{V_0 I_0}$$

If the cathode voltage is -18 kV and the collector voltage is depressed to -7.5 kV determine the efficiency of the GTWT.